

Characterization of the Oncogenic Role of BCL9-2 in Breast Tumorigenesis

Dissertation for the award of the degree

“doctor rerum naturalium”

of the Georg-August-University Göttingen

submitted by

Nathalie Zatula

from Amursk

Göttingen 2012

Prof. Dr. Felix H. Brembeck (Referee)

Hematology/Oncology / Tumor Biology and Signal Transduction
Göttingen University Medical School

Prof. Dr. Matthias Dobbelsstein (Second Referee)

Molecular Oncology
Göttingen University Medical School

Prof. Dr. Heidi Hahn (Third Referee)

Human Genetics / Molecular Developmental Genetics Group
Göttingen University Medical School

Date of the oral examination:

Statement of Authorship

I hereby certify that the dissertation

“Characterization of the Oncogenic Role of BCL9-2 in Breast Tumorigenesis”,

was composed by myself and is based on my work, with no other sources and help than indicated and acknowledged in the text

Göttingen, 07. February 2012

(Nathalie Zatula)

Table of contents

List of Abbreviations	8
1. Introduction.....	8
1.1 Breast development and cancer.....	8
1.1.1 Key stages of breast development.....	8
1.1.2 Morphology of mammary gland	9
1.1.3 Breast cancer	11
1.2 Wnt/ β -catenin signaling in breast development and cancer	12
1.2.1 Overview of Wnt/ β -catenin signaling.....	12
1.2.2 Wnt/ β -catenin signaling in breast development.....	13
1.2.3 Wnt/ β -catenin signaling in breast cancer	15
1.3 BCL9-2 and its function in development and tumorigenesis.....	17
1.3.1 BCL9-2 encodes a member of BCL9 protein family	17
1.3.2 The role of BCL9-2 in normal development and cancer.....	18
2. Aims of the study	21
3. Materials	22
4. Methods.....	42
4.1 In vivo experiments.....	42
4.1.1 Generation of K19-BCL9-2 transgenic mice	42
4.1.2 Generation of compound APC ^{Min/+} ; K19-BCL9-2, MMTV ^{Cre} ; Catnb ^{+/Δex3} ; K19-BCL9-2 and K5-CreER ^{T/+} ; Catnb ^{+/Δex3} ; K19-BCL9-2 females	43
4.1.3 Induction of K5-CreER ^{T/+} expression by tamoxifen.....	43
4.1.4 BrdU incorporation	43
4.2 Isolation of genomic DNA (gDNA).....	43
4.3 Genotyping PCR analyses	44
4.4 Isolation of total RNA using TRI Reagent.....	44

4.5 Detection of BCL9-2 transcripts by PCR	45
4.6 Carmine whole mount staining	46
4.7 Tissue processing for immunohistochemistry.....	46
4.8 Histological staining on tissues.....	47
4.8.1 Hematoxylin and Eosin staining (H&E)	47
4.8.2 Immunohistochemistry.....	47
4.8.3 Immunohistochemical detection of <i>in vivo</i> BrdU labeled cells	48
4.8.4 Immunofluorescent staining on paraffin embedded tissues	48
4.9 Scoring	49
4.10 Primary culture of mouse tumor cells	50
4.10.1 Isolation of primary cells from K19-BCL9-2 and non-transgenic control animals	50
4.10.2 Cultivation of primary cells from K19-BCL9-2 and non-transgenic control animals	50
4.11 MTT assay.....	51
4.12 BrdU incorporation assay.....	51
4.13 2D collagen assay.....	52
4.14 Immunofluorescent staining on primary cells.....	52
4.15 Cell culture of stable human breast cancer cell lines	53
4.16 Transient RNA interference	53
4.17 Quantitative Real Time PCR (qRT-PCR)	53
4.18 Isolation of whole cell protein lysates for Western blot	54
4.19 Isolation of nuclear proteins for Western blot	54
4.20 Western blot analysis	55
4.21 Statistics	56
5. Results	57
5.1 Characterization of K19-BCL9-2 transgenic mouse model.....	57

5.1.1 Analysis of the K19-BCL9-2 transgene expression in K19-BCL9-2 mice.....	57
5.1.2 Phenotype of K19-BCL9-2 transgenic animals	58
5.1.3. Characterization of K19-BCL9-2 transgene expression in mammary gland tumors of transgenic females	60
5.2 BCL9-2 expression during different stages of mammary gland development	60
5.3 Histological analyses of mammary tumors from K19-BCL9-2 mice	63
5.3.1 The tumors of K19-BCL9-2 show distinct differentiations of the tumor cells.....	63
5.3.2 The tumors of K19-BCL9-2 females are estrogen receptor positive	65
5.4 Transgenic females display delayed age-related and post-postlactational involution of the breast epithelium	69
5.4.1 Aged K19-BCL9-2 females display premalignant alterations of the mammary gland.....	69
5.4.2 The mammary glands of K19-BCL9-2 females displayed delayed postlactational involution.....	73
5.5 Transgenic overexpression of BCL9-2 in different Wnt mammary tumor models	75
5.5.1 Transgenic overexpression of BCL9-2 leads to a higher mammary tumor susceptibility in compound APC ^{Min/+} ; K19-BCL9-2 mice.....	75
5.5.2 Transgenic overexpression of BCL9-2 leads to mammary tumor development in MMTV ^{Cre} ; Catnb ^{+/Δex3} ; K19-BCL9-2 compound mutant mice	76
5.5.3 Transgenic overexpression of BCL9-2 does not induce mammary tumor development in K5-CreER ^{T/+} ; Catnb ^{+/Δex3} ; K19-BCL9-2 compound mutant mice.....	80
5.6 Primary culture of breast tumor and hyperplastic glands from K19-BCL9-2 females	82
5.6.1 Characterization of cultured tumors cells from transgenic females.....	82
5.6.2 Estrogen treatment of cultured tumor cells enhances their viability.....	87

5.6.3 Tamoxifen treatment of cultured tumor cells reduces their proliferation .	90
5.6.4 Mammary tumor cells from K19-BCL9-2 generate tamoxifen sensitive colonies in vitro.....	91
5.7 BCL9-2 is overexpressed in hormone receptor positive human mammary breast cancers	92
5.7.1 Human breast cancer cell lines express different levels of BCL9-2	92
5.7.2 Knock down of BCL9-2 in MCF7 leads to reduced expression of ER α and its target genes.....	95
5.7.2 BCL9-2 expression correlates with the expression of ER α , PR and HER2.....	95
6. Discussion.....	100
6.6 BCL9-2 overexpression in human breast cancer correlates with high hormone receptor expression.....	107
7. Summary	111
8. Zusammenfassung.....	113
9. References	115
10. Curriculum Vitae	129
11. Acknowledgements.....	130

List of Abbreviations

APC	<i>adenomatous polyposis coli</i>
BCL9	B-cell CLL/lymphoma 9 protein
BCL9-2	B-cell CLL/lymphoma 9-like protein
BD	binding domain
BGH	bovine growth hormone
bp	Base pairs
BrdU	Bromodeoxyuridine
BRG1	brahma-related gene 1
CBP	CREB-binding protein
cDNA	complementary DNA
CK1	casein kinase 1
DCIS	ductal carcinoma <i>in situ</i>
Dkk1	Dickkopf-related protein 1
DMSO	Dimethylsulfoxide
DNA	Desoxyribonucleic acid
dNTP	Desoxyribonucleotide triphosphate
DSS	dextran sulfate sodium
EDTA	ethane-1,2-diyl dinitrilo tetraacetic acid
EMT	epithelial-mesenchymal transition
ER α	estrogen receptor alpha
ERBB2	v-erb-b2 erythroblastic leukemia viral oncogene homolog 2
EtOH	Ethyl alcohol
EZH2	Enhancer of zeste (Drosophila) homolog 2
FACS	fluorescence activated cell sorting
FBS	fetal bovine serum
For (primer)	forward

List of Abbreviations

gDNA	Genomic DNA
GH	growth hormone
GREB1	Growth regulation by estrogen in breast cancer 1
GSK3	Glycogen Synthase Kinase 3
HAN	hyperplastic alveolar nodule
HD	homology domain
H&E	Hematoxylin & Eosin
HER2	Human Epidermal Growth Factor 2
HRP	Horse radish peroxidase
IDC	Invasive ductal carcinoma
IGF-1	Insulin-like Growth Factor 1
IgG	Immunoglobulin G
IHC	immunohistochemistry
K19	keratin 19
kDa	kilo Dalton
LRP	Low Density Lipoprotein Receptor-related Protein
MaSC	mammary stem cells
MMTV	mouse mammary tumor virus
miRNA	microRNA
Min	multiple intestinal neoplasia
mRNA	messenger RNA
MTT	Methyl Thiazolyl Diphenyl-tetrazolium Bromide
NLS	nuclear localization signal
PBS	Phosphate Buffered Saline
PFA	paraformaldehyde
PCR	polymerase chain reaction
PR	progesterone receptor
qRT-PCR	quantitative real time PCR
Rev (primer)	reverse

List of Abbreviations

RNA	ribonucleic acid
RT	reverse transcriptase or room temperature
SDS	Sodium Dodecyl Sulfate
SDS-PAGE	SDS polyacrylamide gel electrophoresis
siRNA	short interfering RNA
TBP	TATA-Box Binding Protein
TBST	Tris-Buffered Saline Tween-20
TCF/LEF	T cell factor/lymphoid enhancer factor
TEB	terminal end buds
TEMED	N,N,N',N'-Tetramethylethan-1,2-diamin
TG	transgenic
β -TRCP	beta-transducin repeat containing
UTR	untranslated region

1. Introduction

1.1 Breast development and cancer

1.1.1 Key stages of breast development

The basic morphology of the mammary gland and important developmental events during mammary organogenesis are comparable between mice and human (1-4). The mouse mammary gland development is characterized by different stages. The first step of embryonic mammary development occurs approximately at mid-pregnancy. This is when the mammary line appears laterally and extends from the fore to the hind limb of the embryo (5, 6). Shortly after, mammary placodes arise as a result of migration of cells from this mammary line (7). This is followed by invagination of the cells into the underlying mesenchyme, which simultaneously differentiates into mammary mesenchyme. The mammary bud is formed (6, 7). The last step of the embryonic mammary development is the formation of rudimentary ductal tree. The mammary bud cells start to proliferate and invade from the mesenchyme into the fat pad in the dermis. This process is sex hormone independent (8-10). As a result, the rudimentary ductal tree is present in the mammary fat pad at birth (6).

The first step of postnatal mammary gland development is the ductal outgrowth that takes place during the puberty. Here, extensive hormone-dependent branching of the rudimentary ductal tree occurs. This process is driven by the proliferation of the cells, which reside in the terminal end buds (TEB) at the tip of the ducts (10). The outgrowth of the mammary ducts is regulated by estrogen and its receptor ER α (estrogen receptor alpha), GH (growth hormone) and IGF-1 (insulin-like growth factor 1) (11). At this stage, lateral secondary and tertiary side branches appear as a consequence of proliferating activity of the TEBs resulting in complex system of branched ducts and terminal and side alveolar buds in the adult mammary gland (3, 10, 12).

During pregnancy, massive alveologenesis occurs from the alveolar buds, which represent the most hormone sensitive structures in the rodent and human mammary gland (3, 13). The alveolar buds proliferate and differentiate into single alveoli,

which are organized into functional lobular-alveolar units, capable of milk production after pregnancy (3, 13).

After weaning, the mammary gland goes through postlactational involution, where the lobular-alveolar units collapse and undergo apoptosis. Thereafter the mammary gland is remodeled to a pre-pregnancy state with only a few remaining lobular units (3, 13, 14). With aging of the females, the lobular-alveolar epithelium of the breast undergoes irreversible lobular involution, which is characterized by loss of the alveolar units and the function of the breast epithelium (4, 15).

1.1.2 Morphology of mammary gland

Mice are commonly used animal models to study breast development and cancer. Although the general mechanisms of mammary morphogenesis are presumably similar in mammals, there are a number of differences between the mouse and human mammary gland. The mouse mammary gland comprises an epithelial ductal tree embedded in an adipocyte rich mammary fat pad. The epithelium of the breast is generated by two cell lineages, which originate from a common progenitor (2, 16). The inner epithelial cell layer, termed luminal, can be subdivided into ductal and alveolar, lining the ducts and alveoli, respectively. The luminal cells are surrounded by the myoepithelia, bounded by the basement membrane. Stem/progenitor cells are believed to reside in a suprabasal position between luminal and myoepithelial cells (2). In the mouse mammary gland, the whole epithelium is surrounded by fatty tissue with a few fibroblasts in between (Figure 1A). This represents the major difference between human and mice mammary gland, since the human gland contains much more connective tissue (2, 10).

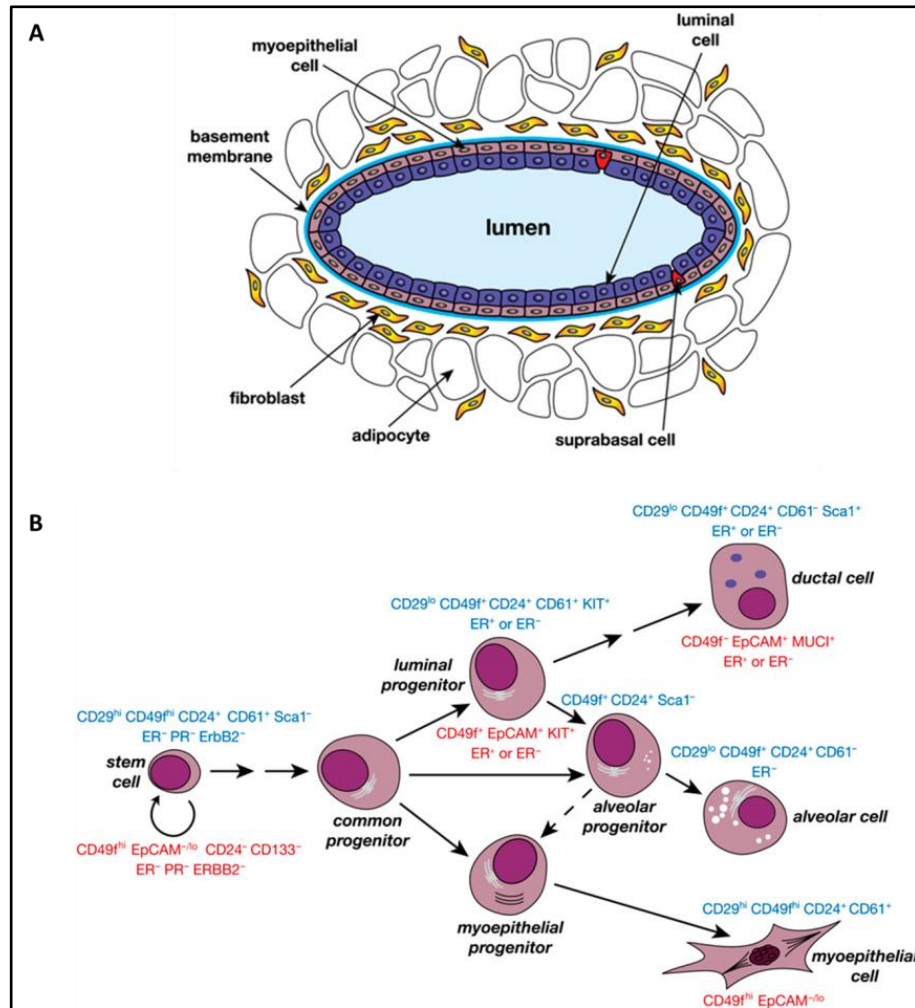


Figure 1. Schematic overview of a mouse mammary duct (A) and hierarchy of different mammary stem/progenitor (2).

A. Different cell types of mammary gland as indicated. **B.** Characteristic cell surface marker compositions for different stem/progenitor populations identified in mouse (blue) and human (red) mammary gland.

Ductal outgrowth and differentiation of different cell types in the postnatal mammary gland originates from mammary stem and progenitor cells (17, 18). The existence of mammary stem cells (MaSC) was proved by mammary epithelium reconstitution assays after transplantation of donor epithelium (19). In the adult breast there is a hierarchical organization of progenitor differentiation (2). A combination of different cell surface markers allowed the isolation of distinct mammary cell populations. Mammary stem cells were reported to be enriched in the CD49f^{high}/CD29^{high}/CD24⁺/Sca1⁻ cell subset (19-21). A certain combination of different levels of these and other used cell surface markers defined different progenitor populations, such as two primary epithelial cell lineages (myoepithelial and luminal) and alveolar progenitors (Figure 1B) (19, 20).

1.1.3 Breast cancer

Breast cancer is a heterogeneous disease based on histopathological features and molecular subtypes. Six molecular subtypes of breast cancer were defined based on their gene expression profiles. These include normal-breast-like, claudin-low, basal-like, luminal A or B, and HER2/ERBB2-overexpressing subtypes. The differences in subtypes are presumed to originate from different mutations and different cells of origin, thus indicating the implication of transformed stem/progenitor cells (22-24).

The most important criterion of the tumor types by immunohistochemistry is the expression of nuclear hormone receptors ER α (estrogen receptor α), PR (progesterone receptor) and of HER2 (Human Epidermal Growth Factor 2, erbB2, neu). This histopathological classification is essential for therapeutic treatment.

Most tumors, especially the common invasive ductal and lobular carcinoma are associated with luminal subtypes and are ER α and PR positive, which respond to the endocrine therapy and are associated with good prognosis (25-28). The most used anti-estrogen is tamoxifen, which is an ER α antagonist and prevents ER α mediated signal transduction (29). As a result, tamoxifen inhibits the expression of ER α target genes, including growth factors, which stimulate the proliferation of tumor cells. However, many patients acquire tamoxifen resistance or do not respond despite the expression of ER α . The possible reasons for that could be loss or reduction of ER α expression, alternative ER α isoforms, altered receptor interaction partner expression or interfering with other signaling pathways (30-35). Another anticancer drug is named Fulvestrant. It is a pure ER α antagonist and acts by preventing the dimerization of the receptor and its binding to the DNA. Unfortunately, Fulvestrant displays poor oral bioavailability (30). Aromatase inhibitors are the third group of endocrine therapeutics, usually used for treatment of postmenopausal patients. As in case of tamoxifen, the breast cancers treated with aromatase inhibitors can gain endocrine resistance (30).

HER2 is deregulated in breast cancers by overexpression or amplification mutations (26, 27, 36). HER2 is a member of the EGFR family and regulates different cellular processes including proliferation and survival. Tumors with HER2 overexpression show usually poor differentiation and are associated with poor outcome. Often tumors with nuclear hormone expression and HER2 overexpression display resistance to endocrine therapy. This often occurs because of a cross talk between HER2 and

ER α pathways, where HER2 signaling dominates. A combination therapy of anti-estrogens and anti HER2 antibody trastuzumab or a tyrosine kinase inhibitor lapatinib reduces risk of tumor progression and metastases (37).

Around 20% of human breast cancers belong to the basal-like subtype. Tumors of this subtype are the most aggressive and usually do not express HER2, ER α or PR and are, therefore termed as triple-negative (36, 38). Interestingly, basal-like tumors are reported to express marker of embryonic stem cells (24, 39). However, basal-like tumors display gene expression signature similar to luminal mammary progenitor cells, whereas luminal A and B as well as HER2 positive cancers correlate with a gene signature from a more differentiated progenitor of the luminal lineage (2).

The tumors of claudin-low type display loss of adherence junctions and show mesenchymal characteristics (40). This tumor subtype displays the greatest overlap with gene signature of mammary stem cells (2).

1.2 Wnt/ β -catenin signaling in breast development and cancer

1.2.1 Overview of Wnt/ β -catenin signaling

Only a few highly conserved signaling pathways regulate cell proliferation and tissue organization during embryogenesis and in the adult organism. One of these pathways represents the so called canonical Wnt or Wnt/ β -catenin signaling cascade. Moreover, deregulated Wnt signaling is of particular importance for malignant transformation and tumor progression (17, 41-48)

The central component of the canonical Wnt signaling pathway is β -catenin (44, 49). In the cell, β -catenin has two functions. It is a component of adherence junctions at the cell membrane and is a transducer of Wnt signals in the cell (41, 48, 50). These two functions are balanced by degradation of β -catenin. In the absence of extracellular Wnt signals, free cytosolic β -catenin is tightly controlled by a cytosolic destruction complex. This complex consists of the tumor suppressor *adenomatous polyposis coli* (APC), casein kinase 1 (CK1), glycogen synthase kinase 3 (GSK3) and a scaffold protein axin. The protein complex phosphorylates N-terminal residues of β -

catenin (Ser 33, 37, 41, 45). The N-terminal phosphorylation results in a subsequent ubiquitination of the protein by β -TRCP (beta-transducin repeat containing), a subunit of the E3 ubiquitin ligase. Finally, proteasomal degradation of β -catenin takes place (41, 45, 48, 51). Binding of Wnt ligands to the transmembrane Frizzled/LRP receptor complex leads to a repression of the destruction complex, a stabilization and nuclear translocation of β -catenin. In the nucleus β -catenin binds to DNA-bound TCF/LEF (T cell factor/lymphoid enhancer factor) transcriptional factors. The consequence is a transcriptional activation of Wnt/ β -catenin dependent target genes (Figure 2) (44, 45, 50-52).

The nuclear function of β -catenin as a transcriptional activator is specified by several co-factors, such as CBP, p300, BRG1, TBP and many more (52, 53). Recently, novel nuclear co-factors of BCL9 and Pygopus proteins families were identified to co-regulate β -catenin dependent transcription of target genes (54-56). The predicted function of Legless/BCL9 was to act as an adaptor protein, which tethers another co-factor of Wnt/ β -catenin signaling Pygopus to the β -catenin/TCF complex. Members of the Pygopus protein family Pygo1/Pygo2 have been implicated in recruitment of chromatin remodeling factors to the protein/DNA assembly and modulation of histones (57-59).

1.2.2 Wnt/ β -catenin signaling in breast development

Wnt signaling is essential for embryonic specification of the mammary placode lineage and postnatal morphogenesis of the mammary gland (7, 18). Wnt10b is the first marker of the mammary line during the embryonic development (5). Several other Wnt genes are expressed when the mammary placodes develop (5, 6). Dkk1 (Dickkopf-related protein 1) acts as an antagonist of canonical Wnt signaling. Overexpressed in mice during mammary line development, Dkk1 inhibits mammary line specification and subsequently mammary placodal development (60). Similar phenotypes were observed in knock out models of different Wnt/ β -catenin pathway components, such as Lrp5 and 6 (Low-density lipoprotein receptor-related protein) or Pygopus2 (61-63).

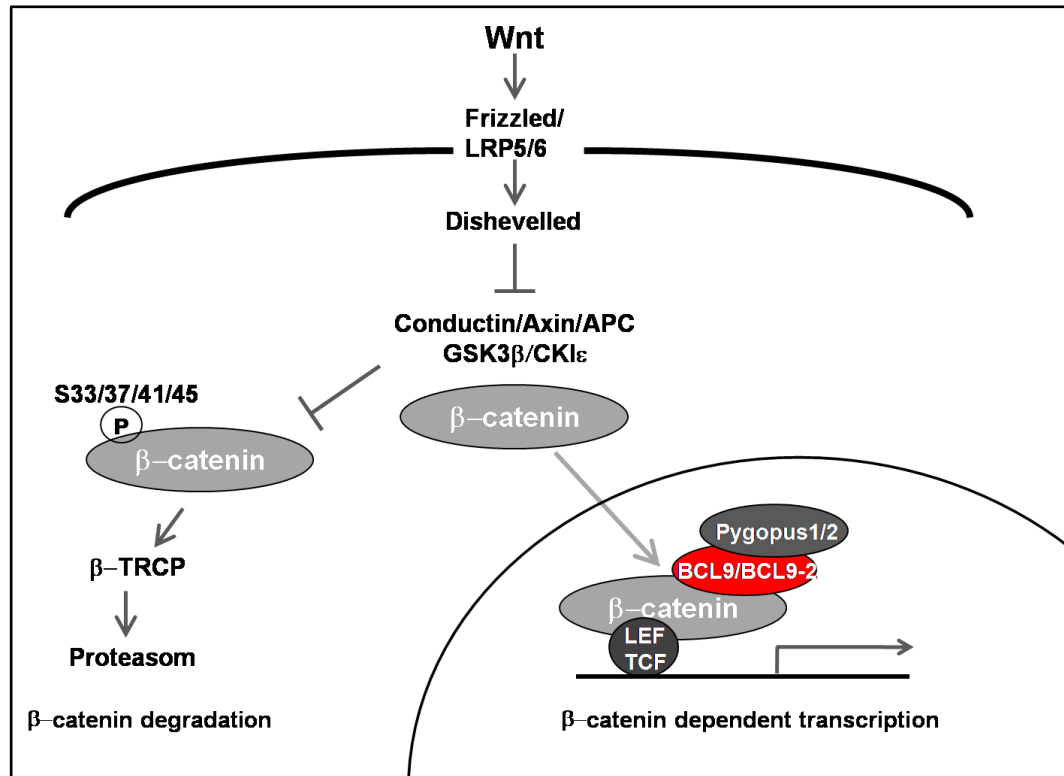


Figure 2. Schematic overview of Wnt/β-catenin signaling pathway.

In the absence of extracellular Wnt molecules, the destruction complex marks cytosolic β-catenin for proteasomal degradation. Binding of Wnt ligands to the transmembrane Frizzled/LRP receptor complex leads to a repression of the destruction complex, a stabilization and nuclear translocation of β-catenin. In the nucleus β-catenin binds to DNA-bound TCF/LEF transcriptional factors and activates the transcription of target genes. The figure was adapted from Brembeck et al. 2006.

During puberty, the expansion of ductal tree takes place. This process is mainly driven by estrogen and ER, growth hormone and insulin-like growth factor (IGF) (11). The role of canonical Wnt pathway during postnatal mammary development was established in different mouse models. For example, glands from MMTV-Wnt10b transgenic virgin mice displayed ductal hyperbranching (64). Similarly, overexpression of stabilized β-catenin from K14 promoter led to precocious branching and lateral bud formation (62). *Lrp6*^{+/-}; *Lrp5*^{-/-} double knock out mutants failed to undergo a proper ductal outgrowth (63). Vice versa, the overexpression of *Lrp6* from the MMTV promoter induced accelerated ductal branching in the mammary glands of virgin mice (65).

The importance of canonical Wnt signaling during pregnancy associated processes was also established from observations from multiple mouse models. The hallmark of pregnancy is extensive lobular-alveolar development (3, 13, 66). As shown by the

expression of the canonical Wnt signaling reporters, TOPGAL and TOPlacZ *in vivo*, Wnt/ β -catenin pathway is activated during pregnancy, as the reporters were both active in mammary epithelium at this developmental stage (60, 67). MMTV driven expression of Wnt1 or Wnt10b induced lobulo-alveolar hyperplasia (64, 68). Similarly, expression of stabilized β -catenin or overexpression of CyclinD1 led to precocious alveologenesis (69, 70). Expression of stabilized β -catenin from K5 promoter induced accelerated side branching and secretory cell differentiation in pregnancy (71). In contrast, ductal branching was postponed in recipient mice during early pregnancy following a transplantation of Wnt4^{-/-} mammary cells into cleared fat pad (72).

The significance of canonical Wnt signaling during the postlactational involution is poorly studied. However, involution defects were detected in MMTV-Wnt10b transgenic mice (64). EZH2 is a histone methyltransferase, which promotes nuclear translocation of β -catenin and transcriptional activity. In MMTV-EZH2 mice the overexpression of EZH2 leads to delayed involution (73).

1.2.3 Wnt/ β -catenin signaling in breast cancer

Roeland Nusse and Harold Varmus described in 1982, that mice infected with mouse mammary tumor virus (MMTV) developed breast tumors due to activation of the *Wnt1* gene (74). MMTV-Wnt1 transgenic mice developed mammary adenocarcinoma, confirming the oncogenic potential of Wnt1 (68). Generation of MMTV-Wnt10b animals led to growth of mammary cancers histologically very similar to MMTV-Wnt1 tumors (64). Transgenic expression of stabilized β -catenin from MMTV promoter again showed increased susceptibility of transgenic females to breast tumor development, approving the association of increased Wnt/ β -catenin signaling with breast cancer development in mice (69).

In human breast cancers stabilization mutations of β -catenin or loss of APC are uncommon (18). Nevertheless, atypical β -catenin expression or localization is often found in human mammary tumors. Elevated cytosolic and nuclear expression of β -catenin was detected in up to 66% of breast tumors and correlated with poor prognosis (75-78). However, deregulations of Wnt/ β -catenin pathway components upstream

of β -catenin are documented. Usually, there is enhanced expression of Wnt ligands, inactivation of antagonists or mutations of receptors, which promote β -catenin activation (75, 78, 79). In addition, overexpression of nuclear cofactors such as Pygopus2 was detected in a panel of human breast cancers (80). Moreover, proteins aside from Wnt/ β -catenin signaling, which however interact with β -catenin, such as EZH2, are overexpressed in breast cancers (73, 81).

The knowledge, that canonical Wnt signaling controls mammary epithelium growth and differentiation established a link between the pathway and mammary stem cells. The evidences came from FACS sorting analyses of different mammary epithelium cell populations followed by transplantation assays. Zeng and Nusse 2010 demonstrated a greater mammary reconstitution capacity for stem cells with activated Wnt/ β -catenin signaling compared to those where Wnt signaling was low (82). In breast cancer mouse models, a reduction of stem cell activity was detected in *Lrp5*^{-/-} animals, indicating the implication of Wnt/ β -catenin pathway in stem/progenitor cell regulation in the mammary epithelium (61). Moreover, MMTV-Wnt1 and Δ N89 β -catenin mice showed an increase in stem/progenitor cell population in the normal breast and tumors (19, 83, 84). These findings demonstrated that canonical Wnt signaling not only controls stem/progenitor population in the normal breast, but also may be involved in oncogenic transformation of these cells leading to tumorigenesis.

Indeed, in human breast cancers recent studies suggest Wnt signaling for (de-) regulation of mammary stem/progenitor cell population. For example, the expression of *Lrp6* is higher in triple-negative breast cancers (85). Cytoplasmic and nuclear expression of β -catenin was associated with basal-like hormone receptor negative type of human breast cancers with poor prognosis. Moreover, cytoplasmic and nuclear expression of β -catenin in these tumors corresponds to the CD24⁻/CD44⁺ stem cell like phenotype (76, 86). In contrast, absence of β -catenin expression was associated with invasive lobular carcinoma (86). Taken together, the recent studies on β -catenin indicate its implication in basal-like type of breast cancer (86).

1.3 BCL9-2 and its function in development and tumorigenesis

1.3.1 BCL9-2 encodes a member of BCL9 protein family

BCL9-2 is a member of the novel BCL9 protein family in vertebrates. Its human homologue BCL9 was initially identified as the product of the *B cell lymphoma 9* gene, which was translocated and overexpressed in B-cell malignancies with chromosomal translocations (87). The function of BCL9 was disclosed in a genetic screen by discovery of the *Drosophila* orthologue *Legless* as a component of Wg/Wnt signaling (see below). *Legless* was identified as an essential co-factor of Wnt/ β -catenin signaling during *Drosophila* development, which binds to β -catenin. *Legless* was functionally replaced by human BCL9 in rescue experiments (57, 88). BCL9-2 was identified as another BCL9 related binding partner of β -catenin in a yeast-two-hybrid screen of a mouse embryo cDNA library (54).

The overall sequence identity of the proteins of BCL9 family is relatively low (approximately 35 %). The similarities are comprised within the seven highly conserved homology domains (HDs). These short sequences contain a Pygopus binding domain, β -catenin binding domain and a nuclear localization signal (NLS) coding domain (HD1, HD2 and HD3, respectively) in the N-terminus. All proteins of BCL9 family share an additional N-terminal domain, which encodes for a putative sumoylation site and, but only in case of BCL9-2 a further NLS. C-terminus of BCL9 proteins includes three additional homology domains termed C-HD 1-3, which are less conserved in *Drosophila* (Figure 3) (54, 57, 89).

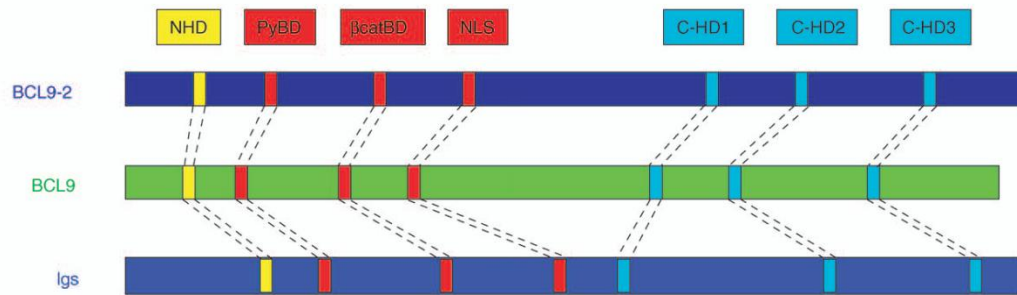


Figure 3. Schematic view of the domain structure of the BCL9 protein family (48).

NHD: N-terminal homology domain, containing a second nuclear localization signal (NLS) in BCL9-2 sequence. PyBD: Pygopus binding domain (HD1), β catBD: β -catenin binding domain (HD2), NLS: classic nuclear localization signal containing domain (HD3). C-HD1, C-HD2 and C-HD3, C-terminal homology domains-1, -2 and -3, respectively.

The analyses of domain functions revealed some unique features of BCL9-2. In contrast to Legless/BCL9, BCL9-2 is a nuclear protein (54, 89). Deletion of the second NLS from the N-terminal homology domain (NHD) of BCL9-2 sequence resulted in cytoplasmic localization of the mutant protein (54, 89, 90).

Binding to Pygo2 is crucial for Legless/BCL9 to promote its co-activator function in Wnt/ β -catenin dependent manner in *Drosophila* and vertebrates. In contrast, BCL9-2 does not require interaction with Pygo2 to co-activate Wnt/ β -catenin dependent transcription in vertebrates (54, 89, 90). Moreover, it was suggested that BCL9-2 translocates β -catenin to the nucleus thereby regulating β -catenin's adhesion and transcriptional functions. Phosphorylation of tyrosine 142 of β -catenin promotes BCL9-2 binding, which in turn enhances β -catenin transcriptional activity (54).

The function of the C-terminal domains is not yet completely understood. However, they seem to be important for promotion of Wnt/ β -catenin signaling, since a deletion of a C-terminus in BCL9 abolished the Wnt/ β -catenin dependent expression of a reporter construct in cultured cells (91).

1.3.2 The role of BCL9-2 in normal development and cancer

Considerable number of studies in the last decade described the requirement of BCL9 and BCL9-2 for the Wnt/ β -catenin in normal cells and in tumors. However,

BCL9 was reported to present its transcriptional co-activator function only in particular type of cells and tissues (e.g. in lymphoid or muscle cells), which are in part distinct from BCL9-2 (91-93). Together, these findings demonstrate distinct, cellular context dependent functions of two proteins believed to fulfill similar tasks.

In vivo studies provided insights into the function of the proteins. In a recent study by Matsuura et al., 2011 a conventional knock-out of BCL9-2 was used to analyze the role of Wnt/ β -catenin signaling in the regulation of the GCM1/syncytin pathway *in vivo*. They reported that BCL9-2^{+/-} mice were healthy and fertile. In contrast, BCL9-2^{-/-} mice died at approximately embryonic day (E) 10.5. However, embryonic lethality was rather due to maternal placental defects (94). Studies on inducible BCL9/BCL9-2 double knockout mice and on K19-BCL9-2 transgenics showed that deregulation of BCL9 proteins is dispensable for normal homeostasis in the intestine (92, 93, 95).

BCL9/BCL9-2 double mutant mice showed altered expression of several genes specifically expressed in intestinal stem cells including *Lgr5*. Moreover, the regeneration capacity of BCL9/BCL9-2 intestinal epithelium was diminished after an induction of colitis by treatment of mice with DSS (dextran sulfate sodium). Furthermore, double mutant mice showed a reduced expression of EMT (epithelial-mesenchymal transition) markers in the intestinal adenoma and reduced size of colon tumors (95). The limiting condition of the double knock out study was the lack of evidence that both proteins share precisely the same function. So, it is not sure, if the resulting phenotype was caused by deregulation of both proteins or if the mutation of one was sufficient. However, the results of the study by Deka et al., 2010 are consistent with our previous findings on BCL9-2 function in normal and cancer cell. Overexpression of BCL9-2 promoted EMT in normal epithelial cells and reconverted a mesenchymal phenotype of colon cancer cells into more epithelial (54). Furthermore, BCL9-2 enhanced local invasion of the APC^{Min/+} adenoma. In addition, overexpression of BCL9-2 induced intestinal tumorigenesis in transgenic K19-BCL9-2 mice (93). Consequently, the role of BCL9 proteins rather under pathological conditions became more evident.

While an oncogenic role of BCL9 was implicated for B- and T-cell malignancies, BCL9-2 was associated with epithelial cancers. High BCL9-2 levels were found in

colon cancer cell lines and HeLa (54, 89, 93, 96). We recently described, that in colon cancer cells BCL9-2 co-regulated only a subset of Wnt/ β -catenin dependent genes. In addition, for the first time we demonstrated that BCL9-2 also controls the expression of the EphB3/B4 receptors and EphrinB1/B2/B3 ligands independently of β -catenin (93). These BCL9-2 specific target are implicated in intestinal cancer (97). The examination of human colorectal neoplasia and invasive cancers revealed a correlation of high BCL9-2 protein level and progressive tumor stages (93, 98).

The expression of BCL9-2 was studied in a single study on human breast cancer samples (99). Here BCL9-2 was described to be higher expressed in breast cancer tissues than in the normal breast. In ductal carcinoma *in situ* (DCIS), the immunohistochemical BCL9-2 expression was significantly associated with the nuclear grade and the expression of HER2, c-myc and p53. Moreover the expression of BCL9-2 tended to correlated with β -catenin and ER. Similarly, in invasive ductal carcinoma (IDC) BCL9-2 expression correlated significantly with nuclear grade and the expression of HER2.

Although the implication of BCL9-2 in development and progression of colon cancers is clear, the mechanisms of its deregulation are still not known. The mechanisms and factors, which regulate the expression of BCL9 proteins, are poorly analyzed. However, recently a first hint in this regard was published. BCL9 was found to be regulated by miRNAs in ovarian cancer (100). Moreover, the potential new functions of C-terminal domains remain to be discovered. Since it is now evident that BCL9-2 can regulate genes independently of β -catenin (93), a detection of candidate pathways, which may interact with BCL9-2, could provide new insights into additional functions of BCL9-2 and contribute to understanding of its oncogenic mechanism.

2. Aims of the study

The aim of this study was to assess the oncogenic role of β -catenin's co-factor BCL9-2, a homologue of the human proto-oncogene product BCL9, in the formation and progression of breast cancer. To analyze if BCL9-2 can contribute to breast cancerogenesis, the overexpression of BCL9-2 was analyzed *in vivo* using a K19-BCL9-2 transgenic mouse model. The mammary glands of transgenic females were examined for the development of early premalignant changes. Furthermore, mammary tumors from K19-BCL9-2 females were analyzed regarding their differentiation and hormone receptor status by immunohistochemistry. To investigate the dependency of these tumors on estrogen receptor activity, primary cell cultures of K19-BCL9-2 tumors were established. MTT and BrdU functional assays were performed to examine the viability and proliferation of K19-BCL9-2 tumor cells after estrogen and tamoxifen treatment.

To study the implication of BCL9-2 in human mammary cancers, cell lines and tissue samples derived from breast cancer patients were used. The BCL9-2 expression levels in different breast cancer cell lines were analyzed by Western blot. Additionally, the mRNA levels of estrogen receptor α and its target genes were examined after siRNA-mediated BCL9-2 knock down, to assess a possible mechanism of how BCL9-2 may regulate estrogen receptor expression and function. To evaluate a correlation of BCL9-2 overexpression and hormone receptor status, human breast cancer tissue arrays were analyzed by immunohistochemistry.

3. Materials

3.1 General material

Materials	Manufacturers
Cryovials	Nunc
Culture plates (100 mm Ø)	Nunc
Cuvettes	Roth
Cell Strainer	Falcon
Filters for solutions (0.2 µm and 0.45 µm)	Sartorius
Flasks for cell culture (75 cm ² and 175 cm ²)	Sarstedt
Gloves (nitrile, latex)	Sempermed
Hybond-P PVDF membrane	GE Healthcare
Hypodermic needle (23 G)	BBraun
Parafilm	Pechiney Plastic Packaging
Pasteur pipettes	Peske OHG
Petri dishes	Falcon
Pipettes (2, 5, 10 and 25 ml)	Eppendorf
Pipette tips (10, 200 and 1000 µl)	MbP
Pipette tips (10, 200 and 1000 µl with a filter)	Biozym
Plates for cell culture (6-well, 24-well and 96-well)	TPP, Nunc
Scalpels	Technic cut

Materials

Tubes for cell culture (polystyrene, 15 and 50 ml)	Falcon, Sarstedt
Tubes for cell culture (polypropylene, 15 ml and 50 ml)	Falcon
Tubes for molecular biology, Safelock (1.5 ml and 2 ml)	Eppendorf, Sarstedt
Whatman paper	Whatman

3.2 Instruments and equipment

Type of device		Manufacturer
Camera	DC 300 FX	Leica
Camera	DFC 290	Leica
Cell counting chamber	Neubauer	Brand
Cell culture incubator	BBD 6220	Heraeus
Cell culture sterile bench	LaminAir HB 2448	Heraeus
Centrifuge	Refrigerated Microcentrifuge	Eppendorf
Centrifuge	Microcentrifuge	Eppendorf
Centrifuge	Refrigerated Bench-Top Hood Centrifuge	Eppendorf
Centrifuge	Microcentrifuge MCF 2360	MS Co. LTD
Controlled-freezing box		Nalgene
Electrophoresis chambers for agarose gels		Peqlab
Electrophoresis chambers		BioRAD

Materials

for SDS-PAGE		
ELISA Reader	SUNRISE A-5082	TECAN
Freezer (-150 °C)	Ultra low temperature freezer MDF-C2156VAN	Sanyo
Freezer (-20 °C)	PremiumNoFrost	Liebherr
Freezer (-80 °C)	Ultra low temperature freezer U725	New Brunswick Scientific GmbH
Fridge (+4 °C)	AEG Electrolux SANTO	AEG
Gel documentation	BioDocAnalyze	Biometra
Heating block	Thermostat plus	Eppendorf
Ice machine	ZBE 70-35	Ziegra
Incubator		Memmert
Micropipettes	(0.5-10 µl, 10-100 µl, 20-200 µl, 100-1000 µl)	Eppendorf
Microscope	DM 500	Leica
Microscope inverted	DM IRB	Leica
Microwave oven		Powerwave
PCR cycler	T3 Thermocycler	Biometra
Pipetting assistant	MATRIX	Thermo Scientific
Power supplier	EV231	Peqlab
Printer		Mitsubishi

Materials

Pump	VDE0530	Adam.Baumüller GmbH
Real Time PCR device	7900HT Fast Real-Time PCR System	Applied Biosystems
Rotator		GLW
Shaker	IKA-Schüttler MTS4	W.Krannich GmbH+Co.KG
Sonifier		dr. Hielscher GmbH
Spectrophotometer	ND-1000	NanoDrop
Stereomicroscope	MZ FL III	Leica
Transilluminator	UV Star	Biometra
UV lamp	EBQ100 isolated	Leica
Vortexer	IKA ® Vortex	IKA
Water bath	GFL 1003	W.Krannich GmbH+Co.KG
Water purification system		Millipore
Western Blot Documentation	LAS-4000	Fujifilm
Wet Transfer Apparatus	Fastblot	Biorad

3.3 Chemical and biological reagents

Reagents	Manufacturer
Acetic acid	Roth
Agarose	Invitrogen

Materials

Ammonium persulfate (APS)	Roth
BrdU	Roche
β -Mercaptoethanol	Roth
Prestained Protein Ladder	Invitrogen
Bradford reagent	BioRAD
Bromphenol Blue	Roth
Carmin	Roth
Chloroform	Roth
Collagen	Sigma
Collagenase/Hyaluronidase Cocktail	Stemcell
D(+)-trehalose dihydrat	Roth
DAPI	Sigma
DEPC (diethyl pyrocarbonate)	Roth
Dexamethasone	Sigma
Dispase	Sigma
DMEM/F12 medium with GlutaMAX™	Invitrogen
DMSO (dimethyl sulfoxide)	Roth
DNA Ladder	Fermentas
DNase	Roche
DTT (DL-Dithiothreitol)	Sigma
EDTA (ethylenediaminetetraacetate)	Roth
EGTA (ethylene glycol tetraacetic acid)	Roth

Materials

β -estradiol	Sigma
EtBr (ethidium bromide)	Roth
Ethanol	Chemie Vertrieb Hannover
FBS (fetal bovine serum)	Invitrogen, Sigma
Glycerol	Sigma
Glycine	Roth
HCl (hydrochloric acid)	Roth
HEPES	Roth
HOT FIREPol DNA Polymerase	Solis BioDyne
H ₂ O ₂	Roth
Immu-Mount	ThermoScientific
Insulin	Sigma
Insulin-Transferrin-Selenium	Invitrogen
Isopropanol	J.T.Backer
KCl (potassium chloride)	Sigma
KAlS ₂ O ₂ · 12H ₂ O (potassium aluminium sulfate)	Sigma
L-glutamine	Invitrogen
Lipofectamin 2000	Invitrogen
Luminol	Sigma
mEGF (mouse Epidermal Growth Factor)	Invitrogen
MEM Non-Essential Aminoacids	Invitrogen
Methanol	J.T.Backer, Merck

Materials

MgCl ₂	Roche
NaCl (sodium chloride)	Roth
NaHCO ₃ (sodium hydrogen carbonate)	Merck
NaOH (sodium hydroxide)	Sigma
Nicotinamid	Sigma
Nonidet-P40 (NP40)	Sigma
Optimem	Invitrogen
p-Coumaric acid	Sigma
Penicillin / streptomycin	Invitrogen
PFA (paraformaldehyde)	Merck
PMSF (phenylmethanesulfonylfluoride)	Sigma
Polyacrylamide (30% Acrylamide / Bis)	Roth
Protease Inhibitor cocktail tablets	Roche
Proteinase K	Roche
Reverse transcriptase, MMLV-RT	Fermentas
RNA sample buffer	Fermentas
RNase A (Ribonuclease A)	Roche
RNase Inhibitor	Fermentas
Roti [®] -Histokitt	Roth
Roti [®] -Phenol/Chloroform/Isoamylalkohol	Roth
RPMI 1640 medium	Invitrogen
SDS	Sigma

Materials

SYBR GREEN I	Sigma Aldrich
Powdered milk	Roth
Streptavidin-biotinylated HRP	GE Healthcare
TEMED (N,N,N',N'-Tetramethylethan-1,2-diamin)	Roth
Tris	Roth
Triton X-100	Sigma
Trypan blue	Sigma
Trypsin / EDTA	Invitrogen
Tween 20	Sigma
Xylene Cyanol	Roth
Xylol	Roth

3.4 Commercial reagent kits

Name	Manufacturer
Cell proliferation ELISA BrdU Kit	Roche
Dako EnVision+ System HRP labeled	DakoCytomation
Fast Start Taq DNA Polymerase (dNTPs pack)	Roche
TRI Reagent RNA Isolation Kit	Ambion

3.5 Buffers, solutions and media

Table 1. Buffers for genomic DNA Isolation

Name	Ingredients
Lysis buffer	100 mM Tris-HCl pH 8.5, 5 mM EDTA pH 8.0, 200 mM NaCl 0.2 % SDS including 200 µg/ml ProteinaseK

Table 2. Buffer and Gel for DNA / RNA electrophoresis

Name	Ingredients
1x TAE Running buffer	0.4M Tris, 0.01M EDTA-NaOH , 0.2M acetic acid
Electrophoresis gel	200 ml TAE buffer (1 x), 0.7-3% agarose, 3 µl EtBr
Blue Juice DNA sample buffer	30 % (v/v) Glycerol, in 1x TAE, 1-2 grains Bromophenol Blue, 1-2 grains Xylene Cyanol

Table 3. Buffers and Gels for Western blot analysis

Name	Ingredients
1 x RIPA buffer	50 mM Tris pH 7.4, 150 mM NaCl, 1 mM EDTA, 1% NP-40
4 x Protein sample buffer	100 mM Tris-HCl pH 8.0, 4% SDS, 0.2% Bromophenol blue, 20% Glycerol
Buffer A	10 mM Hepes, pH 7.9, 10 mM KCl, 0.1 mM EDTA, 0.1 mM EGTA
Buffer C	20 mM Hepes, pH 7.9, 400 mM NaCl, 1 mM EDTA, 1 mM EGTA
Stripping buffer	0.15 M glycine pH 2.5, 0.4% SDS
SDS running buffer (1x)	2.5 mM Tris, 19.2 mM Glycine, 0.01% (w/v) SDS

Materials

Separating buffer (4x)	1.5 M Tris, 0.4% SDS, adjusted to pH 8.8 with HCl
Separating gel (8-12.5%)	(10%): 2.5 ml 30% Acrylamide / Bis, 2.5 ml Separating Buffer (4 x), 5 ml water, 100 µl APS (10%), 10 µl TEMED
Stacking buffer (4x)	0.5 M Tris, 0.4% SDS, adjusted to pH 6.8 with HCl
Stacking gel (4%)	1 ml 30% Acrylamide / Bis, 2.5 ml Stacking Buffer (4 x), 6.5 ml water, 100 µl APS (10%), 10 µl TEMED
Transfer buffer (1x)	2.5 mM Tris pH 8.3, 19.2 mM Glycine, 20% (v/v) Methanol
TBS (1x)	50 mM Tris.HCl, pH 7.4 and 150 mM NaCl.
TBST	1 x TBS including 0.05% (v/v) Tween 20
Blocking Solution	5% powdered milk in TBST
ECL reagent solution A	2.5 mM Luminol, 0.4 mM p-coumaric acid, 0.1 M Tris-HCl pH 8,5
ECL reagent solution B	0.05% (v/v) 35% H ₂ O ₂ , 0.1 M Tris-HCl pH 8,5
ECL detection solution	1 part ECL reagent solution A, 1 part ECL reagent solution B

Table 4. Stock solutions for *in vivo* studies

Name	Ingredients
Tamoxifen stock solution	4% PFA in 1 x PBS, adjusted to pH 7.4 with NaOH
BrdU Solution	10mg/ml in sterile 1x PBS

Table 5. Buffers and solutions for tissue processing

Name	Ingredients
4% paraformaldehyde	4% PFA in 1 x PBS, adjusted to pH 7.4 with NaOH
Carmine Alum Solution	1g carmine natural red, 2.5g aluminium potassium sulphate, 500 ml dH ₂ O
Antigene retrieval buffer	10 mM Tris, 1mM EDTA, pH 9.0
IHC Blocking Buffer	10% <u>rabbit</u> serum, 1% BSA in 1x PBS
AB buffer	0.1% Tween, 10 % horse serum in 1x PBS
PBS (1x)	137 mM NaCl, 2.7 mM KCl, 4.3 mM Na ₂ HPO ₄ , 1.47 mM KH ₂ PO ₄
PBST	1 x PBS, 0.05% Tween
Blocking Solution for immunofluorescent staining on cells	0.5% Triton X-100; 0.5% BSA in 1 x PBS

Table 6. Media, buffers and solutions for cell culture

Name	Ingredients
Dexamethasone stock solution	For 20 µg/ml: 1 mg Dexamethasone was solved in 1 ml 100% EtOH, filled up with 49 ml sterile medium while mixing. Stored at -20 °C.
Nicotinamide stock solution (10 x)	1M in sterile 1x PBS, stored at -20 °C
Isolation and culture medium for primary mouse mammary cells	DMEM/F12 medium with GlutaMAX™ I supplemented with: 5% FBS, 20ng/ml mEGF, 5 µg/ml Insulin, 10 ng/ml Dexamethasone, 10 mM Nicotinamide, 1x MEM Non-Essential Aminoacids, 1x Insulin-Transferrin-Selenium, 1% Pen/Strep

Culture medium for functional assays on primary mouse mammary cells	DMEM/F12 medium with GlutaMAX™ I supplemented with: 5% FBS, 20ng/ml mEGF, 5 µg/ml Insulin, 1% Pen/Strep
Collagenase/Hyaluronidase Cocktail Working Solution (1 x)	1x Collagenase/Hyaluronidase Cocktail in culture medium for primary mammary cells
Dispase Stock Solution (10 x)	20 mg/ml in sterile 1x PBS, stored at -20 °C
Dispase Working Solution (1 x)	2 mg/ml Dispase
DMEM culture medium	DMEM supplemented with 10% FCS, 1% Penicillin/Streptavidin
DMEM transfection medium	DMEM supplemented with 10% FCS
RPMI culture medium	RPMI supplemented with 10% FCS, 1% Penicillin/Streptavidin
Medium for cryopreservation of cells	Culture medium containing 20% FBS and 10% DMSO

Table 7. Solution for MTT Assay

Name	Ingredients
MTT stock solution	5 mg/ml in 1x PBS
MTT solvent	33% DMSO, 5% formic acid, 62% Isopropanol

Table 8 GREEN PCR Master Mix

Name	Ingredients
GREEN PCR Master Mix	75 mM Tris-HCl pH 8.8, 20 mM (NH ₄) ₂ SO ₄ , 0.01% Tween-20, 3 mM MgCl ₂ , 0.2 mM dNTP's, 20 U/ml HOT FIREPol DNA Polymerase, 0.25% TritonX-100, 500 mM D(+)-Trehalose Dihydrat, Cybr Green was added to a final dilution of 1:80000

3.6 Antibodies

Table 9. Antibodies for Western Blot

Antibody	Source	Dilution	Product No.	Manufacturer
Anti-Flag-HRP	mouse	1:500	A8592	Sigma
anti-BCL9-2	rabbit	1:100	Self-made	(93)
anti-β-catenin	rabbit	1:1000	Self-made	(93)
anti-ERα	rabbit	1:300	sc-7207	Santa Cruz
anti-Pygopus2	rabbit	1:1000	Self-made	(93)
anti-α-tubulin	mouse	1:10000	T9026	Sigma
anti-LaminB1	goat	1:100	sc-6216	Santa Cruz
anti-goat IgG HRP	rabbit	1:10000	705-035-147	Jackson Immuno-research
anti-rabbit IgG HRP	goat	1:10000	111-035-144	Jackson Immuno-research
anti-mouse IgG HRP	goat	1:10000	115-035-062	Jackson Immuno-research

Table 10. Antibodies for immunofluorescent staining on cells and tissue

Antibody	Source	Dilution / Amount	Product No.	Manufacturer
anti-BCL9-2	rabbit	1:100	Self-made	(93)
anti-β-catenin	rabbit	1:1000	Self-made	(93)
anti-ERα	rabbit	1:300	sc-7207	Santa Cruz
anti-panCK	mouse	1:300	C2562	Sigma
anti-E-cadherin	mouse	1:100	610 182	BD
anti-αSMA	rabbit	1:1500	A2547	Sigma
anti-K18	mouse	1:300	C8541	Sigma
anti-PR	rabbit	1:250	sc-539	Santa Cruz
anti-rabbit IgG Cy2	donkey	1:500	711-226-152	Jackson Immuno- noresearch
anti-rabbit IgG Cy3	donkey	1:1000	711-166-152	Jackson Immuno- noresearch
anti-mouse IgG Cy2	donkey	1:500	715-226-150	Jackson Immuno- noresearch
anti-rabbit IgG Cy3	donkey	1:1000	715-166-150	Jackson Immuno- noresearch

Table 11. Antibodies for immunohistochemistry

Antibody	Source	Dilution	Product No.	Manufacturer
anti-BCL9-2	rabbit	1:400	Self-made	(93)
anti-β-catenin	rabbit	1:1000	Self-made	(93)
anti-ERα	rabbit	1:300	sc-7207	Santa Cruz
anti-panCK	mouse	1:300	C2562	Sigma
anti-E-cadherin	mouse	1:100	610 182	DB
anti-αSMA	rabbit	1:1500	A2547	Sigma
anti-K19	rabbit	1:250	ab154631	Abcam
anti-PR	rabbit	1:250	sc-539	Santa Cruz
anti-BrdU	rat	1:100	ab6326	Abcam
anti-Cleaved caspase 3	rabbit	1:50	9661L	Cell Signaling Technology
anti-rat biotin IgG	Goat	1:100	B7139	Sigma

3.7 Small interfering RNAs

Small interfering RNAs (siRNAs) were obtained from Thermo Scientific.

Table 12. Small interfering RNA used for transient transfection

siRNA Name	Target Sequence (5'-3')
ON-TARGETplus Non-targeting Pool	Negative control siRNA with at least 4 mismatches to any human, mouse, or rat gene
ON-TARGETplus BCL9-2 (pool)	5'-GAA AGC CUC CCU CGC AGU U-3' 5'-AAC CAG AUC UCG CCU AGC A-3'

3.8 Primers for quantitative RT-PCR and conventional PCR

Table 13. Primer sequences used for qRT-PCR

Name	Sequence (5'-3')
hBCL9-2 sense	5'-AAT CAT GGC AAG ACA GGG AAT GGC T-3'
hBCL9-2 antisense	5'-TCT TCA GAC TTG AGT TGC TAG GCG-3'
*ESR1 sense	5'-GCA TTC TAC AGG CCA AAT TCA-3'
*ESR1 antisense	5'-TCC TTG GCA GAT TCC ATA GC-3'
*PGR sense	5'-TCC ACC CCG GTC GCT GTA GG-3'
*PGR antisense	5'-TAG AGC GGG CGG CTG GAA GT-3'
**GREB1 sense	5'-GTG GTA GCC GAG TGG ACA AT-3'
**GREB1 antisense	5'-ATT TGT TTC CAG CCC TCC TT-3'
h β -actin sense	5'-ATA GCA CAG CCT GGA TAG CAA CGT AC-3'
h β -actin antisense	5'-CAC CTT CTA CAA TGA GCT GCG TGT G-3'

* Sequences were kindly provided by Prof. Dr. Steven Johnsen, Dept. of Molecular Oncology, Georg August University Göttingen, Germany

** Primer sequences published by Kininis et al.,2009

Table 14. Primer sequences for conventional PCR

Name	Sequence (5'-3')
MIN-sense-1 primer (wildtype)	5'-GCC ATC CCT TCA CGT TAG-3'
MIN-sense-2 primer (mutation specific)	5'-TTC TGA GAA AGA CAG AAG TTA-3'
MIN-antisense primer	5'-TTC CAC TTT GGC ATA AGG C-3'
β -cat fwd (662) primer	5'-ACT GCC TTT GTT CTC TTC CCT TCT G-3'

β -cat-rev (803) primer	5'-CAG CCA AGG AGA GCA GGT GAG G-3'
mBCL9-2-intron-TG-sense primer	5'-CTG GTC ATC ATC CTG CCT TT-3'
mBCL9-2-exon1-sense primer	5'-TCC TGG CTA ACA AGA CAA GG-3'
mBCL9-2-exon2-antisense primer	5'-CTC TGA ATC GAG GGA TGG AG-3'
Flag-tag-sense primer	5'- CAA GGA CGA CGA CGA CAA GG-3'
MMTV-CRE-fwd33 primer	5'- CAA TTT ACT GAC CGT ACA C-3'
MMTV-CRE-rev1058n primer	5'- TAA TCG CCA TCT TCC AGC AG-3'

3.9 Human cell lines, mouse strains

Human cell lines MCF7, T47D, MDA-MB-231, BT549, MCF10A and HEK 293 cells were purchased from ATCC. SB-BR-3 was kindly provided by Dr. med. Tobias Pukrop (Dept. Hematology/Oncology, University Medicine Göttingen, Germany).

Table 15. Description of utilized human cell lines

Cell Line	Description
MCF7	Breast adenocarcinoma cell line, derived from pleural effusion of a 69-year old Caucasian woman. The MCF-7 line retains several characteristics of differentiated mammary epithelium. The cells express the wildtype and variant estrogen receptors as well as progesterone receptor.
T47D	Breast carcinoma cells were isolated from a pleural effusion obtained from a 54 year old female patient with an infiltrating ductal carcinoma of the breast (101). The cells express estrogen and progesterone recep-

	tors.
MDA-MB-231	Breast adenocarcinoma cell line, derived from pleural effusion of a 51-year old Caucasian woman. The cells are estrogen and progesterone receptor and HER2 negative.
BT549	The cell line was isolated from a papillary, invasive ductal breast carcinoma from a 72 year old female patient. The cells are estrogen and progesterone receptor and HER2 negative.
SK-BR-3	Breast adenocarcinoma cell line, derived from pleural effusion of a 43-year old Caucasian woman. The cell line overexpresses HER2.
MCF10A	Adherent epithelial cells isolated from a 36-year old Caucasian female patient suffering from a fibrocystic disease of the breast
HEK 293	Human embryonic kidney cell line with epithelial properties. For immortalization the cells were transformed with adenovirus 5 DNA.

Table 16. Description of utilized mouse strain

Mouse strain	Characteristics	Origin
APC ^{Min/+}	This mouse strain was established from an ethylnitrosourea-treated C57BL/6J (B6) male mouse. The single point mutation causes APC loss-of-function mutant allele and is inheritable. Young adult Min mice develop numerous adenomas throughout their intestinal tract.	Jackson Laboratories, Sulzfeld, Germany (102)
Δ N β -catenin	Transgenic mice carry a transgenic construct, in which exon 3 of mouse β -catenin gene is located between two <i>loxP</i> sites. A conditional deletion of exon 3	(103)

	induced by a Cre recombinase results in a stabilized mutant β -catenin protein.	
K5-CreER ^{T/+}	The tissue and cell specific regulation of Cre expression is controlled by keratin 5 (K5) promoter. For temporal control of the Cre recombinase, the recombinase sequence is fused with the mutated hormone-binding domain of the estrogen receptor (ERT). This can be activated by the synthetic estrogen analog tamoxifen or 4-OHT, but not by the physiological ligand 17 β -estradiol.	The mice were provided by Prof. Dr. Heidi Hahn, Institute of Human Genetics, University of Göttingen, Göttingen, Germany. (104)
K19-BCL9-2	In this transgenic model BCL9-2 is over-expressed under the promoter of the mouse keratin-19 (K19) gene. The expression of the transgene is found in tissue containing simple epithelia, including mammary gland, stomach, intestine, pancreas.	(93)
MMTV-Cre	The transgenic mice express Cre recombinase under the control of the MMTV LTR promoter. The MMTV LTR promoter directs the expression of the Cre recombinase in the virgin and lactating mammary gland, salivary gland, seminal vesicle, skin, erythrocytes, B and T cells.	(105)

3.10 Human Tissue Array

Paraffin-embedded human breast cancer tissues were purchased from Pantomics, Inc, Richmond, USA and US Biomax, Inc, Rockville, USA. The arrays included TNM classification, pathology grade and ER, PR and HER2 immunohistochemistry data.

Table 17. Description of utilized tissue arrays

Code of the tissue array	Description	Manufacture
BRC481	Breast cancer tissue array, containing 16 invasive ductal carcinoma samples with duplicate cores per case and 16 matched normal breast tissue from each patient	Pantomics, Inc
BRC482	Breast cancer tissue array, containing 16 invasive ductal carcinoma samples with duplicate cores per case and 16 matched normal breast tissue from each patient	Pantomics, Inc
BR1503a	Breast cancer tissue array, containing 3 cases of normal tissue, 7 intraductal carcinoma and 60 invasive ductal carcinoma with duplicate cores per case	US Biomax, Inc

4. Methods

4.1 In vivo experiments

4.1.1 Generation of K19-BCL9-2 transgenic mice

To analyze the oncogenic potential of BCL9-2 *in vivo*, a transgenic mouse model was established (93). BCL9-2 transgenic vector was generated by linking a 2,1 kb genomic fragment containing the 5' UTR and promoter region of the mouse keratin 19 (K19) gene (106), rabbit β -globin intron sequence. This construct was fused to the flag-tagged cDNA of the mouse BCL9-2 and the BGH-polyA (Figure 4A). Five different founder lines were established on a pure C57BL/6N background. For the transgene integration, a Southern Blot was performed. For this, 40 μ g of tail genomic DNA was digested with *Bgl*II (Figure 4). Genotyping of K19-BCL9-2 transgenic offspring was performed by standard PCR using specific primer for the BCL9-2 transgene (Table 14).

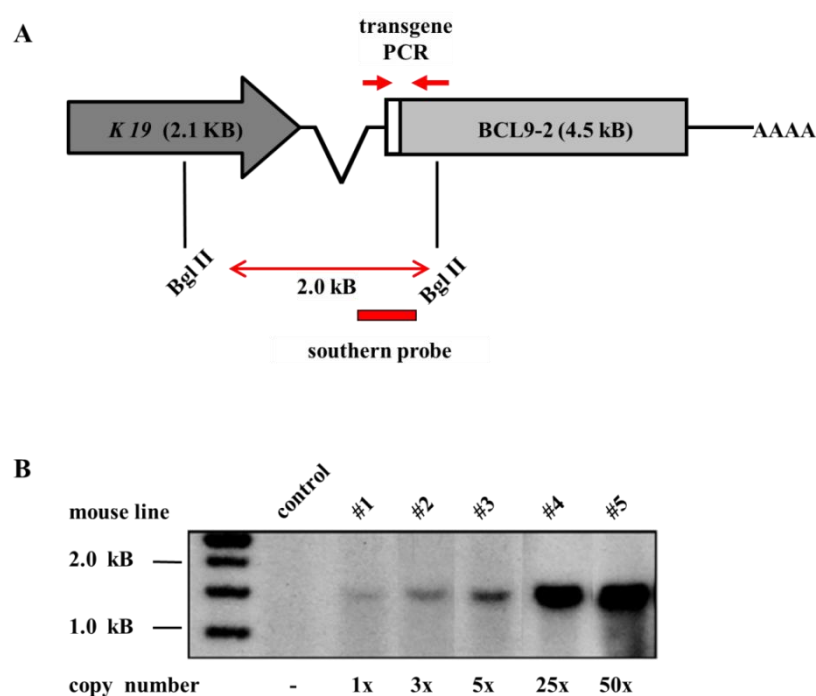


Figure 4. Overexpression of BCL9-2 under control of the K19 promoter in C57BL/6 mice.

(A) Schematic view of the transgene construct for overexpression of BCL9-2 under control of a K19 promoter. The sites for probing of DNA integration by Southern blotting and for the transgene-specific PCR primers are indicated. (B) Identification of K19-BCL9-2 founder lines with different copy numbers by Southern blot analyses.

4.1.2 Generation of compound APC^{Min/+}; K19-BCL9-2, MMTV^{Cre}; Catnb^{+/ Δ ex3}; K19-BCL9-2 and K5-CreER^{T/+}; Catnb^{+/ Δ ex3}; K19-BCL9-2 females

To determine, if transgenic BCL9-2 expression may enhance or modulate mammary tumor formation in other mouse models, K19-BCL9-2 mice were bred with APC^{Min/+}; MMTV^{Cre}; Catnb^{+/ Δ ex3} and K5-CreER^{T/+}; Catnb^{+/ Δ ex3} animals.

The APC^{Min/+}; K19-BCL9-2 females were followed up to 9 months and were sacrificed as they started to suffer from intestinal adenoma.

The MMTV^{Cre}; Catnb^{+/ Δ ex3}; K19-BCL9-2 females were followed up to 10 months and were sacrificed as they started to suffer from skin defects.

The K5-CreER^{T/+}; Catnb^{+/ Δ ex3}; K19-BCL9-2 females were followed up to 4 months and were sacrificed as they started to suffer from skin defects.

4.1.3 Induction of K5-CreER^{T/+} expression by tamoxifen

For the induction of Cre recombinase, the K5-CreER^{T/+}; Catnb^{+/ Δ ex3} females and K5-CreER^{T/+}; Catnb^{+/ Δ ex3}; K19-BCL9-2 females were IP treated with tamoxifen. Prior the injection, 100 mg tamoxifen were dissolved in 1 ml 100% EtOH following a dilution in sun flower oil to 10 mg/ml (Table 4). 1mg tamoxifen per 20 g animal weight was administrated.

4.1.4 BrdU incorporation

To label the proliferating cells *in vivo*, 100 μ g/g of body weight of pre-warmed (37°C) BrdU (Table 4) were administrated by IP (intraperitoneal) injection 2 h prior to necropsy.

4.2 Isolation of genomic DNA (gDNA)

For genotyping, total DNA was isolated from mouse tail tissues. A small piece of tail from 20 days-old mice was incubated overnight at 55°C on a shaker with 50-100 μ l lysis buffer containing fresh Proteinase K (Table 1) After 1:10 dilution with H₂O the

genomic DNA was boiled for 10 min at 95°C, centrifuged for 2 min at maximum speed and the supernatant was used for genotyping PCR analysis.

4.3 Genotyping PCR analyses

Following primers and cycler conditions were used for genotyping PCR to detect different integrated transgenes and APC Min mutation. PCR analyses were performed using 1x Taq buffer without MgCl₂, 0.6 units FastTaq DNA Polymerase, 0.5 µM primer each (Table 14), 0.2 mM dNTPs each, 1.5-2.5 mM MgCl₂ and 1 µl gDNA in a final volume of 15 µl per reaction. Genomic DNA of an appropriate tested transgenic mouse was used as positive and H₂O as a negative control. Separation of DNA fragments occurred in 1-2% agarose gel by electrophoresis.

Table 18. Cycler conditions and PCR product sizes for genotyping PCR

Genotyping of	Cycler conditions	PCR products
APC ^{Min/+}	10 min 95°C; [30 s 95°C; 30 s 54°C; 60 s 72°C] 35 x; 10 min 72°C; ∞ 4°C	wildtype: 619 bp; mutant: 331 bp
ΔNβ-catenin	10 min 95°C; [30 s 95°C; 30 s 62°C; 45 s 72°C] 35 x; 10 min 72°C; ∞ 4°C	wildtype: 140 bp; lox/+ mutant: 140 bp, 190 bp; lox/lox mutant: 190 bp
K19-BCL9-2	10 min 95°C; [30 s 95°C; 30 s 60°C; 150 s 72°C] 35 x; 10 min 72°C; ∞ 4°C	wildtype: 1593 bp; transgene: 400-500 bp
MMTV-Cre, K5-CreER ^{T/+}	10 min 95°C; [30 s 95°C; 30 s 58°C; 60 s 72°C] 35 x; 10 min 72°C; ∞ 4°C	transgene: 200-300 bp

4.4 Isolation of total RNA using TRI Reagent

Isolation of RNA from fresh/frozen mouse tissue was done using TRI Reagent RNA Isolation Kit according to manufacturer's instructions (Ambion Manual Version 0610). Briefly, fresh/frozen tissue was homogenized in an appropriate volume of TRI Reagent and incubated for 5 min at RT. After addition of 100 µl chloroform per 0.5 ml TRI Reagent, probes were vigorously vortexed for 15 s, incubated 10 min at RT and centrifuged at 10500 rpm for 15 min (4°C). The aqueous RNA phase was

transferred into a new reaction tube and RNA was precipitated by adding 250 μ l isopropanol per 0.5 ml TRI Reagent. Samples were shaken well, incubated 10 min at RT and again centrifuged at 10500 rpm for 10 min (4°C). The RNA pellet was washed with 0.5 ml 70% ethanol and centrifuged at 8000 rpm for 10 min (4°C). After removal of ethanol the pellet was air-dried for 2-5 min and dissolved in 20-100 μ l DEPC-dH₂O. RNA concentration was determined photometrically at 260 nm and RNA was stored at – 80°C.

4.5 Detection of BCL9-2 transcripts by PCR

To examine transgenic expression of BCL9-2, isolated RNA was treated with DNase I and reverse transcribed into complementary DNA (cDNA) using MMLV reverse transcriptase and random hexamer primers. To digest residual gDNA 20 μ g of total RNA was incubated for 90 min at 37°C with 2.5 μ l 10x DNase buffer, 1.25 μ l 20mM DTT, 0.5 μ l RNase Out and 0.2 μ l RNase-free DNase I at a final volume of 25 μ l. Subsequently, additional 0.2 μ l RNase-free DNase I was added for further 60 min at 37°C and diluted with nuclease-free H₂O to a final volume of 100 μ l. After phenol:chloroform extraction to precipitate the RNA, 7-10 μ g RNA was incubated with 0.3 μ g random hexamer primers (final volume 35 μ l) for 5 min at 65°C and cooled on ice, rapidly. While 5 μ l of the sample was saved to measure residual gDNA contamination, 30 μ l of the sample was mixed with 12 μ l 5x MMLV RT buffer, 3 μ l 20 mM DTT, 1.5 μ l RNase Out, 3 μ l 10 mM dNTPs and 0.75 μ l reverse transcriptase at a final volume of 60 μ l. After incubation at 42°C for 90 min and addition of 60 μ l nuclease-free H₂O, the reverse transcribed cDNA was immediately used for PCR or stored at -20°C.

For the detection of the transgenic BCL9-2, specific flag tag primer and the mBCL9-2-exon2-antisense primers were used (Table 14). To amplify β -actin gene transcripts human β -actin primers were used (Table 13). PCR was performed using 1x Taq buffer without MgCl₂, 0.6 units FastTaq DNA Polymerase, 0.2 μ M primer each, 0.2 mM dNTPs each, 2.5 mM MgCl₂ and 10 μ l cDNA in a final volume of 15 μ l per reaction. H₂O was used as negative control. Separation of PCR products occurred in 1% agarose gel by electrophoresis.

Table 19. Cyclor conditions and PCR product sizes to detect β -actin and transgenic BCL9-2 transcripts

Detection of	Cycler conditions	PCR products
TG BCL9-2	10 min 95°C; [30 s 95°C; 30 s 60°C; 150 s 72°C] 35 x; 10 min 72°C; ∞ 4°C	500 bp
β -actin	10 min 95°C; [30 s 95°C; 30 s 60°C; 30 s 72°C] 30 x; 10 min 72°C; ∞ 4°C	400 bp

4.6 Carmine whole mount staining

Carmine whole mount staining of the mammary glands were performed to identify neoplastic changes of breast tissues derived from different founder lines of transgenic mice. The breast tissue was fixed overnight at 4°C in fresh cold 4% PFA. Subsequently, the tissue was washed in dH₂O and stained with carmine alum staining solution (Table 5) for at least 3 h at RT dependent on size of the gland and amount of fatty tissue. After washing in dH₂O, the tissue was dehydrated in 70%, 95% and 100% EtOH (2 x 15 min incubation each) and cleared in Xylol for at least 2 x 60 min. For imaging the fixed and stained tissue was pressed between two glass slides to flatten and mounted on slides.

4.7 Tissue processing for immunohistochemistry

Tissue samples of transgenic and control mice were fixed in 4% paraformaldehyde at 4°C overnight, then washed with cold 1x PBS and transferred into 70% ethanol for long-term storage. For dehydration and paraffinisation the tissue samples were incubated in 75% EtOH, 80% EtOH, 90% EtOH, 96% EtOH, 2 x 100% EtOH for 1.5 h each, followed by incubation in Xylol 2 x 1.5 h as well as 1.5 h and up to 12 h in a Paraffin-series. Tissue samples were cut into 3 μ m-thick sections and stored at RT.

4.8 Histological staining on tissues

4.8.1 Hematoxylin and Eosin staining (H&E)

For a histological overview staining, the 3 µm-thick paraffin sections were then stained with (H&E). To dewax and rehydrate, the tissue sections were incubated in Xylol (3 x 5 min), EtOH (100%, 96%, 80% and 70% for 3 min each step) and then washed in dH₂O. The samples were incubated in Hematoxylin (2 min), rinsed with dH₂O (5-10 min) and then incubated in Eosin for additional 2 min. For imaging, stained sections were dehydrated in a rising EtOH-series (70% 10 sec, 80% 10 sec, 96% 3 min and 100% 2 x 3 min) and Xylol (3 x 3 min) and then mounted with Roti[®]-Histokitt.

4.8.2 Immunohistochemistry

To detect protein expression, corresponding specific antibodies (Table 11) and the indirect immunoperoxidase staining were used. The paraffin sections were rehydrated by incubation in Xylol (3 x 5 min), EtOH (100%, 96%, 80% and 70% for 3 min each step) and then washed in dH₂O. Following rehydration, the antigene retrieval was performed by boiling the samples in preheated Antigene retrieval buffer (Table 5) for 20 min. The samples were cooled down in a cold water bath to RT. To block endogenous peroxidase the sections were incubated for 10 min (RT) with 1% H₂O₂ and then washed once in dH₂O (5 min) and twice in 1 x PBS (5 min each). After blocking for 30 min (RT) in IHC blocking solution (Table 5) the sections were incubated overnight (4°C) with the specific primary antibody (diluted in IHC blocking solution) in a humidified atmosphere. After washing (3 x 5 min in 1 x PBS) the samples were incubated for 30-45 min (RT, humidified atmosphere) with the secondary HRP-conjugated antibody (Dako EnVision Kit) and then washed again in 1 x PBS (3 x 5 min). Antibody-antigen complexes were detected according to manufacturer's protocol and counterstaining was performed with Hematoxylin (10 sec incubation with Hematoxylin, 5-10 min rinsed in dH₂O). For imaging, stained sections were dehydrated in a rising EtOH-series (70% 10 sec, 80% 10 sec, 96% 3 min and 100% 2 x 3 min) and Xylol (3 x 3 min) and then mounted with Roti[®]-Histokitt.

4.8.3 Immunohistochemical detection of *in vivo* BrdU labeled cells

To detect BrdU labeled cells, corresponding specific antibody (Table 11) and the indirect immunoperoxidase staining were used. The paraffin sections were treated as described in 3.8.2 including the primary antibody incubation. After the labeling the tissues with the anti-BrdU primary antibody, the sections were incubated with biotin-conjugated secondary antibody (diluted in IHC blocking solution) for 60 min at RT, washed 3x in 1x PBS. The HRP addition was performed by incubation of the sections for further 30 min with streptavidin-biotinylated HRP (diluted in IHC blocking solution) at RT. Antibody-antigen complexes were detected using Gold and Silver tablets (1 Gold and 1 Silver tablet per 1 ml dH₂O) and counterstaining was performed with Hematoxylin (10 sec incubation with Hematoxylin, 5-10 min rinsed in dH₂O). For imaging, stained sections were dehydrated in a rising EtOH-series (70% 10 sec, 80% 10 sec, 96% 3 min and 100% 2 x 3 min) and Xylol (3 x 3 min) and then mounted with Roti[®]-Histokitt.

4.8.4 Immunofluorescent staining on paraffin embedded tissues

To detect protein expression, corresponding specific antibodies (Table 10) and the indirect fluorescent staining were used. The paraffin sections were rehydrated by incubation in Xylol (3 x 5 min), EtOH (100%, 96%, 80% and 70% for 3 min each step) and then washed in dH₂O. Following rehydration, the antigene retrieval was performed by boiling the samples in preheated Antigene retrieval buffer (Table 5) for 20 min. The samples were cooled down in a cold water bath to RT. After 30 min (RT) blocking of sections in AB buffer (Table 5), the sections were incubated overnight (4°C) with the specific primary antibody (diluted in blocking solution) in a humidified atmosphere. After washing (3 x 20 min in PBST) the samples were incubated for 30-45 min (RT, humidified atmosphere) with the secondary fluorofore-conjugated antibody (diluted in AB buffer) and then washed again in PBST (3 x 20 min). The counterstaining with DAPI was performed in the pre-last washing step by diluting DAPI stock solution to 0.1 µg/ml in PBST. For microscopy the sections were mounted in Immu-Mount and stored at 4°C in the dark.

4.9 Scoring

For the quantification of the BCL9-2, nuclear ER α and PR expression in mouse and human breast cancer tissues, an expression score was applied. The same expression score we already used to evaluate the immunohistochemical expression of nuclear BCL9-2 in human colon cancers (93). The percentage of positive epithelial cells was scored as follows: 0 (0%), 1 (<30%), 2 (30%–60%), and 3 (>60%). The staining intensity was classified as 0 (negative), 1 (low), 2 (moderate), and 3 (strong). The immunoreactive score (0 to 9) was calculated by multiplication of the scores of positive cells and staining intensity. Stainings were scored by 3 independent investigators. The histopathology of the mouse tumor samples was also assessed by a pathologist (Dr. med. Christina Perske, Department of Pathology; UMG).

For the quantification of the early neoplastic changes, a score was developed, that evaluated the severity of the preneoplastic changes and the amount of involved tissue in the mammary gland. The definition of severity and amount of involved tissue is described in (Table 20). The score (0 to 9) was calculated by multiplication of the scores of severity of the preneoplastic changes and amount of involved tissue.

Table 20. Definition of severity of preneoplastic changes and amount of involved mammary tissue

Score for severity of the preneoplastic changes and amount of involved tissue	Definition of severity			Definition of amount of involved tissue
	Ductal dilatation	Hyperplastic Alveolar Nodules (HANs)	Alveolar morphology	
0	no dilatation	no HANs	no alveolar morphology	0%
1	moderate	<0,5 mm on average	moderate	<30%
2	strong	0,5-0,75 mm on average	strong	30%–60%

3	severe	> 0,75 mm on average	severe	>60%
---	--------	----------------------	--------	------

4.10 Primary culture of mouse tumor cells

4.10.1 Isolation of primary cells from K19-BCL9-2 and non-transgenic control animals

Primary cultures of mammary tumors and from hyperplastic glands obtained from aged K19-BCL9-2 females have been established as follows. Mammary gland tissue/tumor tissue were isolated, washed in cold 1 x PBS and transferred into ice-cold tumor isolation medium (Table 6) until digestion. For digestion, the medium was removed, the tissue was chopped with scissors and then resuspended in Collagenase/Hyaluronidase-Solution (Table 6) with 10 ml per 1 g tissue. After lysis (1.5 hours at 37°C in a tissue incubator) the cells were centrifuged at 1000 rpm for 5 min and the pellet was resuspended in dispase solution (Table 6) with 10 ml per 1 g tissue and incubated for another hour at 37°C in a tissue incubator. The digest was filtered through a 40 µm BD Falcon Cell Strainer, centrifuged at 1200 rpm for 5 min and washed twice with tumor medium. The strained primary cells were cultured in DMEM/F12 medium with supplements (Table 6) at 37°C (5% CO₂) in a humidified atmosphere or cryopreserved at -150°C (see 4.10.2).

4.10.2 Cultivation of primary cells from K19-BCL9-2 and non-transgenic control animals

When cells grew to confluence (every 3-4 days) the medium was removed and cells were split 1:2. To detach the tumor cells they were washed once with 1 x PBS and incubated 5 min with 2 ml of 1 x trypsin at 37°C (5% CO₂). Detached cells were resuspended in fresh culture medium, centrifuged at 1200 rpm for 7 min and spread in new culture flasks. Dependent on tumor cell line concentrations between 1 x 10⁶ and 1 x 10⁷ cells per 1 ml culture medium/ 20% FBS / 10% DMSO were frozen at -150°C. After resuspension of cell pellets in an appropriate volume of medium for cryopreservation (Table 6), 1 ml aliquots of the cell suspension were transferred into pre-cooled cryovials. The cryovials were placed into controlled freezing boxes, stored 12-18 h at -80°C and were then transferred to -150°C for long-term storage.

To re-culture the cryopreserved cells, cryovials were thawed at 37°C in the water bath until only small ice crystals were seen floating inside the cryovial. The content of a vial was rapidly transferred into a 50 ml Falcon tube containing 20 ml of fresh culture medium. Cells were pelletized by centrifugation at 1200 rpm for 7 min, re-suspended in pre-warmed culture medium and transferred into culture flask. Cell amounts were determined using Neubauer hemocytometer.

4.11 MTT assay

To analyze cell vitality by MTT assay, 5×10^3 primary cells were seeded in triplicates at a final volume of 100 µl Optimem (for starvation) into 96-well plates. After incubation overnight at 37°C (5% CO₂) in a humidified atmosphere, cells were treated with 3.6 µM tamoxifen or estrogen for 24 h, 48 h or 72 h in the culture medium for functional assays (Table 6). The media were changed every 24 h. After appropriate incubation time 10 µl of MTT stock solution (Table 7) was added to the cells/control wells without cells and incubated for 3.5 h at 37°C (5% CO₂) in a humidified atmosphere. The media was carefully removed and primary cells were incubated with 150 µl MTT solvent / well for 15 min at RT (shaker). Absorbance (590 nm) was measured in an ELISA reader.

4.12 BrdU incorporation assay

Cell proliferation was quantified using Cell Proliferation ELISA, BrdU (colorimetric) Kit according to manufacturer's protocol (Roche Instruction Manual 08/2007). Briefly, 5×10^3 primary cells per 96-well were seeded in triplicates at a final volume of 100 µl Optimem (for starvation) and incubated at 37°C (5% CO₂) in a humidified atmosphere. After an overnight starvation, the cells were treated with 3.6 µM tamoxifen or estrogen for 12 h, 24 h, 36 h or 48 h in the culture medium for functional assays (Table 6). BrdU labeling solution was added 12 h prior the defined measurement times (0 h, 12 h, 24 h, 36 h, 48 h after treatment). After appropriate incubation time cells were lysed and incubated with a specific peroxidase conjugated anti-BrdU-antibody to detect incorporated BrdU. Reaction product was quantified by measuring the absorbance (450 nm) using an ELISA reader. The mean value and standard devi-

ation are displayed graphically using Microsoft Excel. Determination of the statistical significance was carried out by using the conventional t-test. The absorbance values directly correlate to the amount of DNA synthesis and hereby to the proliferation rate of cells.

4.13 2D collagen assay

For 2D collagen assay, 96 Well plates were coated with 50 μ l of Collagen matrix (1.5 mg/ml Collagen solution, 2.2 mg/ml NaHCO₃, 5% FCS, 20 mM Hepes in medium for functional assay and dried 30min at 37°C.

1x10³ cells were then suspended in 100 μ l Optimem and the cell were cultured for 7-12 days on top of collagen pad in triplicates at 37°C, 5% CO₂ und 95% humidity in DMEM-F12, 5% FCS, 1%PenStrep.

For immunofluorescent stainings the collagen pads were fixed in cold 4% PFA solution and stained as described in **4.14**.

4.14 Immunofluorescent staining on primary cells

Immunofluorescence analyses of primary cultured cells from K19-BCL9-2 females as well as of non-transgenic mammary cells grown on coverslips and from 2D collagen assay were performed as described here. After fixation of cells with 4% PFA, permeabilization occurred with 0.5% Triton X-100 in 1 x PBS (15 min at RT). The samples were washed twice in 1 x PBS and then blocked for at least 60 min in blocking solution. After washing, the cells were incubated with the appropriate primary antibody for 12-18 hours at 4°C diluted in blocking buffer (Table 10), washed again (3 x 10 min in 1 x PBS) and incubated for 45 min (RT, in the dark) with a secondary fluorophor-conjugated antibody diluted in blocking solution. Nuclei were stained with DAPI (0.1 μ g/ml). The cells were washed with 1 x PBS (3 x 10 min) and then mounted with Immu-Mount for microscopy, dried overnight at RT and stored at 4°C in the dark.

4.15 Cell culture of stable human breast cancer cell lines

Breast cancer cell lines were cultured in DMEM or RPMI culture medium (Table 6) at 37°C (5% CO₂) in a humidified atmosphere. The volume of medium in a middle-sized culture flask (75 cm² adherence surface) was 20 ml and 30 ml in a large-sized flask (175 cm² adherence surface). When cells grew to confluence (every 3-4 days) the medium was removed and cells were split 1:5 to 1:10. To detach the tumor cells they were washed once with 1 x PBS and incubated 5 min with 1 ml and 2 ml 1 x trypsin at 37°C (5% CO₂), respectively. Detached cells were resuspended in fresh culture medium, centrifuged at 1000 rpm for 5 min and spread in new culture flasks or cryopreserved as described in **4.10.2**.

4.16 Transient RNA interference

For transient protein knock down, transfections with short interfering RNA (siRNA) were done using Lipofectamin 2000 Transfection Reagent according to standard procedures for transfection in 6-well plates (Invitrogen Handbook 07/2011). Briefly, 6 x 10⁵ cells were plated into 6-well plate at a final volume of 1.5 ml transfection medium containing (Table 6) incubated overnight at 37 °C (5% CO₂) in a humidified atmosphere. Following the overnight incubation, 500µl Optimem containing 25 nmol/L siRNA and 5 µl Lipofectamin 2000 Transfection Reagent were added to the cells. The transfection medium was replaced by standard culture medium 8 h after transfection and the cells were incubated for further 48 to 72 h at 37 °C (5% CO₂) in a humidified atmosphere. To analyze transient gene knock down compared to siRNA control, RNA and nuclear proteins were isolated and gene expression was examined by quantitative RT-PCR and Western Blot, respectively (see **4.17** and **4.20**).

4.17 Quantitative Real Time PCR (qRT-PCR)

To examine gene expression by quantitative RT-PCR, the cells were resuspended in 1 ml TRI Reagent per 6-well and the RNA were isolated and reverse transcribed into complementary DNA (cDNA) as described in 3.5 without DNase treatment. qRT-PCR with 40 ng complementary DNA was performed with absolute SYBR Green. Gene expression was calculated relative to a standard curve of β-actin.

Quantification of synthesized cDNA by qRT-PCR allows examination of differential gene expression, as the amount of cDNA correspond to the amount of cellular mRNA. qRT-PCR was performed by use of GREEN PCR Master Mix (Table 8) containing SYBR Green I dye, HOT FIREPol DANN Polymerase, PCR buffer and dNTPs. Gene specific primers (0,3 pmol/ μ l) and 2 μ l cDNA template were added to 8 μ l master mix and adjusted to a final volume of 10 μ l with RNase-free water. Gene expression profiles were normalized to the mRNA levels of β -actin and calculated using the 2-ddCt method. The mean value and standard deviation of duplicates are displayed graphically using Microsoft Excel. Fluorescence was measured with an AB 7300 Real-Time PCR System (Applied Biosystems).

4.18 Isolation of whole cell protein lysates for Western blot

For whole cell lysate protein extraction the cells grown in 10 cm plate were washed twice with ice cold 1 x PBS and resuspended in 500 μ l of 1 x RIPA buffer (Table 3) containing Protease Inhibitor Cocktail (1 tablet per 10 ml buffer). The cells were scrapped off, sonicated for 15 sec (4°C), centrifuged for 15 min at maximum speed (4°C) and the protein containing supernatant was transferred to a fresh tube. After photometrical determination of protein concentration by Bradford test, the appropriate protein concentration was adjusted with 1 x extraction buffer and mixed with the required volume of 4 x protein sample buffer. Aliquots of whole protein lysates and nuclear extracts were stored at -20°C or immediately processed for SDS-polyacrylamide gel electrophoresis (SDS-PAGE).

4.19 Isolation of nuclear proteins for Western blot

For nuclear extraction the cells were scrapped off and resuspended in 100 μ l of buffer A (Table 3) containing Protease Inhibitor Cocktail. After incubation for 15 min on ice 10% NP40 (25 μ l per 500 μ l buffer A) was added and the samples were mixed by vortexing for 20 sec and centrifuged for 2 min at 3000 rpm (4°C). The cytoplasmatic fraction (supernatant) was mixed with the required volume of 4 x protein sample buffer, while the nuclear fraction (pellet) was resuspended in 60 μ l ice cold buffer C (Table 3) and incubated for 15 min at 4°C (shaker). After centrifugation for 5 min at

3000 rpm (4°C) the supernatant was mixed with 4 x sample buffer (20 µl 4 x PP / 60 µl nuclear protein lysate). Aliquots of whole protein lysates and nuclear extracts were stored at -20°C or immediately processed for SDS-polyacrylamide gel electrophoresis (SDS-PAGE).

4.20 Western blot analysis

To examine protein expression by Western blot, whole protein lysates or nuclear protein extracts from cultured cells were used.

Dependent on the molecular weight of separating protein 6-12% polyacrylamide gels were used for SDS-PAGE. Protein sample were boiled at 95°C for 5 min, centrifuged for 1 min at maximum speed and then transferred to the gel. Electrophoresis was carried out at 100-120 V for 3-4 h. Molecular weight of the separated proteins was determined by comparison with a pre-stained molecular weight standard. For immunoblot analysis proteins were transferred onto Hybond-P PVDF membranes for 1.4 h at 0.5 A in a wet blot device in the presence of transfer buffer at 4°C. After electroblotting the transferred proteins are bound to the surface of the PVDF membrane, providing access for reaction with immunodetection reagents. Prior protein transfer, the PVDF membranes were incubation in methanol for approximately 30 sec. Unspecific binding sites were blocked by immersing the membrane in blocking solution (Table 3) for 1-4 h at RT or overnight at 4°C. The membrane was then incubated with primary antibody (Table 9) overnight at 4°C. Antibodies were diluted according to the manufacturer's instructions in blocking solution. The membrane was washed 3 x in 1 x TBST, incubated for 45 min with horseradish peroxidase (HRP) coupled secondary antibody and washed 3 x in 1 x TBST. Antibody-antigen complexes were detected using ECL detection solution (Table 3). This detection system is based on the oxidation of a Luminogen by HRP and peroxide, resulting in a chemoluminescent signal detectable by a CCD camera. Signals were detected with the LAS-4000 imaging system. For long-term storage, the membranes were air dried and stored at -20°C. To reactivate dried PVDF membrane, membrane was incubated in methanol (~30 sec), washed once with 1 x TBST and blocked for 1-4 h. For stripping, the membrane was washed 3 x 5 min in TBST and incubated in freshly prepared stripping buffer (Table 3) for 2 x 15 min. The membrane was then washed

briefly in 1 M Tris pH 6.8 and 3 x 5 min in TBST. After blocking for 1 h the membrane was incubated with primary antibodies.

4.21 Statistics

Determination of the statistical significance of data from MTT, BrdU and 2D collagen assays and qRT-PCR was carried out by the conventional t-test using Microsoft Excel. Significances for protein expression scores and scores for preneoplastic changes in the glands of K19-BCL9-2 females were calculated by Mann-Whitney test using SPSS 19.0 software. The correlations were tested by Spearman's analyses using SPSS 19.0 software.

5. Results

5.1 Characterization of K19-BCL9-2 transgenic mouse model

5.1.1 Analysis of the K19-BCL9-2 transgene expression in K19-BCL9-2 mice

To analyze the oncogenic potential of BCL9-2 *in vivo*, a transgenic mouse model was established (93). Transgenic overexpression of BCL9-2 was achieved by linking the cDNA of BCL9-2 with a 2,1 kb genomic fragment containing the 5' UTR and promoter region of the mouse K19 gene and a β -globin intron sequence (see Material and Methods). The expression of K19 is known to be restricted to simple epithelia of several organs including the proliferative compartments of the stomach, small intestine, colon and ductal epithelia of the pancreas and mammary gland (107-109). To identify the expression pattern of the K19-BCL9-2 transgene, RNA from different epithelial tissues of approximately 10 weeks old transgenic and control females were isolated. This was confirmed for 2 founder lines. To demonstrate transgenic expression of BCL9-2, a reverse transcription PCR using a sense primer that specifically binds to the flag tag sequence encoded by the transgene construct was performed.

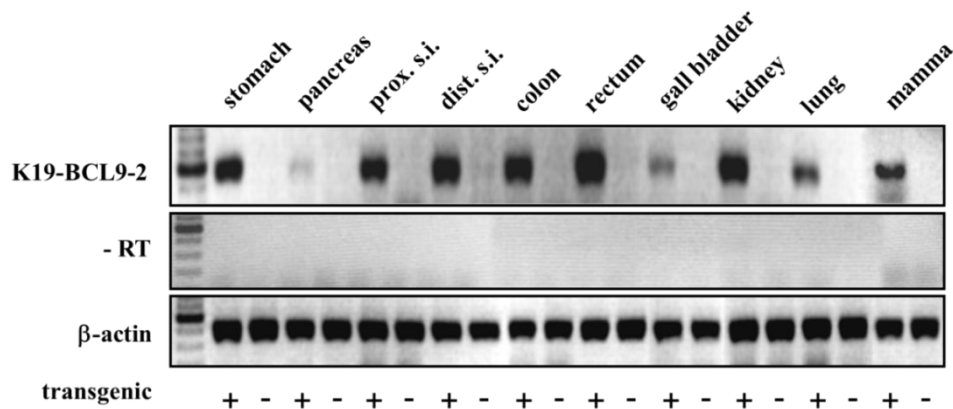


Figure 5. RNA expression of the transgene in different tissues of K19-BCL9-2 mice and non-transgenic littermate controls was analyzed by RT-PCR (93).

Upper panel: 500 ng of cDNA was analyzed using K19-BCL9-2 transgene specific primers. Middle panel: 100 ng RNA samples without reverse transcription were used as control for genomic DNA contamination. Lower panel: 500 ng of cDNA was analyzed using β -actin primer as an internal control.

The expression of the K19-BCL9-2 transgene in transgenic females was detected throughout the gastrointestinal tract (including stomach, small intestine, colon, and rectum), pancreas, liver, kidney and mammary glands. No expression of the K19-BCL9-2 transgene was detected in the respective tissues obtained from control animals (Figure 5).

5.1.2 Phenotype of K19-BCL9-2 transgenic animals

K19-BCL9-2 mice were phenotypically normal at birth. Upon aging (starting at approximately 15 month of age), transgenic mice developed macroscopic tumors of the pancreas, intestine and mammary gland (Figure 6).

The tumor spectrum was similar in all founder lines, however with different incidences for the different founder lines compared to non-transgenic control mice (Table 21, Table 22). In aged control animals, 26% of animals (10 of 39) developed pancreas tumors, whereas the incidence for intestinal tumors was very low ($1/39=3\%$). In contrast, with the exception of one founder line, five of six analyzed founder lines showed higher frequencies of tumors in the pancreas and in the small intestine, ranging from 33 to 55% and 5 to 22% respectively (Table 21).



Figure 6. K19-BCL9-2 mice developed macroscopic tumors of the pancreas (left), small intestine (middle) and breast (right).

In contrast, tumors of the mammary gland were never observed in non-transgenic control mice (Table 22). K19-BCL9-2 transgenic mice developed macroscopic tumors of the breast in 18% of the cases (20 of 109 analyzed animals). The incidence for mammary tumors was not significantly different between all analyzed founder lines. Interestingly, the incidence for breast tumors was higher in parous transgenic females (26%) compared to virgin animals (16%) (Table 22). These tumors developed in transgenic female mice starting at approximately 15 month of age and prog-

Table 21. Frequency of pancreas and small intestine tumors of K19-BCL9-2 animals compared to age-matched non-transgenic littermates.

animals	n	pancreas tumors		si tumors	
		n	%	n	%
ctrl littermates	39	10	26	1	3
transgenics	186	70	38	24	13
# 1	18	9	50	4	22
# 2	22	12	55	4	18
# 3	28	5	18	1	4
# 4	33	12	36	4	12
# 5	21	7	33	1	5
# 6	64	25	39	10	16

ressed very fast within 2 to 4 weeks to large macroscopic tumors. Therefore, the focus of this project was to analyze the mammary gland tumors of K19-BCL9-2 female mice.

Table 22. Frequency of mammary gland tumors of K19-BCL9-2 animals compared to age-matched non-transgenic littermates.

animals	n	breast tumors	
		n	%
ctrl littermates	15	0	0
transgenics	109	20	18
virgins	82	13	16
parous	27	7	26
# 1	18	3	17
# 2	19	4	21
# 3	14	2	14
# 4	25	5	20
# 5	4	1	25
# 6	29	5	17

These findings indicate a relationship between tumorigenesis in K19-BCL9-2 females and overexpression of BCL9-2, pointing to a possible oncogenic potential of BCL9-2.

5.1.3. Characterization of K19-BCL9-2 transgene expression in mammary gland tumors of transgenic females

For the verification of the transgene expression in the breast tumors obtained from transgenic females, RNA from tumor tissues was extracted. To demonstrate transgenic expression of BCL9-2 a reverse transcription PCR using the transgene specific primers was performed. All analyzed mammary gland tumors obtained from the transgenic females showed strong expression of the K19-BCL9-2 transgene. In contrast, mammary gland tumors from $APC^{Min/+}$ that were used here as a negative controls, showed no transgene specific product (Figure 7).

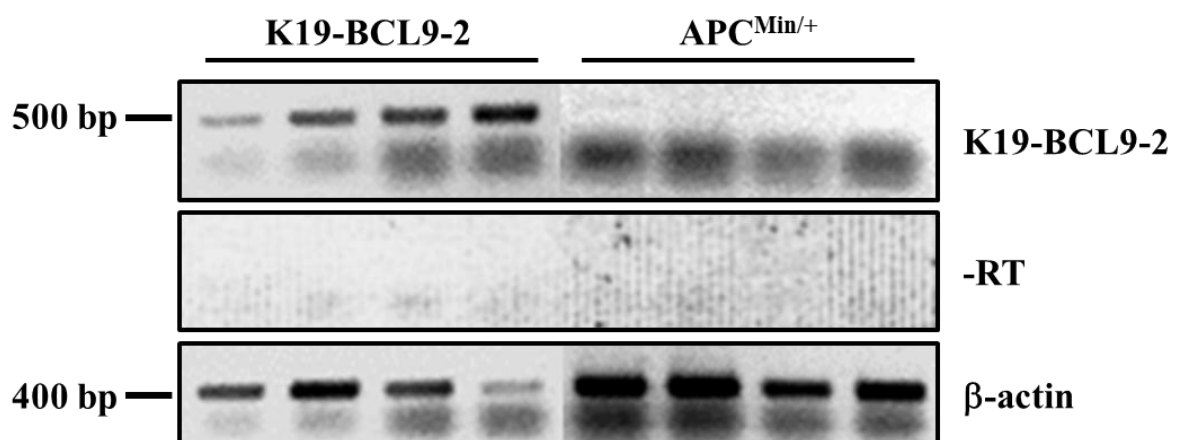


Figure 7. RNA expression of the transgene in mammary tumors from K19-BCL9-2 females. Breast tumors from $APC^{Min/+}$ females were used as negative control.

Upper panel: 500 ng of tumor cDNA was analyzed using K19-BCL9-2 transgene specific primers. Middle panel: RNA samples without prior reverse transcription were used as a control, to exclude the amplification from genomic DNA. Lower panel: 500 ng of tumor cDNA was analyzed using β -actin primer as internal control.

5.2 BCL9-2 expression during different stages of mammary gland development

The tumor development of K19-BCL9-2 females in the breast prompted us to analyze, if BCL9-2 might play a role during different phases of postneonatal mammary gland development. Currently, there is no detailed analysis available about the expression of BCL9-2 in different stages of the normal breast. Therefore, the expression of BCL9-2 in the mammary gland in mice between 4 weeks up to 18 month of age was analyzed by immunohistochemistry using our new specific antibodies (93).

During puberty, the terminal end buds of the primary mammary rudiments start to proliferate and to invade into fat pad. As a result of this process, the entire adult fat pad is filled by a branched ductal tree. During pregnancy, the mammary epithelium differentiates into functional lobular-alveolar structures, which produce milk after pregnancy. After weaning, the mammary gland goes through post-lactational involution, where the lobular-alveolar units collapse and undergo apoptosis. With aging of the females, the lobular-alveolar epithelium of the breast undergoes terminal lobular involution, which is characterized by loss of the alveolar units (3, 10-12).

High expression of BCL9-2 was found in the outgrowing ductal cells and terminal end bud cells of pubertal mammary glands from 4 weeks old virgins (Figure 8A), where the ductal outgrowth takes place due to proliferation of the cap cells in TEBs (10). In contrast, the expression of BCL9-2 in the mature ducts was limited only to a few epithelial cells (Figure 8B). The ductal epithelium of adult 4 month old virgin females still expressed BCL9-2. The levels were comparable to the mature ducts of the pubertal glands (Figure 8C and D). BCL9-2 expression was almost absent or very low as the females aged (starting at 12 month of age) (Figure 8E and F). In contrast, the highest BCL9-2 expression was detected in the breast epithelium during late pregnancy (from E18.5). Here both, alveolar and ductal cells were strongly positive for BCL9-2 (Figure 8G and H, respectively). The expression dropped again during post-lactational involution of the breast epithelium. BCL9-2 was expressed at day 10 of involution in the milk ducts at moderate levels and was weakly detectable in the collapsed alveoli (Figure 8I and J, respectively). As the involution progressed (day20), BCL9-2 was only weakly expressed in the alveolar structures and was almost not detectable in the ductal epithelia, similar to the normal adult ductal epithelium (Figure 8K and L).

The results of the immunohistochemical analyses show that BCL9-2 is highly expressed during developmental stages of wild-type mammary gland, which are characterized by high proliferation of the mammary epithelium.

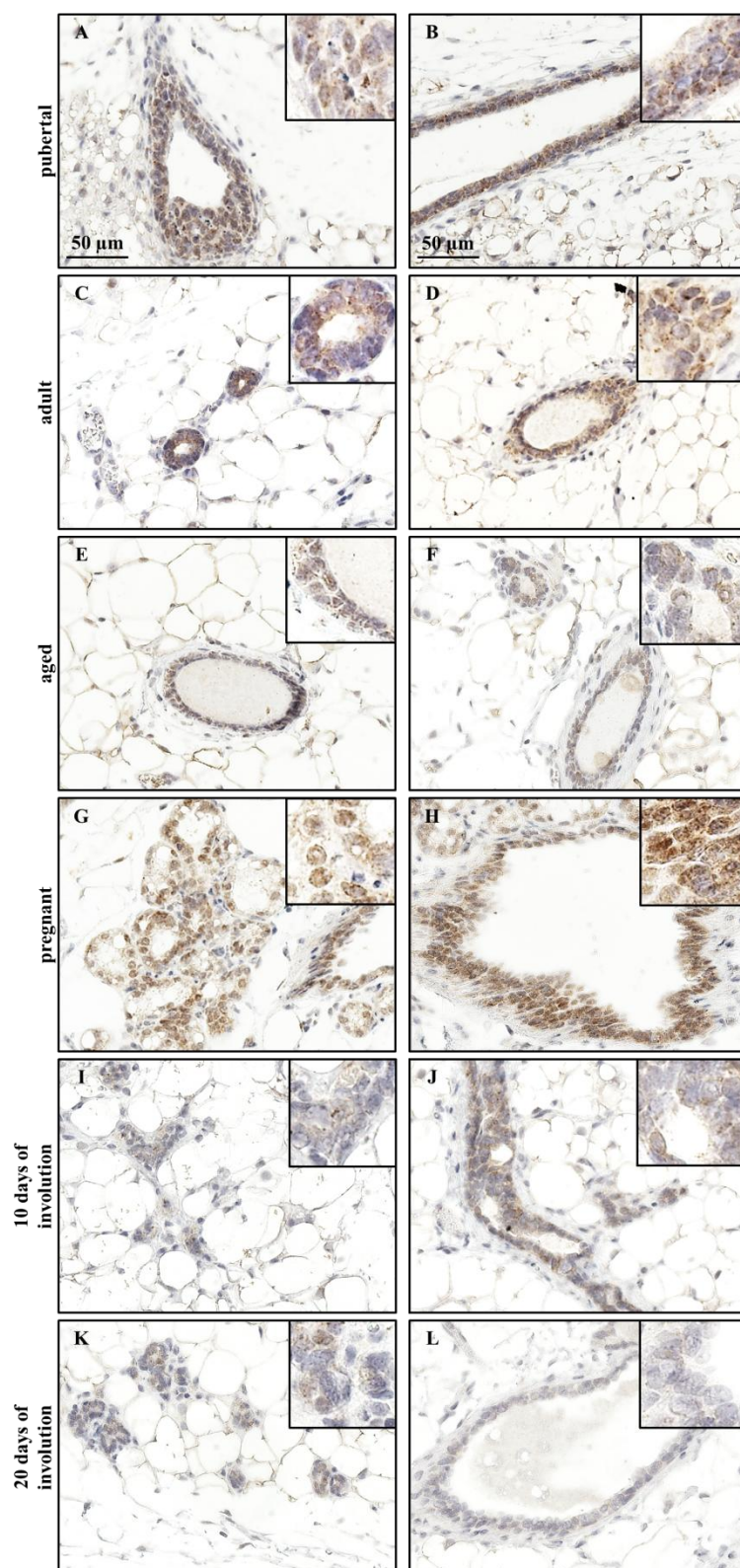


Figure 8. Immunohistochemical BCL9-2 staining of mammary gland tissues from wild-type mice during different postneonatal stages of breast development.

A. TEBS and **B.** mature milk ducts of a pubertal gland. **C.** small and **D.** large ducts of a mammary gland from a 4 month old female. **E.** small and **F.** large ducts of a mammary gland of a 12month old female. **G.** alveoli and **H.** milk ducts of pregnant female (E18.5). **J.** collapsing alveoli and **I.** ductal epithelia on day 10 of involution. **K.** collapsing alveoli and **L.** ductal epithelia on day 20 of involution. Inserts show the mammary tissue at higher magnification. 400x magnification.

5.3 Histological analyses of mammary tumors from K19-BCL9-2 mice

5.3.1 The tumors of K19-BCL9-2 show distinct differentiations of the tumor cells

For a more detailed characterization of the mammary tumors from K19-BCL9-2 transgenics, sections of the tumors were evaluated by H&E stainings and immunohistochemical analyses. The histopathology of the tumor samples was also assessed by a pathologist (Dr. med. Christina Perske, Department of Pathology; UMG). 13 of 20 tumors were clearly evaluated as mammary adenomas or adenocarcinomas. Moreover, 4 of these mammary tumors were defined as lobular breast carcinomas that exhibit the typical histopathological morphology as found in humans. 6 other tumors were poorly differentiated tumors adjacent to the mammary glands.

Our examination of the H&E and immunohistological stainings further revealed that the mammary tumors exhibited distinct regions of differentiation of the tumor cells. We identified well differentiated tumors that consisted of ductal-like and myoepithelial-like tumor cells (Figure 9A and B). In addition, other tumors were moderately differentiated and were characterized by few remaining ductal-like structures embedded into monomorphic tumor cells with irregularly shaped nuclei. Those tumors were classified as lobular carcinomas by the pathologist (Figure 9C).

The expression of specific markers of the mammary gland was analyzed in the tumors by immunohistochemistry. In the normal mammary gland, ducts consist of an inner luminal epithelial, which expresses epithelial markers such as K8/18, K19 and an outer myoepithelial single cell layer that is characterized by the expression of α SMA. Two different areas of tumor cells were identified within cancers with histological ductal-like differentiation. One area was characterized by strong membranous and elevated cytoplasmic β -catenin expression and high expression of cytokeratins, as indicated by prominent Pan-Cytokeratin staining (Figure 9G and J, respectively). These ductal-like tumor cells highly expressed the luminal epithelia marker K19 (Figure 9M). In addition, they exhibited expression of alpha smooth muscle actin (α SMA), which is a marker of mammary myoepithelial cells (Figure 9S). In the tumors, multiple layers of α SMA positive cells surrounded the more irregular, also multi-layered K19 expressing cells (Figure 10A). Since this morphology was remi-

niscent of normal mammary ducts, we therefore described these tumor areas as dysplasia with ductal-like morphology. The second area within the well differentiated tumors was characterized by a large number of α SMA positive cells (Figure 9T). Pan-Cytokeratin expressing cells were also present within these areas, although to a smaller degree (Figure 9K). The expression of β -catenin and K19 was restricted to a few remaining ductal-like structures (Figure 9H and N, respectively). Thus, these tumor areas showed a predominant myoepithelial-like morphology. E-cadherin is usually strongly expressed in the epithelia of the mammary glands and its loss is associated with metastases in breast cancer (110-115). Remarkably, the expression of E-cadherin was only moderately in some ductal-like structures in both luminal and myoepithelial differentiated areas of K19-BCL9-2 tumors. The main tumor mass showed only weak expression of E-cadherin (Figure 9P and Q).

Interestingly, high expression of BCL9-2 could be detected in both, luminal- and myoepithelial-like tumor areas (Figure 9D and E, respectively). In addition, co-immunofluorescence staining confirmed that both, the luminal and myoepithelial cell lineages expressed high BCL9-2 (Figure 10B). Moreover, the luminal- like areas displayed an increased cell proliferation indicated by an intensive BrDU staining (Figure 9V).

In contrast to these well differentiated tumors, the examination of the lobular-like tumors of the K19-BCL9-2 females uncovered a different architecture. They displayed also a high number of proliferating cells, indicated by BrdU incorporation, similar to the well differentiated tumors (Figure 9X). In contrast, the expression of luminal epithelial markers K19 and panCK was restricted to the remaining ductal-like structures and to single cells within the tumor (Figure 9O and L, respectively). A similar expression pattern was detected for E-cadherin (Figure 9R). Those ductal-like were surrounded by α SMA positive cells (Figure 9U).

Intriguingly, the expression of BCL9-2 in these tumors resembled the expression of the K19 with the highest expression in the ducts. The single cells of the tumor mass displayed weak BCL9-2 staining (Figure 9F). Note that the expression of the transgenic BCL9-2 RNA showed in 5.1.3 (Figure 7) was performed with cDNA from tumors with lobular-like differentiation, indicating that the expression of K19-BCL9-2 transgene still took place in this proportion of tumors.

During necropsy of transgenic females displaying mammary tumors, small macroscopic nodes on the lung surface were observed (Figure 11). To assess if these lesions correspond to lung metastasis, we evaluated the sections of the lungs of five K19-BCL9-2 transgenic animals with mammary cancers by H&E staining. The stainings showed multiple areas within the lung tissue, containing round-shaped, epithelia-like structures, very reminiscent of mammary small ducts and alveoli (Figure 11). In total, micro-metastases to the lung were identified in 4 of 5 lungs of transgenic females, which were not seen in two aged matched controls.

Taken together, these findings indicate, that overexpression of BCL9-2 in the breast may lead to a development of breast carcinoma with a potential to metastases.

5.3.2 The tumors of K19-BCL9-2 females are estrogen receptor positive

Expression of the hormone receptors ER α and PR, and of the epidermal growth factor receptor 2 HER2 (ErbB2/Neu) are relevant for the therapeutic regimens of human breast cancers and are highly predictive for the response to the treatment (26, 116). Only a few mouse breast cancer models have been described that can mimic the molecular features of human breast cancers, especially for ER α and PR positive mammary tumors (70, 117, 118).

To analyze the hormone receptor status of the tumors of K19-BCL9-2 females, tumor samples were analyzed for the expression of ER α and PR by immunohistochemical stainings. All tumors showed high expression of nuclear ER α (Figure 12A-C) and the majority of them expressed nuclear PR (Figure 12D-F).

For the quantification of the BCL9-2, nuclear ER α and PR expression, an expression score was applied, that was calculated from the staining intensity and the amount of positive epithelia (see Materials and Methods).

First, the expression of BCL9-2 in the mammary glands of age matched control females and in the tumors of K19-BCL9-2 females were compared.

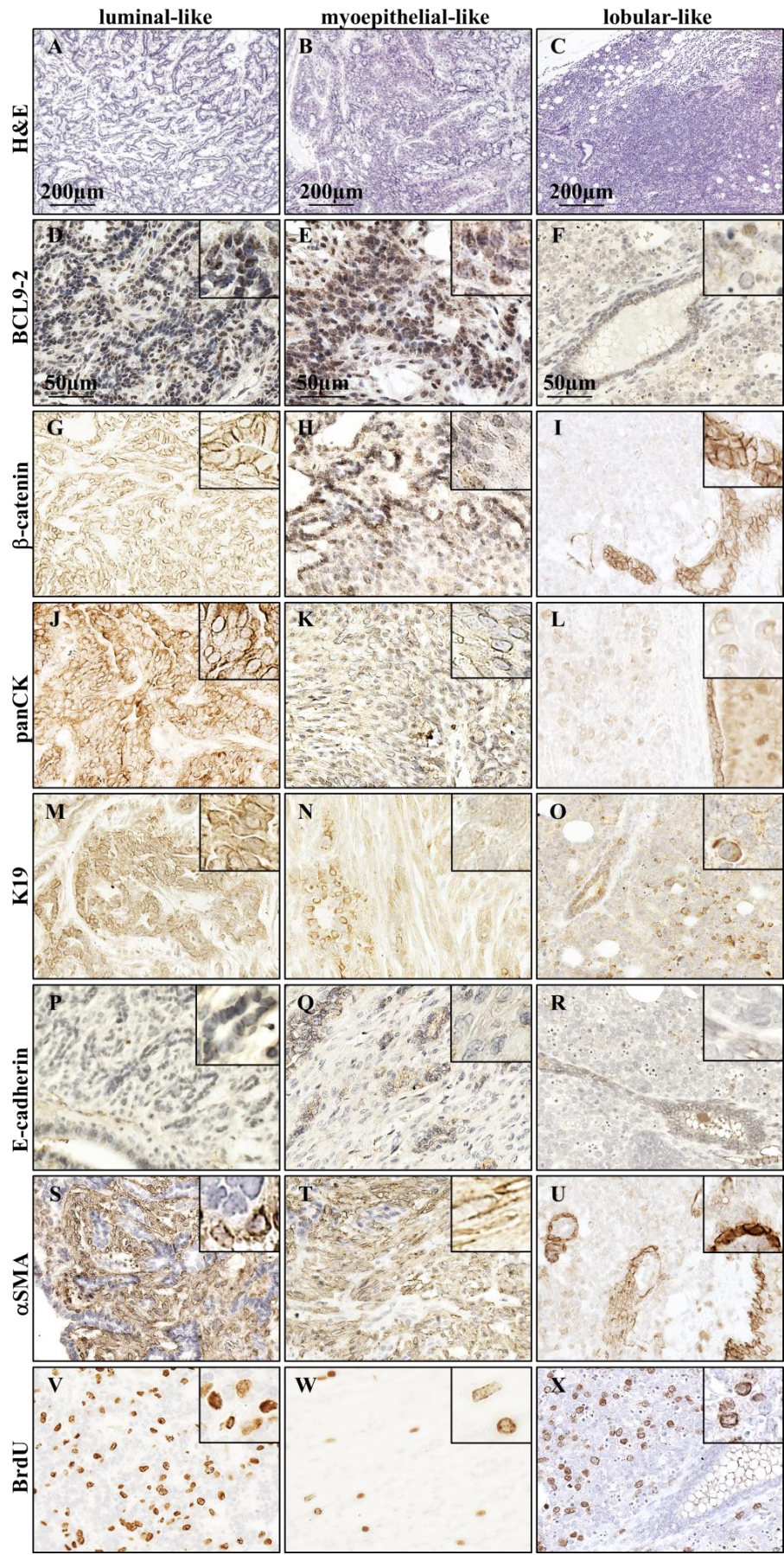


Figure 9. Histopathology of the ductal-like and lobular-like breast tumors from K19-BCL9-2 females.

A, D, G, J, M, P, S, V: Immunohistochemical staining as indicated of luminal-like area of a ductal-like differentiated tumor. **B, E, H, K, N, Q, T, W:** Immunohistochemical staining as indicated of myoepithelial-like area of a ductal-like differentiated tumor. **C, F, I, L, O, R, U, X:** Immunohistochemical staining as indicated of lobular-like differentiated tumor. Inserts show the tumor tissue at higher magnification. H&E: 100x magnification, BCL9-2, β -catenin, panCK, K19, α SMA and BrdU: 400x magnification.

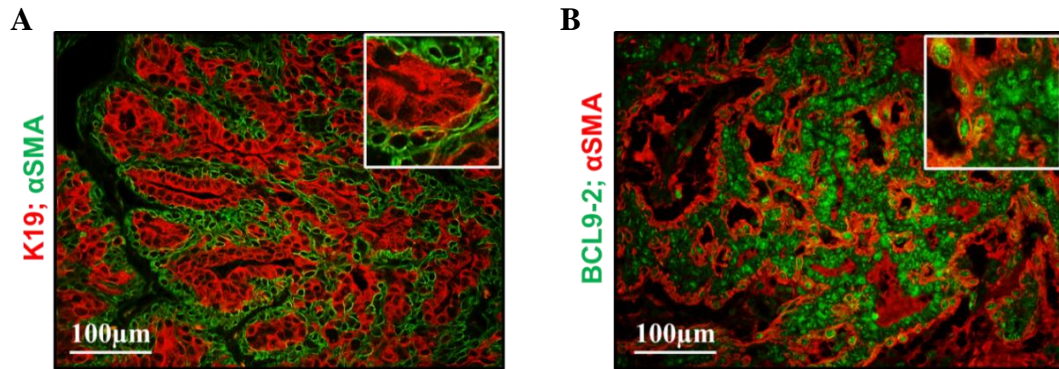


Figure 10. Co-immunofluorescence staining of mammary tumor tissues from K19-BCL9-2 females.

A: Image of a K19 (red) and α SMA (green) co-staining. **B:** Image of a BCL9-2 (green) and α SMA (red) co-staining. Inserts show the tumor tissue at higher magnification. 200x magnification.

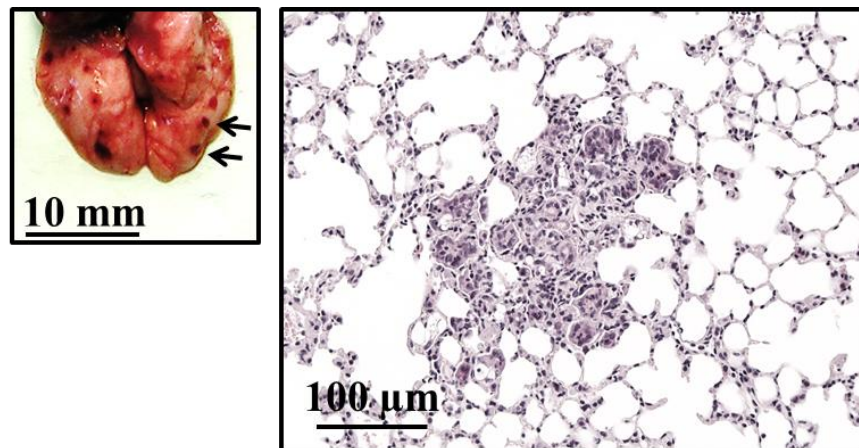


Figure 11. K19-BCL9-2 females bearing mammary tumors displayed pulmonary metastases.

Left: Macroscopic view of pulmonary nodes in the lung from a K19-BCL9-2 female with a breast tumor. Right: H&E staining of paraffin embedded lung tissue from a K19-BCL9-2 female with a breast tumor. H&E: 200x magnification.

The expression score for BCL9-2 in four of five control tissues was low with a median of 2. In contrast, tumors of K19-BCL9-2 females showed higher BCL9-2 expression, although the median for all 13 analyzed tumors was also 2 (Figure 13A).

Results

Eleven tumor samples, which were analyzed by IHC for the expression of BCL9-2, ER α and PR expression of BCL9-2 were divided into 2 groups based on their BCL9-2 expression. Those tumors which were comparable with the BCL9-2 expression in the normal breast were defined as “low BCL9-2” tumors (n= 6). The tumors with an expression score higher than 2 were defined as “high BCL9-2” tumors (n=5). Mann-Whitney analyses revealed that in BCL9-2 high expressing tumors also the expression of both, ER α and PR was higher, compared to those with low BCL9-2 expression (Figure 13B), which however did not reach statistical significance, due to low number of analyzed tissues (Figure 13B). These findings indicate that elevated levels of BCL9-2 may play a role in the development of ER α and PR positive breast tumors in K19-BCL9-2 mouse model.

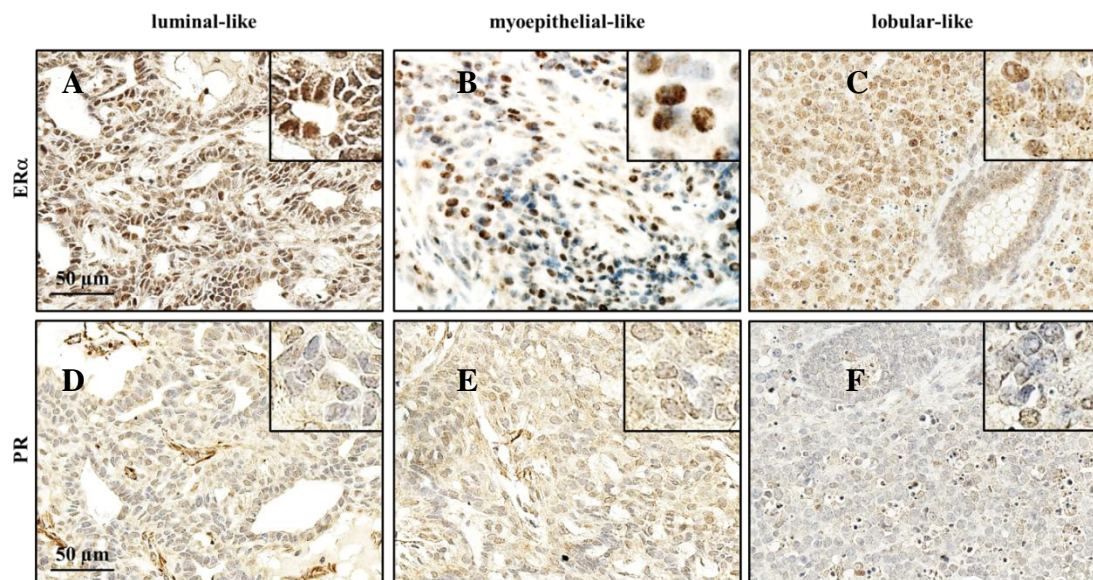


Figure 12. Breast tumors from K19-BCL9-2 females express nuclear ER α .

A-C: Immunohistochemical ER α staining of luminal-like area (A) and of myoepithelial-like area (B) of a ductal-like differentiated tumor, and of lobular-like differentiated tumor (C) **D-F:** Immunohistochemical PR staining of luminal-like area (D) and of myoepithelial-like area (E) of a ductal-like differentiated tumor, and of lobular-like differentiated tumor (F). Inserts show the tumor tissue at higher magnification. 400x magnification.

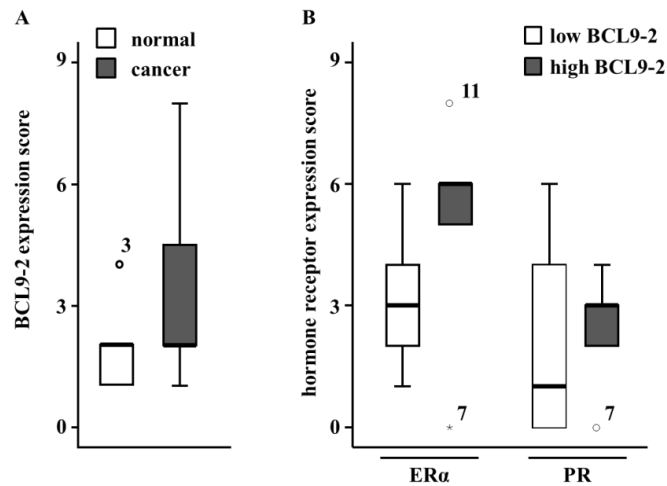


Figure 13. High expression of BCL9-2 in breast tumors from K19-BCL9-2 females correlates with nuclear ER α .

A: Box plot analyses of the BCL9-2 expression score in normal breast tissue from non-transgenic control females and breast tumors from K19-BCL9-2 females. In tumors, the expression of BCL9-2 was higher compared to control mammary glands. **B:** high nuclear expression of BCL9-2 in K19-BCL9-2 tumors correlated with higher levels of nuclear ER α and PR. For statistical analyses a Mann-Whitney-Test was performed.

5.4 Transgenic females display delayed age-related and post-lactational involution of the breast epithelium

5.4.1 Aged K19-BCL9-2 females display premalignant alterations of the mammary gland

The development of epithelial cancers represents a multistep process. Preneoplastic alterations in the mammary gland of the mouse consist of hyperplastic alveolar nodules (HANs) and ductal hyperplasia. They are often accompanied by ductal dilations. Those changes are considered as premalignant (119-121). To identify early neoplastic changes of K19-BCL9-2 breast tissues, carmine whole mount staining of the mammary glands derived from the different founder lines of transgenic mice were performed. For this, mammary tissues from transgenic females without macroscopic mammary tumors of 12 and 20-24 months of age were compared to age matched non-transgenic controls. For the quantification of the early neoplastic changes, a score was developed, that evaluated the severity of the preneoplastic changes and the amount of involved tissue in the mammary gland (see Materials and Methods).

At 12 months of age, transgenic females showed only a slight increase of the ductal dilatation (Figure 14B). The mammary glands of these females did not develop HANs at this age, similar to control littermates. In contrast, at the age of 24 month, mammary glands of 3 of 4 transgenic founder lines clearly developed more HANs, which were also significantly larger in size than in control animals (Figure 14A). In addition, two of four analyzed founder lines of 24 month old K19-BCL9-2 females showed a significantly stronger dilatation of the ducts compared to controls (Figure 14B).

Surprisingly, carmine whole mount staining of the mammary glands of both, 12 and 24 month old transgenic females showed more extensive alveolar structures, compared to control animals (Figure 14C). This morphology of the breast epithelium is unexpected in aged females, since the loss of alveolar structures of the breast is a consequence of the age related involution (4, 13, 122).

The premalignant alterations of the mammary epithelium in K19-BCL9-2 aged females were analyzed by immunohistochemical staining on tissue sections. H&E staining of control tissues revealed only slightly enlarged milk ducts, but almost no alveolar structures (Figure 15C). In contrast, the examination of the breast tissues of transgenic females showed strongly dilated ducts surrounded by numerous enlarged alveoli. The ductal and alveolar structures were filled with secretions (Figure 15D). This morphology was very reminiscent of the histology usually found in the postlactationally involuting mammary gland (see below). While only few ductal cells of control mammary glands expressed BCL9-2, the gland epithelia, especially the epithelium of HANs in K19-BCL9-2 glands displayed higher expression of BCL9-2 (Figure 15E and F, respectively). Similar results were found for the expression of ER α . In the transgenic epithelium, the epithelial cells of HANs expressed high ER α , while only a few ductal cells of control epithelia showed nuclear ER α expression (Figure 15G). Moreover, in the epithelia of hyperplastic alveoli of the transgenics, increased cytoplasmic staining of ER α was detected (Figure 15H). The examination of BrdU stainings revealed high proliferation within the hyperplastic alveolar epithelium of aged K19-BCL9-2 females compared to the mammary epithelia of the control animals (Figure 15J and I, respectively). These results indicate that the development of early

premalignant hallmarks of the mammary tissue may be enhanced by the overexpression of BCL9-2 in the breast epithelium.

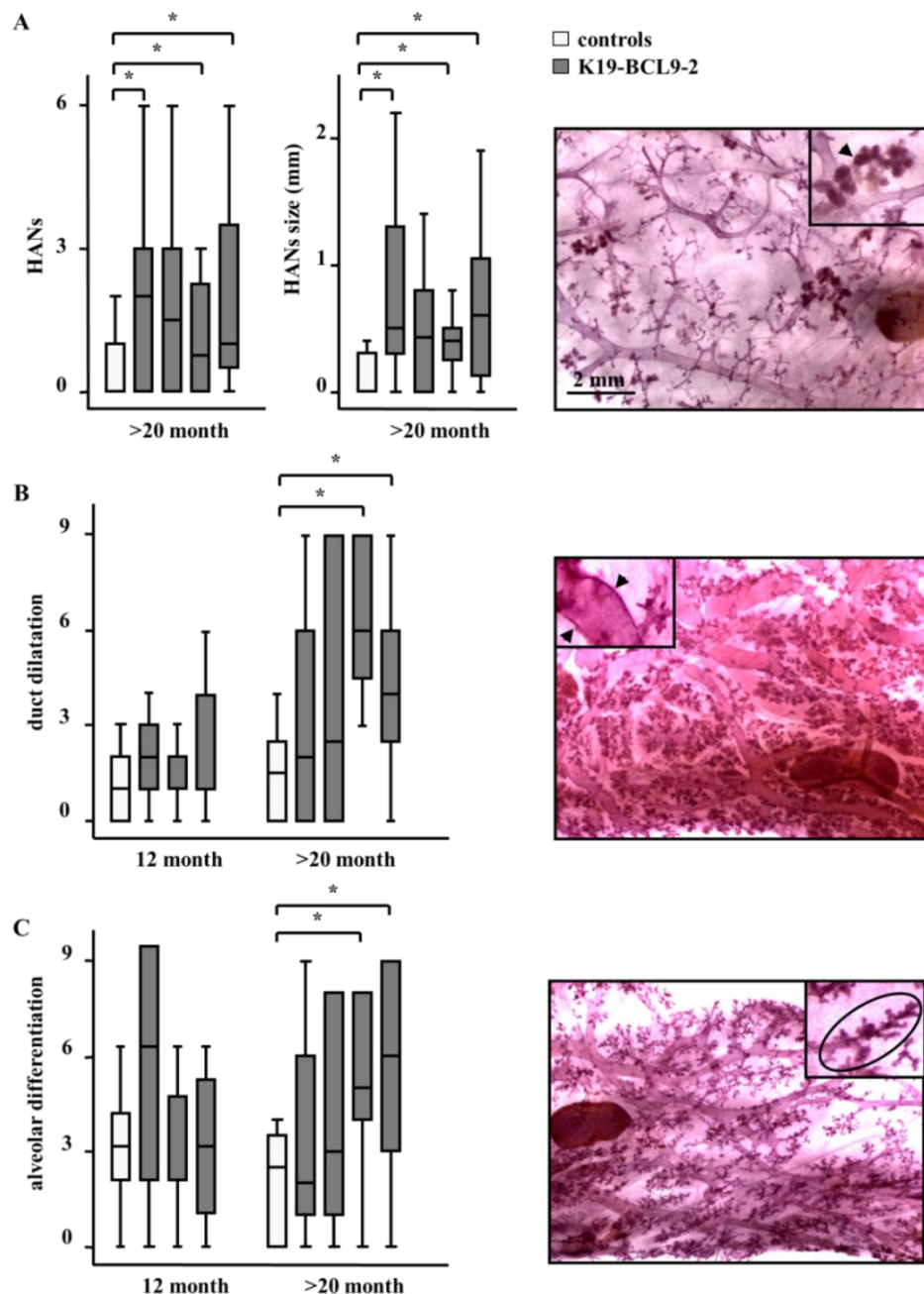


Figure 14. Aged K19-BCL9-2 females develop early breast epithelial neoplasia.

A. Left: Box plot graphs showing that transgenic females at the age of 20 month develop more and greater hyperplastic alveolar nodules (HANs) compared to control littermates. Right: Representative carmine staining. **B.** Left: Box plot graph indicates that duct dilatation was found in the breast tissues of K19-BCL9-2 females starting at 12 month of age. Right: Representative carmine staining. **C.** Left: Box plot graph showing mammary glands from 12 and >20 month old transgenic females that display an extensive alveolar morphology compared to non-transgenic controls. Right: Representative carmine staining. The insets within the pictures display the magnification of respective preneoplastic changes. For statistical analyses, a Mann-Whitney-Test was performed. * $p < 0.05$. Carmine staining: 200x magnification.

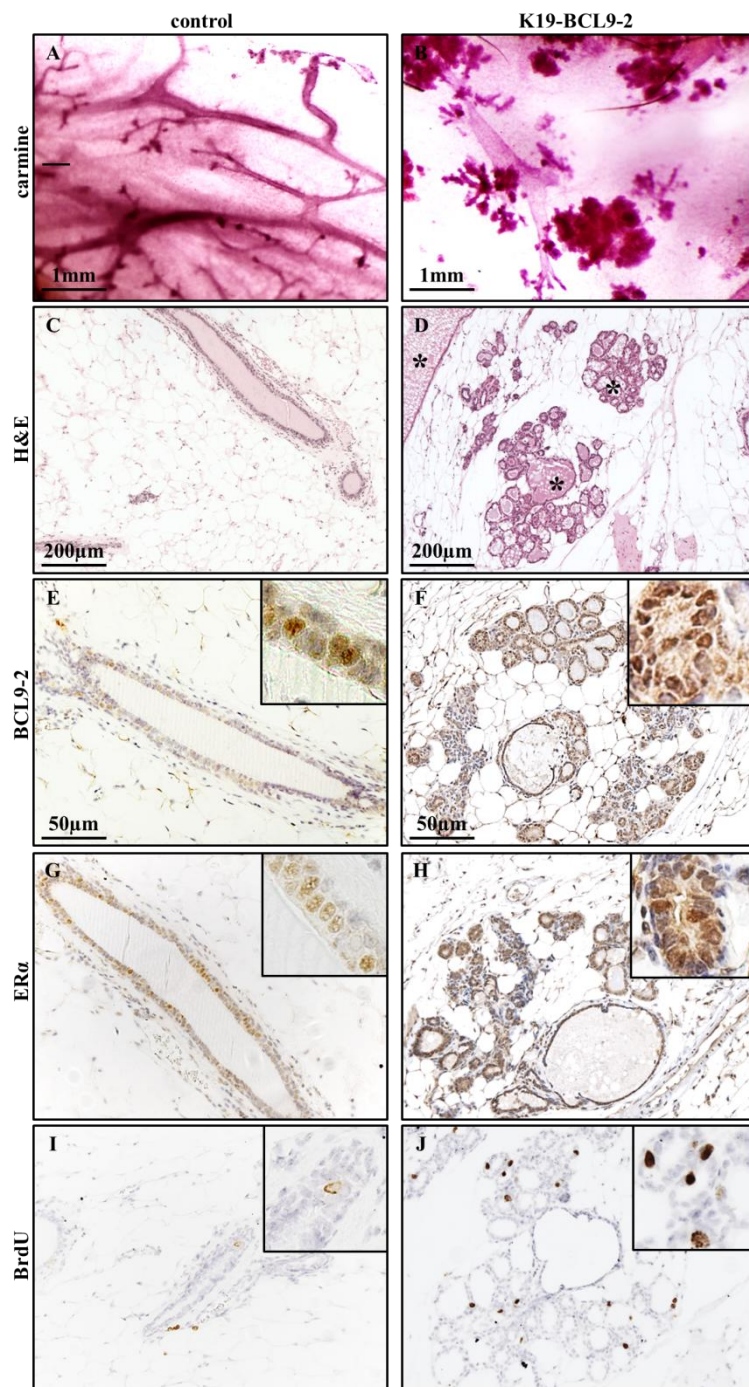


Figure 15. Histopathology of hyperplastic breasts from 24 month old control and K19-BCL9-2 females.

A, B: Whole mount carmine staining of control (A) and transgenic mammary gland (B). **C, E, G, I:** Immunohistochemical staining as indicated of control mammary gland. **D, F, H, J:** Immunohistochemical staining as indicated of transgenic mammary gland. Inserts show the tissue at higher magnification. Carmine staining: 200x; H&E: 100x; BCL9-2, ERα and BrdU: 400x magnification.

5.4.2 The mammary glands of K19-BCL9-2 females displayed delayed postlactational involution

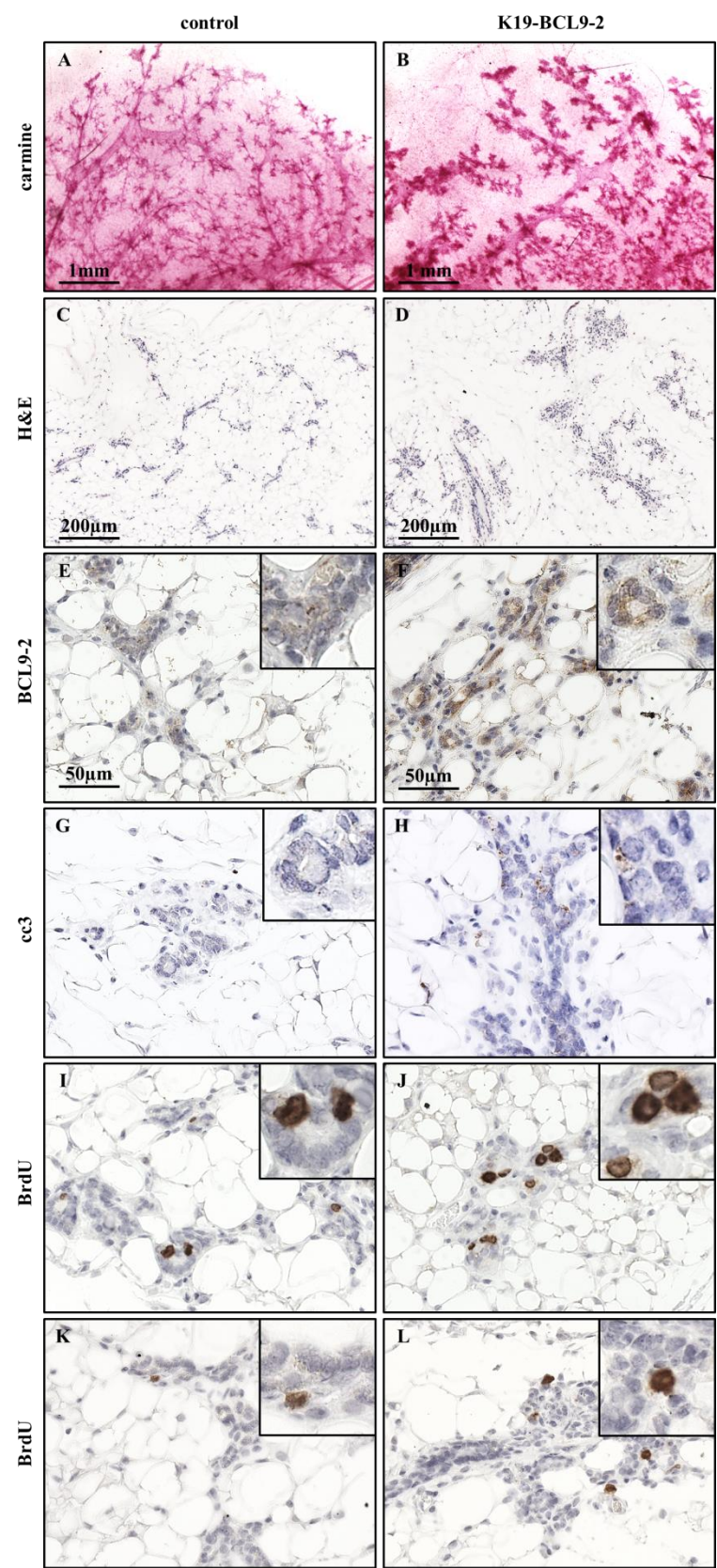
Not only preneoplastic alternations of the breast epithelium were shown to be associated with development of mammary tumors. The risk for breast cancer was reported to increase if the mammary gland has not undergone proper postlactational lobular involution (4).

To analyze the involution of the breast of the transgenic females after lactation, carmine whole mount staining of the mammary glands on day 10 and 20 of the involution was performed. Furthermore, the tissues were analyzed by IHC for BCL9-2 expression, apoptosis and proliferation.

Carmine staining revealed a more dense structure of the transgenic mammary gland on day 10 of involution. The tissues contained more alveolar structures compared to controls (Figure 16B and A, respectively). H&E staining of tissue sections of control mammary glands showed collapsed, small alveolar structures. In contrast, K19-BCL9-2 glands still retained large alveoli at day 10 of involution (Figure 16C and D, respectively). Moreover, the breast epithelia of the transgenic mice expressed BCL9-2. It was hardly detectable in the mammary glands of control animals (Figure 16E and F, respectively). However, the examination of Cleaved caspase 3 by IHC revealed no differences between controls and transgenics (Figure 16G and H). Interestingly, the mammary epithelium of the transgenes showed high proliferation in the alveoli, indicated by BrdU stainings. Only a few BrdU-labeled cells were detected in the glands of the control animals (Figure 16J and I, respectively). On day 20 of involution, the transgenic glands displayed still larger alveolar structures than controls. However, the proliferation in the transgenic epithelium was low as in the control mammary gland (Figure 16K and L). Thus, K19-BCL9-2 displayed delayed postpartum mammary involution with increased epithelial cell proliferation.

Figure 16. Immunohistochemical staining of a mammary gland from a K19-BCL9-2 female during the involution.

A, B: Whole mount carmine staining of control (A) and transgenic mammary gland (B). **C, E, G, I:** Immunohistochemical staining as indicated of control mammary gland. **D, F, H, J:** Immunohistochemical staining as indicated of transgenic mammary gland. **K, L:** BrdU staining of control (K) and transgenic mammary gland (L) on day 20 of involution. Inserts show the tissue at higher magnification. Carmine staining: 200x; H&E: 100x; BCL9-2, Cleaved caspase 3 (cc3) and BrdU: 400x magnification.



5.5 Transgenic overexpression of BCL9-2 in different Wnt mammary tumor models

To determine, if transgenic BCL9-2 expression may enhance or modulate mammary tumor formation in other mouse models, K19-BCL9-2 mice were bred with APC^{Min/+}, MMTV^{Cre}; Catnb^{+/ Δ ex3} and K5-CreER^{T/+}; Catnb^{+/ Δ ex3} animals.

5.5.1 Transgenic overexpression of BCL9-2 leads to a higher mammary tumor susceptibility in compound APC^{Min/+}; K19-BCL9-2 mice

APC^{Min/+} females spontaneously develop mammary gland tumors. They usually display acinar/pilar differentiation with characteristic squamous metaplasia (123-126).

To investigate if overexpression of BCL9-2 can enhance tumor development, transgenic BCL9-2 mice were crossed with APC^{Min/+} mice. Compound APC^{Min/+}; K19-BCL9-2 females, developed tumors of mammary gland starting at approximately 3 month of age similar to APC^{Min/+} mice. However, APC^{Min/+}; K19-BCL9-2 compound females showed an increased incidence for breast tumor development (9/30= 30% vs. 17/35= 49%, respectively).

K19-BCL9-2 females developed hyperplasia of the breast epithelium. To analyze if overexpression of BCL9-2 can induce hyperplasia in the breast of APC^{Min/+} females, glands of 5 month old APC^{Min/+} and compound APC^{Min/+}; K19-BCL9-2 females were analyzed by carmine whole mount staining. Examination of the carmine staining revealed no apparent hyperplastic changes in the mammary glands from APC^{Min/+} and APC^{Min/+}; K19-BCL9-2 females (Figure 17A and B).

The tumors of APC^{Min/+}; K19-BCL9-2 compound females were also analyzed by IHC. The examination of H&E revealed no apparent differences between APC^{Min/+} and APC^{Min/+}; K19-BCL9-2 females. The architecture of APC^{Min/+}; K19-BCL9-2 tumors was similar to the well described mammary tumors from APC^{Min/+} mice. They showed pilar differentiation combined with areas of extensive squamous metaplasia (Figure 18A and B). As indicated by BrdU staining, both tumors exhibited high proliferation (Figure 18C and D). Compared to the tumors from APC^{Min/+} mice, the tu-

mor tissues from APC^{Min/+}; K19-BCL9-2 mice expressed higher levels of nuclear BCL9-2 in the tumor epithelia (Figure 18E and F). Both, the tumors from APC^{Min/+} and APC^{Min/+}; K19-BCL9-2 mice showed also elevated levels of cytoplasmatic β -catenin (Figure 18G and H). In contrast to the tumors of aged K19-BCL9-2 transgenics, tumors of both mutant genotypes on the APC Min background displayed weak or absent staining of nuclear ER α (Figure 18I and J).

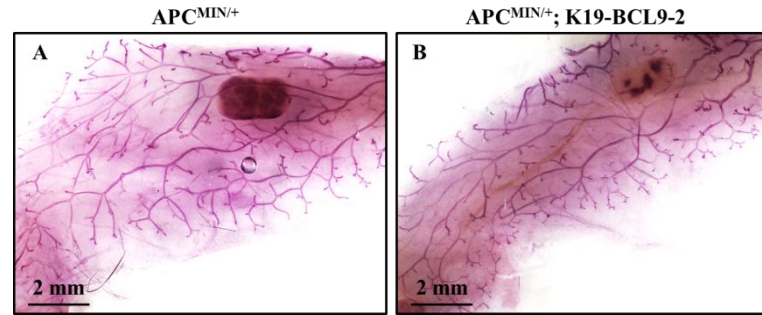


Figure 17. Carmine whole mount staining of breast tissues from APC^{Min/+} and compound APC^{Min/+}; K19-BCL9-2 females.

A: Carmine whole mount staining of the mammary tissue from a 5 month old APC^{Min/+} female. **B** Carmine whole mount staining of the mammary tissue from a 5 month old APC^{Min/+}; K19-BCL9-2 female. 80x magnification.

These findings indicate that overexpression of BCL9-2 in the breast may enhance the tumorigenesis in APC^{Min/+} mice. However, the overexpression of BCL9-2 does not affect the tissue differentiation caused by aberrant stabilization of β -catenin.

5.5.2 Transgenic overexpression of BCL9-2 leads to mammary tumor development in MMTV^{Cre}; Catnb^{+/ Δ ex3}; K19-BCL9-2 compound mutant mice

MMTV^{Cre}; Catnb^{+/ Δ ex3} is a mouse model, in which an constitutive active form of β -catenin is specifically expressed in the mammary gland epithelium. This mutation of β -catenin results in deregulated Wnt signaling in the breast and induces also the transdifferentiation of the alveolar epithelium into epidermal and pilar structures. However, the deregulation of β -catenin does not result in the development of macroscopic mammary tumors (127).

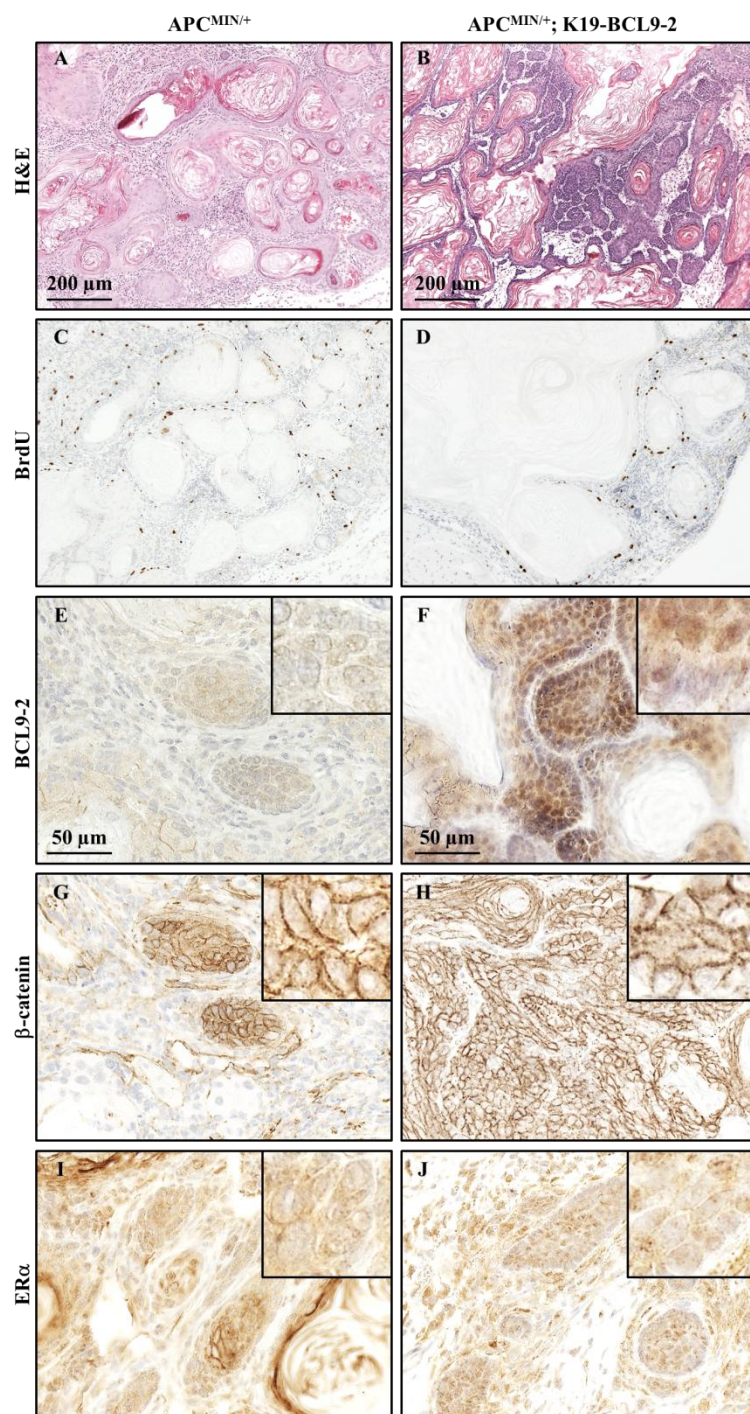


Figure 18. Immunohistochemical staining of breast tumor tissues from APC^{Min/+} and APC^{Min/+}; K19-BCL9-2 compound females.

A, C, E, G, I: Immunohistochemical staining as indicated of the tumor sample from APC^{Min/+} female
 B, D, F, H, J: Immunohistochemical staining as indicated of the tumor sample from APC^{Min/+}; K19-BCL9-2 female Inserts show the tumor tissue at higher magnification. H&E and BrdU: 100x; BCL9-2, β-catenin and ERα: 400x magnification.

To analyze the role of transgenic BCL9-2 overexpression in this model, MMTV^{Cre};Catnb^{+/ Δ ex3}; K19-BCL9-2 compound mice were generated. The females were followed up until 12 month of age.

In contrast to the MMTV^{Cre};Catnb^{+/ Δ ex3} females (n=9), 2 of 10 MMTV^{Cre};Catnb^{+/ Δ ex3}; K19-BCL9-2 females developed macroscopic mammary gland tumors (20%).

The histopathological examination of those tumors revealed a morphology, similar to that found in APC^{Min/+} and APC^{Min/+}; K19-BCL9-2 tumors. The tumors of MMTV^{Cre};Catnb^{+/ Δ ex3}; K19-BCL9-2 females displayed large areas of squamous metaplasia (Figure 19A). The analysis of the hormone receptor status showed that the tumors were also ER α and PR negative (Figure 19C and D). Only a few remaining ducts with normal morphology displayed low nuclear ER α expression (Figure 19C). The expression of nuclear PR was not detected. These tumors expressed low amounts of BCL9-2 in the remaining ductal structures (Figure 19B).

The glands of 5 and 9 month old virgin MMTV^{Cre};Catnb^{+/ Δ ex3} and MMTV^{Cre};Catnb^{+/ Δ ex3}; K19-BCL9-2 females, which did not develop macroscopic tumors, were additionally analyzed by carmine whole mount stainings. An extensive alveolar morphology was evident in both analyzed mutant mouse lines (Figure 20). The number of alveoli increased in the mammary glands of the nine month old animals (Figure 20C and D). Moreover, the alveolar structures were strongly enlarged and dilated. This dilated alveoli were even more frequent in the epithelium of the MMTV^{Cre};Catnb^{+/ Δ ex3}; K19-BCL9-2 females (Figure 20D).

The histopathological analyses revealed a strong hyperproliferation of the ductal epithelium in both, MMTV^{Cre};Catnb^{+/ Δ ex3} and MMTV^{Cre};Catnb^{+/ Δ ex3}; K19-BCL9-2 breasts, indicated by epithelial cell layers growing into the duct lumen. In addition, the glands of both mouse lines showed characteristic regions of squamous metaplasia (Figure 21A and B). Both, MMTV^{Cre};Catnb^{+/ Δ ex3} and MMTV^{Cre};Catnb^{+/ Δ ex3}; K19-BCL9-2 glands showed nuclear expression of ER α within the hyperplastic epithelium (Figure 21E and F). BCL9-2-expression was exhibited by the epithelium of the MMTV^{Cre};Catnb^{+/ Δ ex3}; K19-BCL9-2 mammary glands (Figure 21C and D).

These results indicate that overexpression of BCL9-2 in the breast may enhance the hyperplasia and trigger the tumorigenesis in MMTV^{Cre};Catnb^{+/ Δ ex3} mice. However,

the overexpression of BCL9-2 does not affect the tissue differentiation caused by aberrant stabilization of β -catenin.

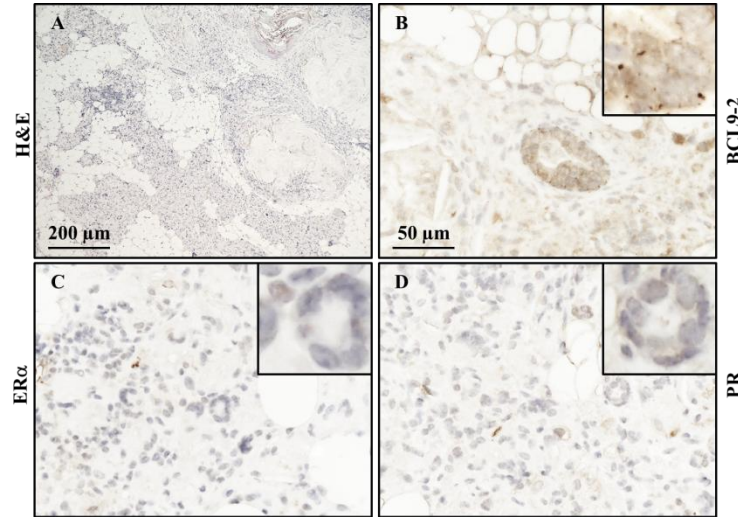


Figure 19. Histopathology of breast tumor tissues from $MMTV^{Cre};Catnb^{+/Δex3}$; K19-BCL9-2 females.

A. H&E. **B.** BCL9-2. **C.** ER α and **D.** PR stainings of the tumor sample. Inserts show the tumor tissue at higher magnification. H&E: 100x; BCL9-2, ER α and PR: 400x magnification.

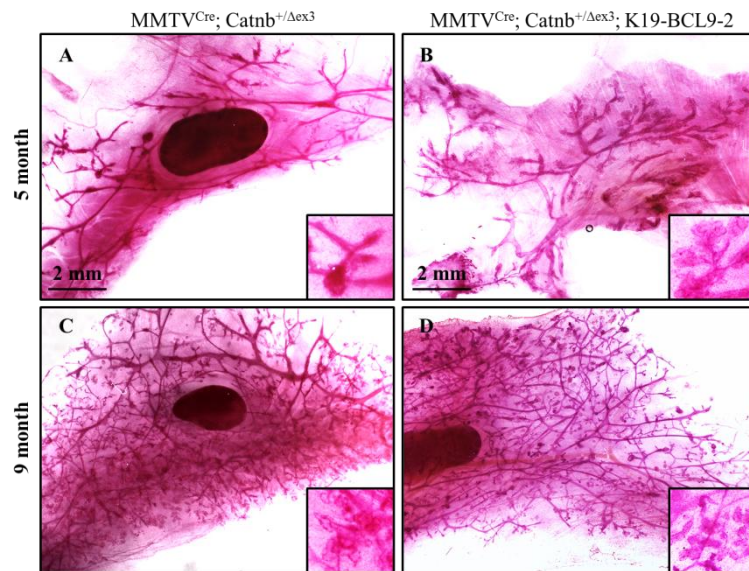


Figure 20. Carmine whole mount staining of breast tissues from $MMTV^{Cre};Catnb^{+/Δex3}$ and $MMTV^{Cre};Catnb^{+/Δex3}$; K19-BCL9-2 females.

A, C: Carmine staining of the mammary tissue from a 5 (A) and a 9 (C) month old $MMTV^{Cre};Catnb^{+/Δex3}$ female. **B, D:** Carmine staining of the mammary tissue from a 5 (B) and 9 (D) month old $MMTV^{Cre};Catnb^{+/Δex3}$; K19-BCL9-2 female. Inserts show dilated alveolar structures at higher magnification. 80x magnification

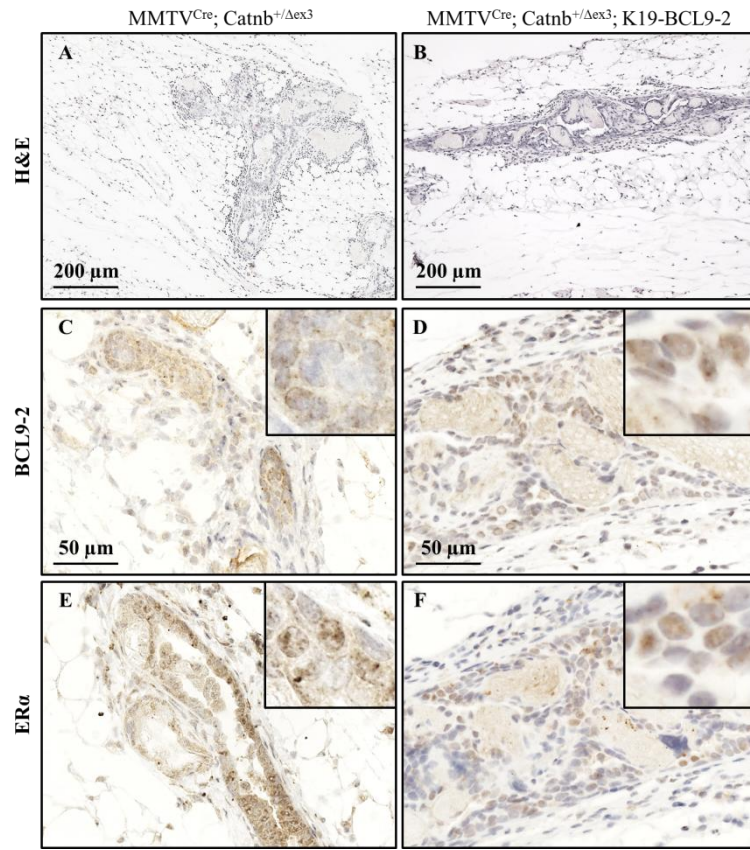


Figure 21. Immunohistological staining of breast tissues from MMTV^{Cre};Catnb^{+/Δex3} and MMTV^{Cre};Catnb^{+/Δex3}; K19-BCL9-2 females.

A, C, E: Immunohistochemical staining as indicated of the mammary gland from a 9 month old MMTV^{Cre};Catnb^{+/Δex3} female. **B, D, F:** Immunohistochemical staining as indicated of the mammary gland from a 9 month old MMTV^{Cre};Catnb^{+/Δex3}; K19-BCL9-2 female. Inserts show the mammary tissue at higher magnification. H&E: 100x, BCL9-2 and ERα: 400x magnification.

5.5.3 Transgenic overexpression of BCL9-2 does not induce mammary tumor development in K5-CreER^{T/+}; Catnb^{+/Δex3}; K19-BCL9-2 compound mutant mice

Compound MMTV^{Cre}; Catnb^{+/Δex3}; K19-BCL9-2 mutant animals were also compared to K5-CreER^{T/+}; Catnb^{+/Δex3}; K19-BCL9-2 mutant mice. MMTV-LTR drives the expression of the Cre-recombinase predominantly in the luminal epithelia of the breast (128, 129). In contrast, K5-CreER^{T/+} drives the expression of stabilized β-catenin in the basal epithelial cells of the breast epithelium due to specific expression of K5 in the myoepithelia. The induction of the Cre expression by tamoxifen injection was performed 6 weeks after birth. At this time point the outgrowth of the ductal tree is completed and cannot be disturbed by overactivation of β-catenin. K5-CreER^{T/+};

Results

$Catnb^{+/\Delta ex3}$ and $K5-CreER^{T/+}; Catnb^{+/\Delta ex3}$; K19-BCL9-2 were sacrificed 4 month after tamoxifen administration, since some females started to suffer from skin defects.

Neither $K5-CreER^{T/+}; Catnb^{+/\Delta ex3}$ nor $K5-CreER^{T/+}; Catnb^{+/\Delta ex3}$; K19-BCL9-2 females developed macroscopic tumors of the breast.

The glands of 5 month old virgin $K5-CreER^{T/+}; Catnb^{+/\Delta ex3}$ and $K5-CreER^{T/+}; Catnb^{+/\Delta ex3}$; K19-BCL9-2 females were further analyzed by carmine whole mount staining. Similar to $MMTV^{Cre}; Catnb^{+/\Delta ex3}$ and $MMTV^{Cre}; Catnb^{+/\Delta ex3}$; K19-BCL9-2; both $K5-CreER^{T/+}$ compound lines displayed extensive alveolar morphology of the mammary glands. In the K5-dependent mouse model, no differences were found between $K5-CreER^{T/+}; Catnb^{+/\Delta ex3}$ and $K5-CreER^{T/+}; Catnb^{+/\Delta ex3}$; K19-BCL9-2 mammary glands (Figure 22A and B).

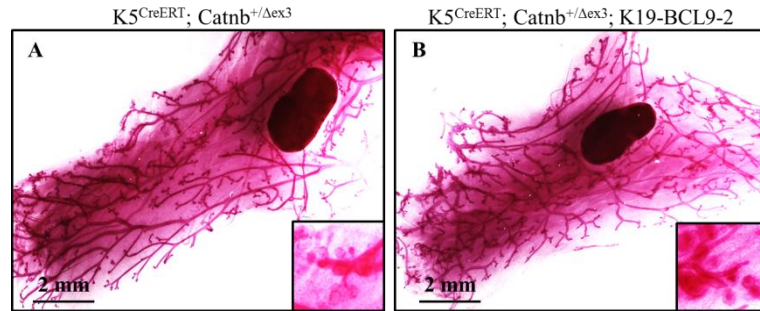


Figure 22. Carmine whole mount staining of breast tissues from $K5-CreER^{T/+}; Catnb^{+/\Delta ex3}$ and $K5-CreER^{T/+}; Catnb^{+/\Delta ex3}$; K19-BCL9-2 compound females.

A: Carmine staining of the mammary tissue from a 5 month old $K5-CreER^{T/+}; Catnb^{+/\Delta ex3}$ female. **B:** Carmine staining of the mammary tissue from a 5 month old $K5-CreER^{T/+}; Catnb^{+/\Delta ex3}$; K19-BCL9-2 female. Inserts show alveolar structures at higher magnification. 80x magnification.

Histological analyses of the breast tissues revealed hyperproliferation of the mammary epithelium in both, $K5-CreER^{T/+}; Catnb^{+/\Delta ex3}$, and $K5-CreER^{T/+}; Catnb^{+/\Delta ex3}$; K19-BCL9-2 glands, indicated by a multilayered ductal epithelium (Figure 23A and B). Weak BCL9-2-expression was found in the epithelium of both, $K5-CreER^{T/+}; Catnb^{+/\Delta ex3}$, and $K5-CreER^{T/+}; Catnb^{+/\Delta ex3}$; K19-BCL9-2 mammary glands (Figure 23C and D). In addition, $K5^{CreERT}; Catnb^{+/\Delta ex3}$ and $K5-CreER^{T/+}; Catnb^{+/\Delta ex3}$; K19-BCL9-2 glands showed a strong nuclear expression of ER α within the hyperplastic epithelium (Figure 23E and F).

These results indicate that overexpression of BCL9-2 in the luminal breast epithelia does not affect hyperplasia development or trigger the tumorigenesis in K5-

CreER^{T/+}; Catnb^{+/ Δ ex3} mice. Moreover, the overexpression of BCL9-2 does not influence the tissue differentiation caused by aberrant stabilization of β -catenin.

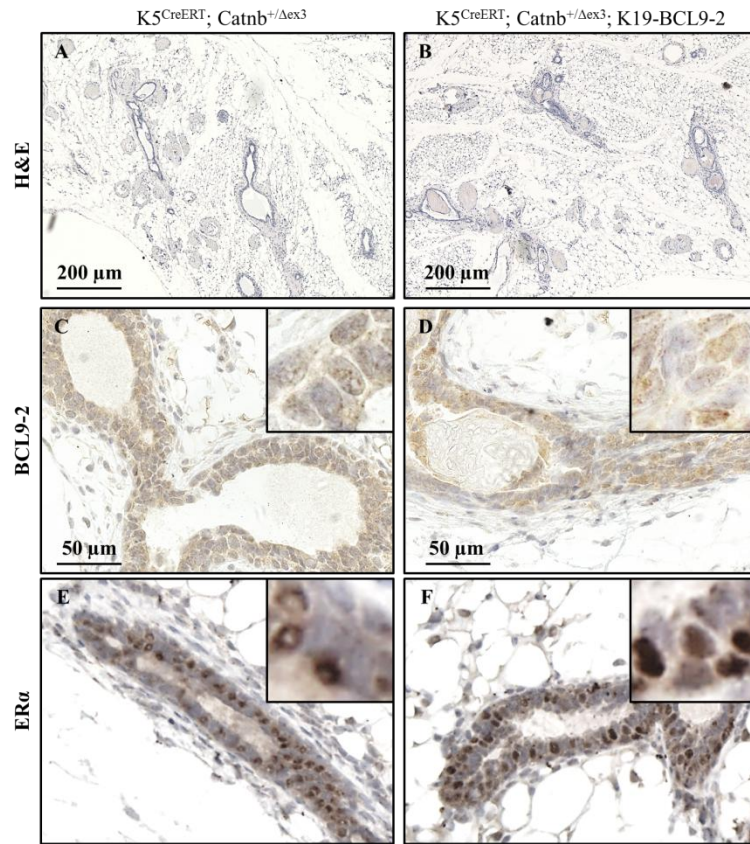


Figure 23. Immunohistological staining of breast tissues from K5-CreER^{T/+}; Catnb^{+/ Δ ex3} and K5-CreER^{T/+}; Catnb^{+/ Δ ex3}; K19-BCL9-2 females.

A, C, E: Immunohistochemical staining as indicated of the mammary gland from a 5 month old K5-CreER^{T/+}; Catnb^{+/ Δ ex3} female. **B, D, F:** Immunohistochemical staining as indicated of the mammary gland from a 5 month old K5-CreER^{T/+}; Catnb^{+/ Δ ex3}; K19-BCL9-2 female. Inserts show the mammary tissue at higher magnification. H&E: 100x, BCL9-2 and ER α : 400x magnification.

5.6 Primary culture of breast tumor and hyperplastic glands from K19-BCL9-2 females

5.6.1 Characterization of cultured tumors cells from transgenic females

For functional experiments, primary cultures of the mammary tumors and from hyperplastic glands obtained from aged K19-BCL9-2 females were established. The primary cells grew as adherent monolayer and showed an epithelial like phenotype (Figure 24A and B).

K19-BCL9-2 hyperplastic breast cells were successfully cultured and maintained for up to 9 passages. The culture of tumor cells obtained from K19-BCL9-2 mice was maintained for up to 23 passages. In addition, the tumor cells achieved much faster full confluence compared to cells from K19-BCL9-2 hyperplastic mammary glands. This indicated stronger proliferation of the primary tumor cells. For functional assays, mammary cells from non-transgenic females were also cultured as controls. Of note, both, the cells from the hyperplastic breasts of the transgenic mice and from non-transgenic controls grew in smaller colonies compared to tumor cells.

Further examinations revealed that the primary hyperplastic gland and tumor cells retained the same markers as found by immunohistochemistry on fixed tissues. Immunofluorescence staining revealed that the cells from hyperplastic glands and tumors were strongly positive for panCK, an antibody which detects all cytokeratins and is a marker of epithelial cells (Figure 24C and D). Moreover, α SMA staining on the cells showed that the cell population contained a subset of α SMA positive myoepithelial cells (Figure 24E and F). Primary tumor cells expressed strongly β -catenin, not only at the membrane, but also in the cytoplasm (Figure 25C and D). In addition, the cells from hyperplastic glands and tumor cells showed E-cadherin staining on the membrane and in the cytoplasm (Figure 25A and B). Moreover, they expressed the luminal epithelia marker K18 and the marker for myoepithelia, SMA α (Figure 25E and F; and Figure 26, respectively). Using our specific antibody against BCL9-2, strong expression of BCL9-2 was detected in cells from hyperplastic glands and tumor cells (Figure 25Figure 26A and B). Interestingly, co-immunofluorescence staining of the tumor cells with antibodies against BCL9-2 and SMA α revealed, that both, SMA α positive and negative cell types, expressed BCL9-2 (Figure 26A). The expression of BCL9-2 was constantly detected even in the late passages.

The tumor cells were further analyzed for the expression of hormone receptors. Nuclear ER α expression was detected in cells from control glands, as well as in cells from transgenic hyperplastic glands and tumors (Figure 25C and D, and data not shown). Similar to the BCL9-2 expression, co-staining of the tumor cells with antibodies against ER α and SMA α revealed, that both SMA α positive and negative cell types, expressed nuclear ER α (Figure 26B). In addition, the expression of nuclear PR was detected in the cells from hyperplastic glands and tumors (Figure 25E and F).

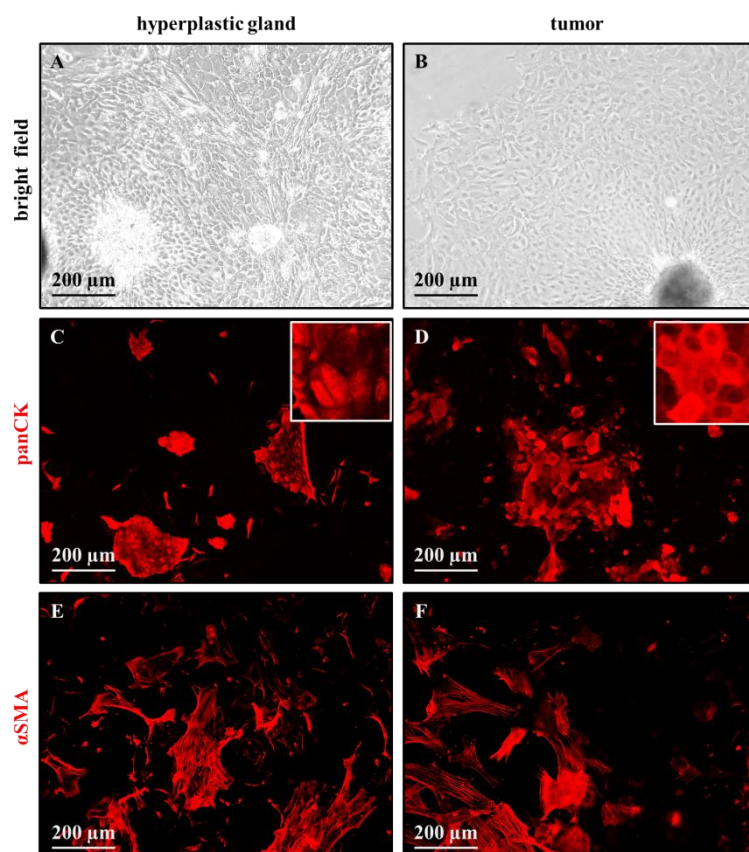


Figure 24. Immunofluorescence analyses of primary cells from hyperplastic mammary glands and mammary tumors from K19-BCL9-2 females.

A, B: Bright field images of cultured primary cells from hyperplastic mammary glands from K19-BCL9-2 females. **C, E:** Immunofluorescence staining of panCK (C) and αSMA (E) on primary cells from hyperplastic mammary glands from K19-BCL9-2 females. **D, F:** Immunofluorescence staining of panCK (D) and αSMA (F) on primary cells from mammary tumors from K19-BCL9-2 females. All images: 100x magnification.

Immunofluorescent stainings described above were performed on the non-transgenic mammary control cells, too. The expression of BCL9-2 and hormone receptors was detected in the nuclei of the cells. The quantification of the BCL9-2 and ERα protein levels in control versus hyperplastic and tumor cells was not possible based of immunofluorescence stainings. Therefore, Western Blot analyses were performed using cell lysates.

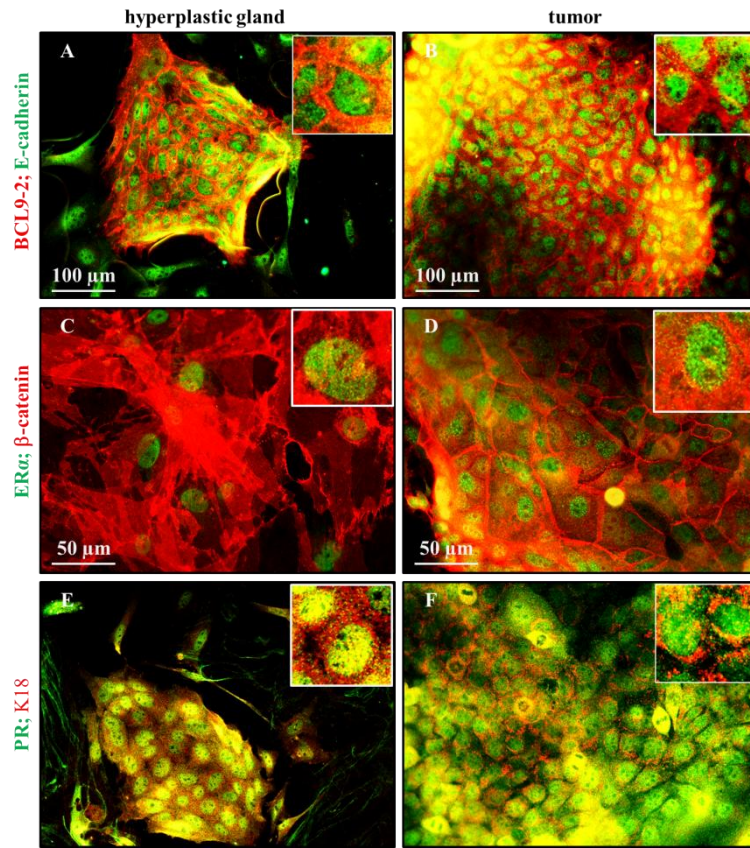


Figure 25. Immunofluorescence co-staining on primary cells from hyperplastic mammary glands and mammary tumors from K19-BCL9-2 females.

A, C, E: Images of BCL9-2 (green)/ E-cadherin (red) (A), ERα (green)/ β-catenin (red) (C), and PR (green)/ K18 (red) (E) co-staining on primary cells from hyperplastic mammary glands from K19-BCL9-2 females. **B, D, F:** Images of BCL9-2 (green)/ E-cadherin (red) (B), ERα (green)/ β-catenin (red) (D) and PR (green)/ K18 (red) (F) co-staining on primary cells from hyperplastic mammary glands from K19-BCL9-2 females. Inserts show the cells at higher magnification. BCL9-2/E-cadherin: 200x, ERα /β-catenin and PR/K18: 400x magnification.

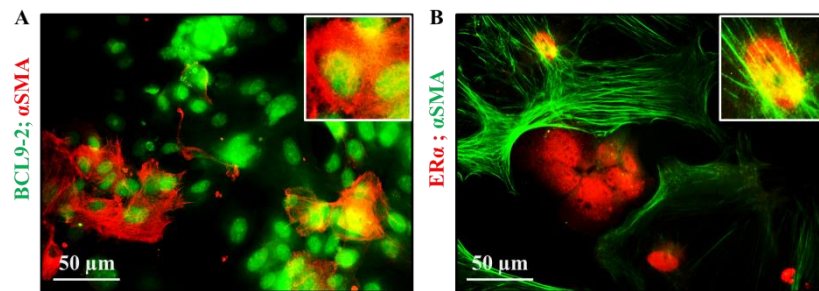


Figure 26. Immunofluorescent co-staining on primary mammary tumor cells from K19-BCL9-2 females.

A: Image of BCL9-2 (green)/ αSMA (red) on primary mammary tumor cells from K19-BCL9-2 females. **B:** Image of ERα (red)/ αSMA (green) on primary mammary tumor cells from K19-BCL9-2 females. Inserts show the tumor cells at higher magnification. 400x magnification.

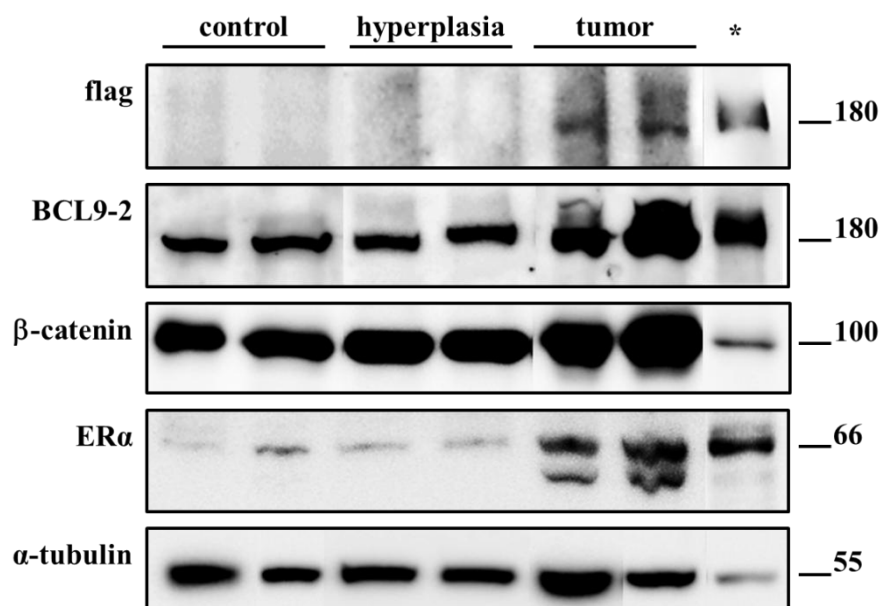


Figure 27. Western Blot analyses of BCL-2, β -catenin and ER α expression in lysates from non-transgenic control cells and from K19-BCL9-2 hyperplastic glands and mammary tumors. For the detection of transgenic BCL9-2, total BCL9-2 and β -catenin, 60 μ g of total protein lysates were used. For the detection of ER α and α -tubulin, 25 μ g of total protein lysates were used. * indicates the Western Blot analysis an whole lysates obtained from HEK293 cells after a transient transfection with the respective cDNAs and were used as positive controls.

As shown in Figure 27, both analyzed transgenic tumor cell lines expressed transgenic BCL9-2, as indicated by a 180 kDa protein band detected by an anti-flag tag specific antibody. The same band was not detected in the non-transgenic cells or in the cells from transgenic hyperplastic glands. Further Western Blot analyses revealed higher BCL9-2 protein in tumor cells compared to controls and hyperplastic cells. In addition, strong β -catenin protein expression was detected in the cell lysates from control, hyperplastic and tumor cells. However, the tumor cells showed even higher β -catenin protein levels compared to control and hyperplastic cells. Finally, the cell lysates were analyzed for ER α expression. Again, both tumor cell lines showed much higher ER α expression compared to a very weak expression in the controls and hyperplastic cells. Interestingly, the antibody against ER α detected an ER α full length specific band of appr. 66 kDa and a second band of appr. 55 kDa. This confirms, that overexpression of BCL9-2 may correlate with high levels of ER α in K19-BCL9-2 tumor cells.

5.6.2 Estrogen treatment of cultured tumor cells enhances their viability

The proliferation of many human ER α positive breast cancers and breast cancer cell lines is known to be dependent on estrogen (130). Since the tumor cells from K19-BCL9-2 females express high nuclear ER α , the aim of the following experiments was to test, if these cells depend on the stimulation or inhibition of the estrogen pathway. Therefore, the viability and proliferation of the K19-BCL9-2 tumor cells after treatment with an anti-estrogen (tamoxifen) or estrogen was analyzed.

The normal culture medium for the propagation of our primary cells was supplemented with 5% calf serum that contains several hormones including estrogen. In addition, this medium contained phenol red, which was reported to have estrogenic action (131-133). To reduce hormone-active supplements from the medium before treatment with estrogen, the primary cells were cultured in phenol red free medium supplemented with charcoal stripped fetal calf serum and their viability was tested. However, it was not possible to perform experiments under hormone reduced conditions, since the cells did not survive in the hormone reduced, phenol red free medium. The MTT and BrdU incorporation assays were therefore performed in complete medium.

First, different concentrations of estrogen and tamoxifen were used to determine the best conditions for stimulation of the cells. Estrogen and tamoxifen at concentrations of 0.5; 1; 3.6; 7 and 10 μ M were administrated. As controls, the cells were treated with 0.1 % (v/v) EtOH, which served as vehicle for estrogen and tamoxifen. The cell viability was measured in a MTT assay after 48 hours.

As shown in the Figure 28, the viability of cells from non-transgenic glands was not affected after 48 hours stimulation with any concentration of estrogen. The stimulation of transgenic tumor cells with estrogen led to a slight increase of cell viability after 48 hours with each hormone concentration used for stimulation. The highest effect on cell viability of the tumor cells was measured after stimulation with 3.6 μ M estrogen.

Treatment with the anti-estrogene tamoxifen showed different effects on cell viability: High concentrations of tamoxifen (7 and 10 μ M) led to death of both, control and transgenic tumor cells after 48 hours of incubation. The viability of control cells was

however not affected by lower tamoxifen concentrations, but they even were further growing after 48 hours of treatment with 0.5-3.6 μM tamoxifen. In contrast, the viability of tumor cells by low concentrations of tamoxifen was not reduced and was comparable to that of the cells treated with vehicle. Thus, treatment with low concentrations of tamoxifen up to 3.6 μM did not show toxic effects on the cells.

However, compared to non-transgenic control cells, the viability of the tumor cells was higher after stimulation with 3.6 μM estrogen.

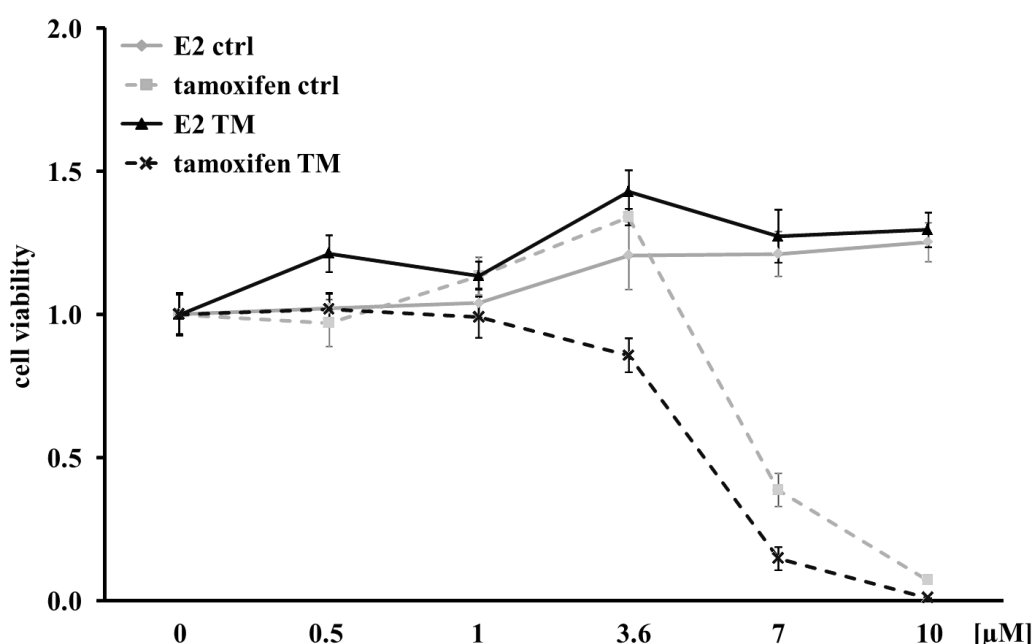


Figure 28. Estrogen and tamoxifen toxicity test on non-transgenic mammary gland cells and K19-BCL9-2 tumor cells.

The non-transgenic control cells and the cells from K19-BCL9-2 breast tumors were treated with the indicated estrogen or tamoxifen concentrations for 48 hours. Cells treated with 0.1% EtOH as vehicle in culture medium were used as untreated control.

Based on the results of the toxicity test, the concentration of 3.6 μM for both estrogen and tamoxifen, were considered as an appropriate non-toxic concentration to carry out MTT cell viability and BrdU proliferation assays.

A time course for cell viability using the MTT assay was performed to address the question if the addition of tamoxifen or estrogen to the medium alters the viability of the primary cultured cells from the transgenic hyperplastic glands or tumors for up to 96h. Cells from non-transgenic females were used as controls.

Results

The cells received 3.6 μ M tamoxifen or estrogen and the viability of cells was measured after 24, 48, 72 and 96 hours.

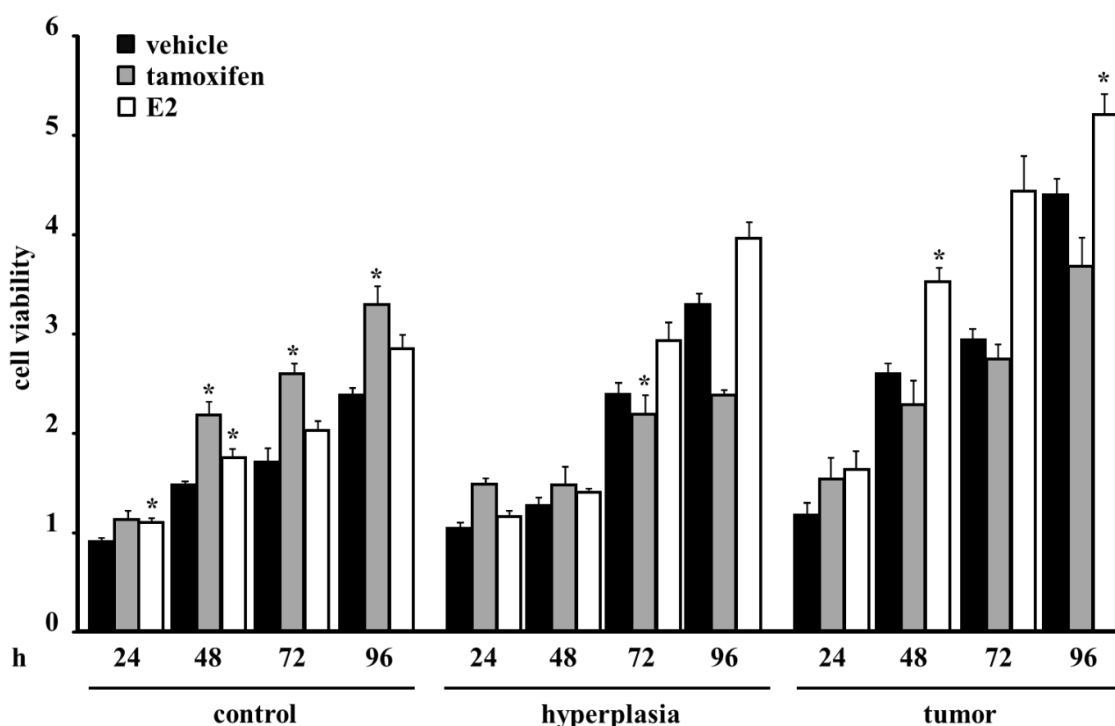


Figure 29. MTT assay on non-transgenic mammary gland cells, cells from K19-BCL9-2 hyperplastic glands and mammary tumors.

The non-transgenic control cells, cells from K19-BCL9-2 hyperplastic glands and mammary tumors were treated with 3.6 μ M tamoxifen or estrogen over 96 hours. Cells treated with 0.1% EtOH as vehicle in the culture medium were used as untreated control. * indicates significant differences with $p < 0.05$.

The stimulation with estrogen led to a slight increase of the viability of control cells. Surprisingly, the treatment of the non-transgenic cells with tamoxifen had similar effect like estrogen, and also increased the cell viability (Figure 29, left graph). The cells from hyperplastic mammary glands of transgenic females behaved differently after treatment with tamoxifen and estrogen.

After 72 and 96 h, the cell viability of the cells from hyperplastic mammary glands was slightly reduced, while the stimulation with estrogen increased the cell viability at these time points (Figure 29, middle graph). Finally, the treatment of transgenic tumor cells with tamoxifen and estrogen showed similar results as found for the cells from hyperplastic mammary glands of K19-BCL9-2 females. While the administration of tamoxifen slightly reduced the viability of the tumor cells after 48 hours, es-

trogen stimulation significantly ($p < 0,002$) increased their viability after 48 and 96 hours compared to vehicle treated cells (Figure 29, right graph). The viability of the tumor cells was still higher after 96 hours of tamoxifen treatment compared to 24 hours of treatment. This indicated that reduced viability of the tumor cells was not due to a toxic effect of tamoxifen at the concentration of 3.6 μM . Moreover, tumor cells showed an increased viability in response to estrogen after 96 hours, which was not observed for control cells.

5.6.3 Tamoxifen treatment of cultured tumor cells reduces their proliferation

The BrdU assay was performed to address the question if the proliferation of the primary hyperplastic and tumor cells can be altered by tamoxifen or estrogen treatment. Cells from non-transgenic females were used as controls. The cells received 3.6 μM tamoxifen or estrogen and the BrdU incorporation was analyzed after 12, 24, 36 and 48 hours. In contrast to the MTT assay, cell proliferation can be directly measured by DNA synthesis based on the incorporation of BrdU into the cells.

The stimulation of the non-transgenic cells with tamoxifen increased the BrdU incorporation after 24 hours. In contrast, after 36 hours of tamoxifen treatment cells proliferated less than cells which received the medium containing the vehicle (Figure 30, left graph). Compared to that, the stimulation of the control cells with estrogen enhanced the BrdU incorporation only after 36 hours. After 48 h, based on the BrdU incorporation, the vehicle treated control cells stopped to proliferate after 48 hours, but the addition of estrogen still stimulated their proliferation (Figure 30, left graph). Treatment of cells from the transgenic hyperplastic mammary glands with tamoxifen showed a slight reduction of BrdU incorporation, while estrogen increased the proliferation of the cells strongly after 48 hours (Figure 30, middle graph). Interestingly, the tumor cells still proliferated strongly after 36 and 48 hours, as shown for the vehicle treated cells (Figure 30, right graph). Moreover, tamoxifen administration significantly ($p < 0.05$) reduced the proliferation of the tumor cells after 36 and 48 hours, while estrogen stimulated their proliferation at that time point.

5.6.4 Mammary tumor cells from K19-BCL9-2 generate tamoxifen sensitive colonies in vitro

To examine the differentiation potential of mammary tumor cells from K19-BCL9-2 females, 2D- and 3D collagen cultures with non-transgenic control cells and cells from K19-BCL9-2 tumors were established. Control and tumor cells cultured in 3D system were unable to proliferate and died. In contrast, cells cultured on 2D collagen proliferated and were organized as

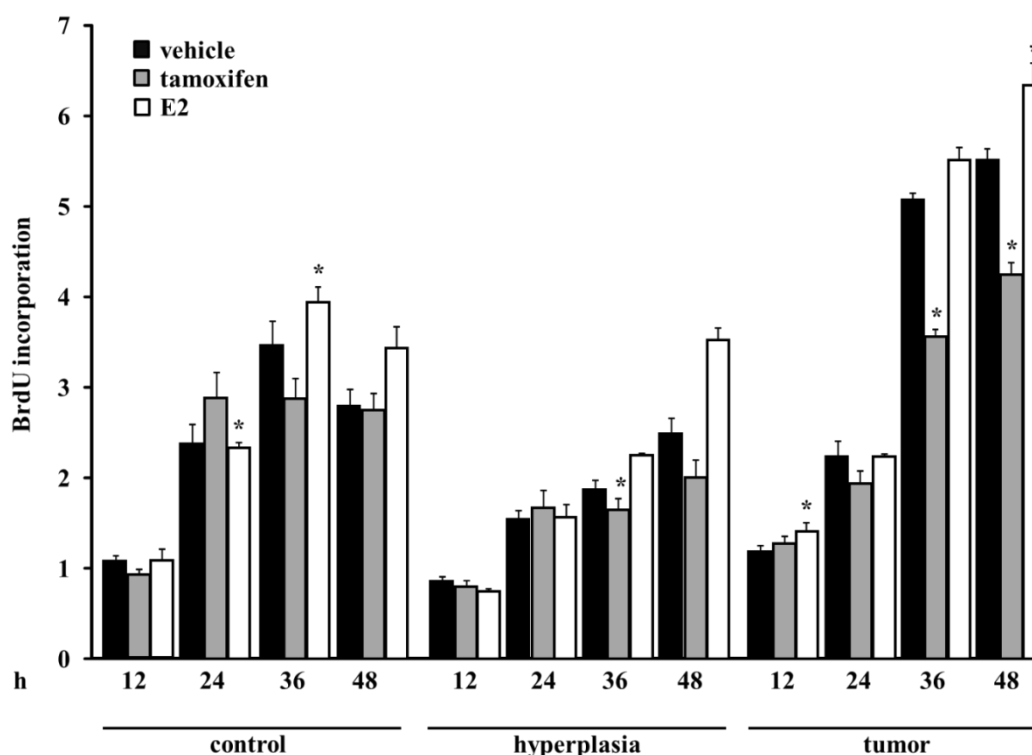


Figure 30. Proliferation assay on non-transgenic mammary gland cells, cells from K19-BCL9-2 hyperplastic glands and mammary tumors.

The non-transgenic control cells, cells from K19-BCL9-2 hyperplastic glands and mammary tumors were treated with 3.6 μ M tamoxifen or estrogen over 48 hours. Cells treated with 0.1% EtOH as vehicle in culture medium were used as untreated control. For BrdU incorporation, the cells were incubated with BrdU solution 12 hours prior to measurement. * indicates significance with $p < 0.05$.

colonies after 4 days. The colonies developed also duct-like structures (Figure 31A). Treatment of the primary tumor cells in 2D culture with estrogen led to an increased number of colonies, while the cells from non-transgenic mammary glands developed similar numbers of colonies compared to vehicle treated cells (Figure 31B). Moreover, the number of colonies generated by tumor cells was reduced by treatment with tamoxifen. In addition, the tumor cell colonies treated with tamoxifen died sooner

than colonies treated with vehicle or estrogen. In contrast, the number of colonies from control cells even increased initially after tamoxifen administration, but then died already after a few days (Figure 31B).

Immunofluorescence studies of the colonies showed that the colonies generated under treatment with vehicle alone or with estrogen, consisted of epithelial cells with tight cell-cell contacts. The cells were strongly positive for panCK and expressed membranous β -catenin (Figure 32A and B).

Taken together, the protein expression analyses and functional examinations of primary cultured cells indicate, that the overexpression of BCL9-2 may account for development of ER positive tumors, which growth depends on the ER action.

5.7 BCL9-2 is overexpressed in hormone receptor positive human mammary breast cancers

5.7.1 Human breast cancer cell lines express different levels of BCL9-2

We recently characterized the expression of BCL9-2 in a panel of human colon cancer cell lines (93). Similarly, the expression of endogenous BCL9-2 in different human breast cancer cell lines was analyzed by Western Blot analyses. High levels of BCL9-2 were detected in ER α positive cell lines (MCF7 and T47D) and in the HER2 positive breast cancer cell line SKBR3 (Figure 33). Triple negative cell lines MDA-MB-231 and BT549 expressed moderate levels of BCL9-2. Furthermore, the expression of BCL9-2 was analyzed in a non-tumorigenic human epithelial breast cell line derived from a fibrocystic breast disease (MCF10a). These cells expressed the lowest amounts of BCL9-2 of all analyzed cell lines. HEK293 cells were used as negative control since they do not express BCL9-2. All analyzed cell lines, with the exception of SKBR3, expressed β -catenin in different amounts (Figure 33). Thus, in human breast cancer cell lines, the amount of BCL9-2 is higher in hormone receptor and HER2 positive cell lines.

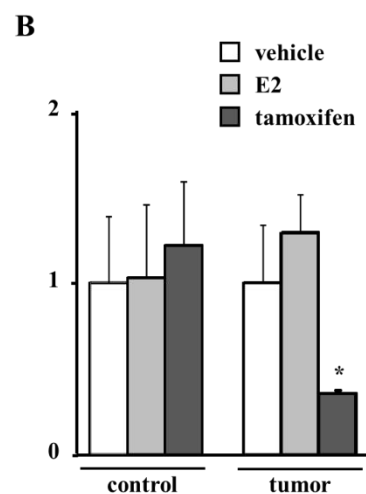
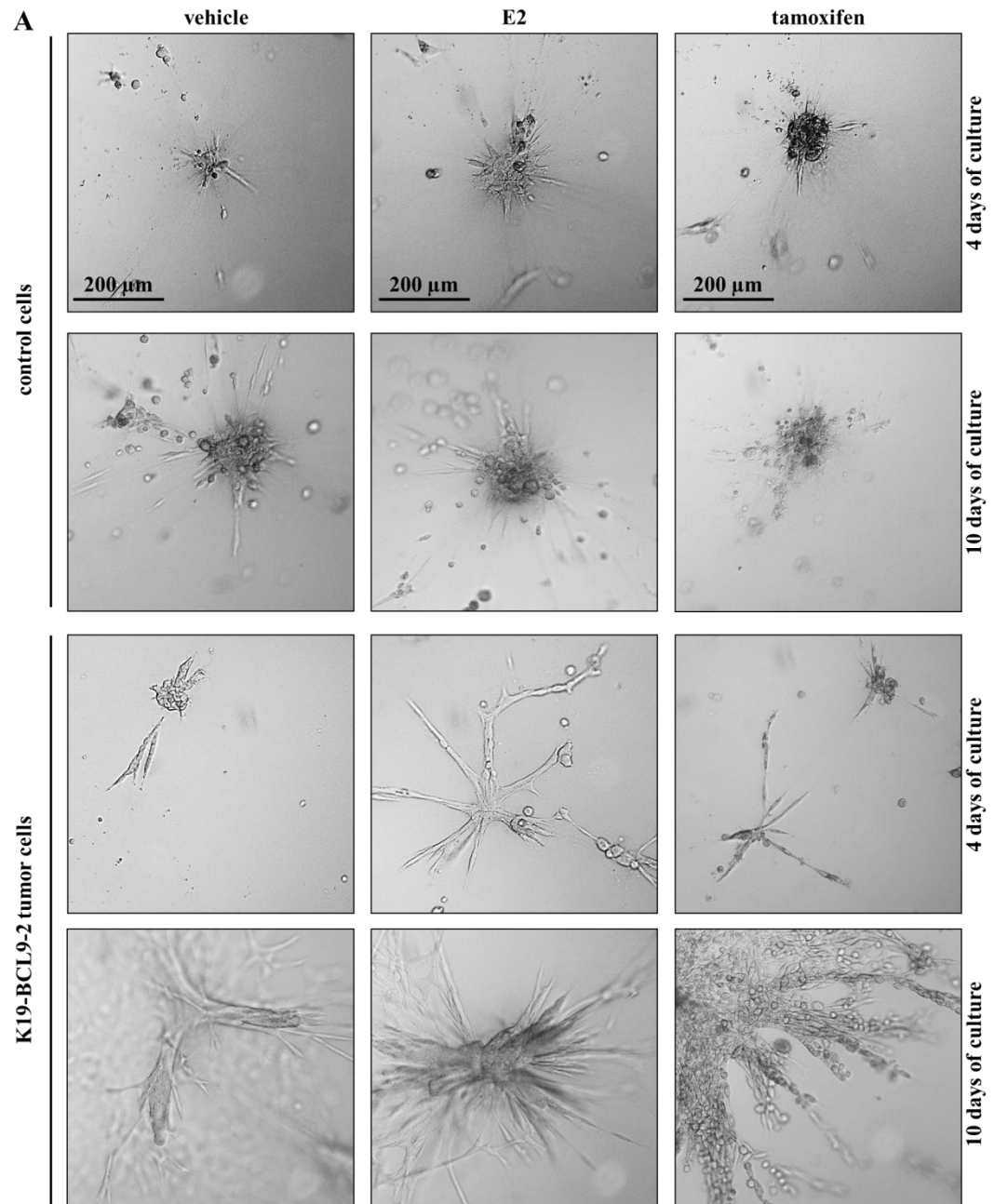


Figure 31. 2D collagen assay.

Cells from non-transgenic glands and K19-BCL9-2 tumors were seeded on top of collagen gels (10^3 cells/96well) and treated with $3,6 \mu\text{M}$ estrogen or tamoxifen. **A.** Upper panel: colonies generated by non-transgenic cells after 4 and 10 days of culture. Lower panel: colonies generated by K19-BCL9-2 cells after 4 and 10 days of culture. 100 x magnifications. **B.** Quantification of colony numbers after estrogen or tamoxifen treatment made by cells from non-transgenic glands and K19-BCL9-2 tumors after 4 days of culture.

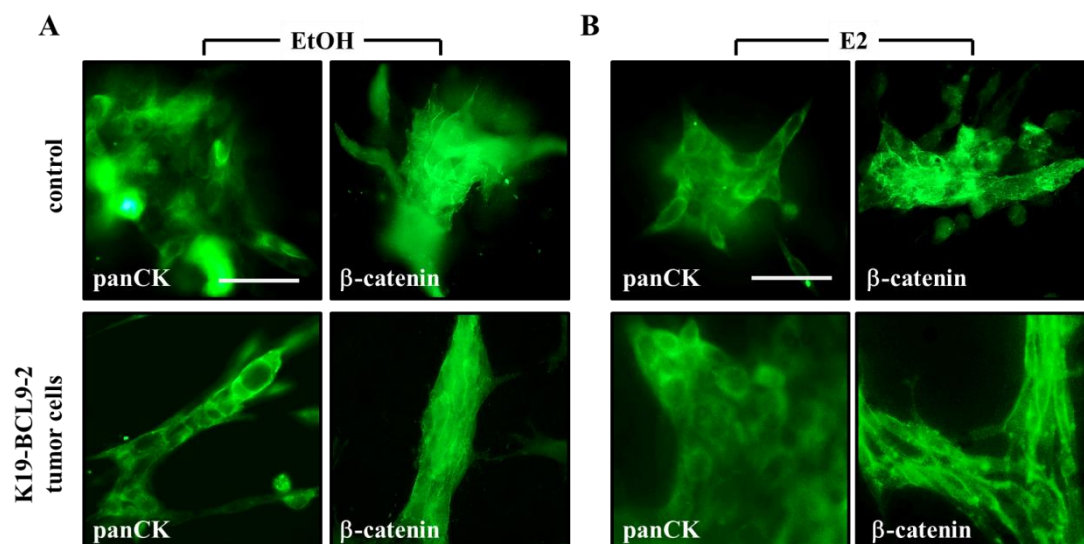


Figure 32. Immunofluorescent staining on colonies from non-transgenic mammary cells and mammary tumor cells from K19-BCL9-2 females in a 2D collagen assay.

A: Representative images of panCK and β -catenin staining on colonies from non-transgenic and K19-BCL9-2 tumor cells after 10 days of vehicle (0.1% EtOH) treatment. **B:** Representative images of panCK and β -catenin staining on colonies from non-transgenic and K19-BCL9-2 tumor cells after 10 days of estrogen treatment. All images were taken at 200x magnification.

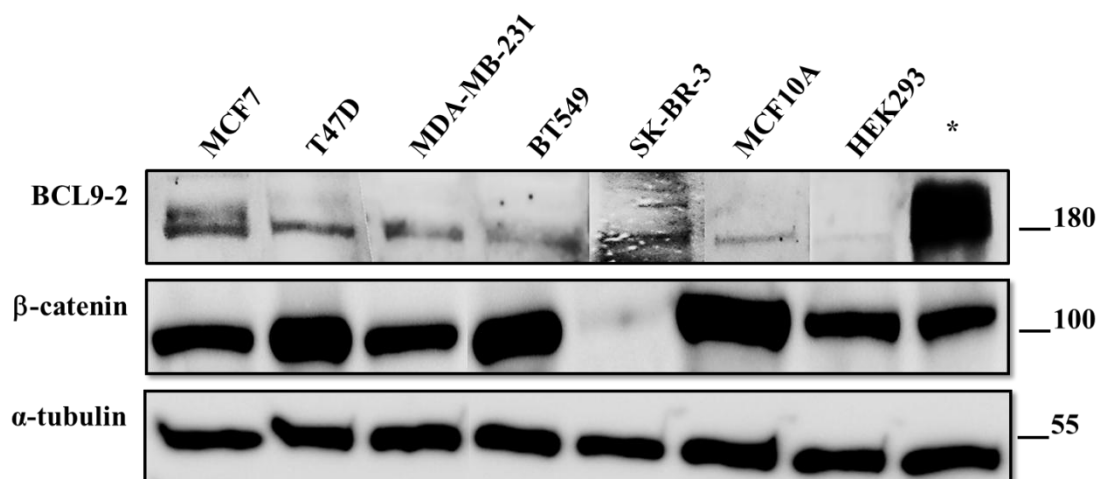


Figure 33. Western Blot analyses of endogenous BCL9-2 expression in different human breast cancer cell lines

60 μ g of total protein from whole cell lysates from the indicated cell lines were used to detect BCL9-2 and β -catenin. Whole cell lysates from HEK293 were used as control. * indicates protein lysates obtained from HEK293 cells after transient transfection as positive controls.

5.7.2 Knock down of BCL9-2 in MCF7 leads to reduced expression of ER α and its target genes

To examine if BCL9-2 is able to regulate ER α itself and its target genes, a siRNA-mediated BCL9-2 knock down in the hormone receptor positive cell line MCF7 was performed. The expression of ER α was analyzed by qRT-PCR and Western Blot. In addition, the expression of ER α regulated genes GREB1 and PR was analyzed by qRT-PCR. All experiments were performed and analyzed together with a bachelor student, Christopher Diederichs.

Using specific siRNAs against BCL9-2, the BCL9-2 protein expression was reduced after 48 and 72h (Figure 34A). qRT-PCR revealed that transfection of cells with siRNA against BCL9-2 led to an approximately 70 % reduction of BCL9-2 RNA at 48 and 72h (Figure 34B).

Western Blot analyses of ER α protein expression revealed only a reduction after 48 hours of siBCL9-2 treatment, which was not detected after 72 hours (Figure 34A). Similarly, qRT-PCR results showed a 50 % and 25 % reduction of ER α RNA expression after 48 and 72 hours of siBCL9-2 treatment, respectively (Figure 34B).

The qRT-PCR analyses of ER α target gene expression revealed, that the expression of both PR and GREB1 was significantly reduced after 48 hours of siBCL9-2 treatment (20% and 25 %, respectively), but no reduction was found after 72 hours (Figure 34B). These results indicate an implication of BCL9-2 in ER α signaling.

5.7.2 BCL9-2 expression correlates with the expression of ER α , PR and HER2

Toya et al. 2007 characterized for the first time BCL9-2 expression in human normal breast epithelium and breast cancer tissues by immunohistochemical analyses. Immunohistochemical stainings on three breast cancer tissue microarrays was performed to analyze the BCL9-2 expression. In total, the tissue microarrays provided 194 breast cancer samples from 99 patients. In addition, they contained 30 cases of corresponding uninvolved breast tissue. To estimate the immunohistochemical expression of nuclear BCL9-2 in normal and cancer epithelium an expression score was calculated. The same expression score we already used to evaluate the immunohisto-

chemical expression of nuclear BCL9-2 in human colon cancers (93). It contained a rating of staining intensity and amount of positive epithelia (see Material and Methods).

First, a comparison of histologically normal breast epithelium from uninvolved breast tissue samples and cancer cases for the BCL9-2 expression was performed (Figure 35A). In normal breast epithelia the expression of BCL9-2 showed median expression of 3. In contrast, the expression of BCL9-2 in breast cancer epithelium of 194 cancer cases was significantly higher than in controls and showed the median expression of 5 (Figure 35B, left).

The tissue microarrays provided grading data for the tumors. The expression of BCL9-2 was analyzed in tumors of grade one to three (n= 16, 116, 38, respectively). Mann-Whitney analyses revealed a decrease of BCL9-2 expression as the tumor grade became higher. However, BCL9-2 expression in tumors of grade three was still significantly higher (median expression of 4) than in control tissue (Figure 35B, left).

The tissue microarrays provided immunohistological expression data for ER, PR and HER2. To analyze if BCL9-2 expression correlates with the expression of these receptors, the cancer cases were subdivided into four groups. The expression of BCL9-2 in the group of tumors which were defined as triple negative (n= 48) was slightly higher compared to control tissue. This group of tumors included tumors with no expression of nuclear hormone receptors and with HER2 expression score of 0 and 1. BCL9-2 expression was significantly higher in tumors which were HER2 receptor positive (n= 64), or expressed nuclear hormone receptors ER α and PR (n= 26), or were defined as HER2, ER α and PR positive (n= 53) (Figure 35B, right).

To further analyze, that BCL9-2 expression correlates with the expression of these receptors, the cancer cases were subdivided into 3 groups based on their BCL9-2 expression score as follows: 0-3 for low (n = 42), 4-6 for moderate expression (n = 72); and 7-9 for high expression of BCL9-2 (n = 45). Mann-Whitney test revealed that the group of the tumors with the highest expression of BCL9-2 showed a significantly higher expression of ER, PR and HER2 compared to tumors with low BCL9-2 expression ($p < 0.05$). Moreover, a Spearman-Rho analysis showed that the expres-

sion of all 3 analyzed receptors positively correlated with the expression of BCL9-2 ($p < 0.00007$, < 0.00002 , and < 0.03 , respectively) (Figure 36).

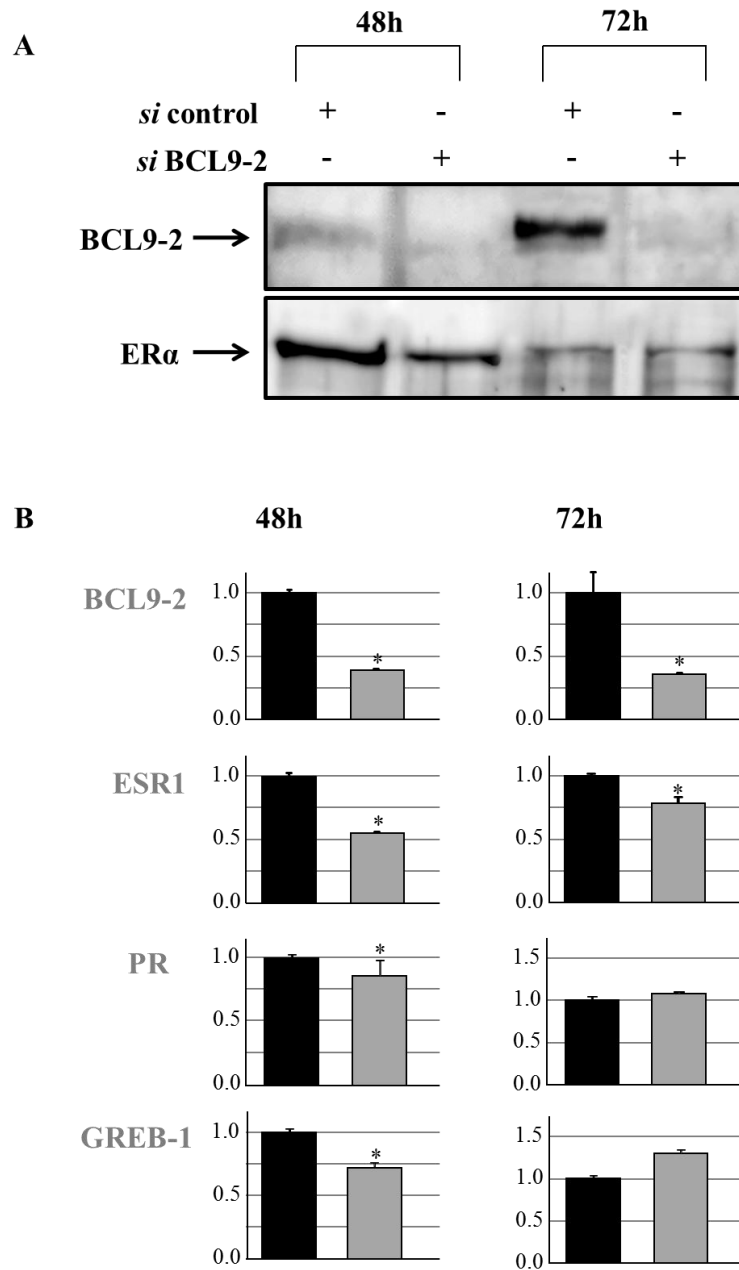


Figure 34. Expression analyses of BCL9-2, ER α and its target genes in MCF7 after BCL9-2 knock down.

A: Western Blot analyses of BCL9-2 and ER α protein expression after BCL9-2 knock down. Nuclear protein extracts 48 and 72 hours after BCL9-2 knock down were used. **B:** qRT-PCR analyses of ER α and its target genes after BCL9-2 knock down. qRT-PCR was performed 48 and 72 hours after BCL9-2 knock down. 40 ng of cDNA from MCF7 48 and 72 hours after BCL9-2 knock down were used.

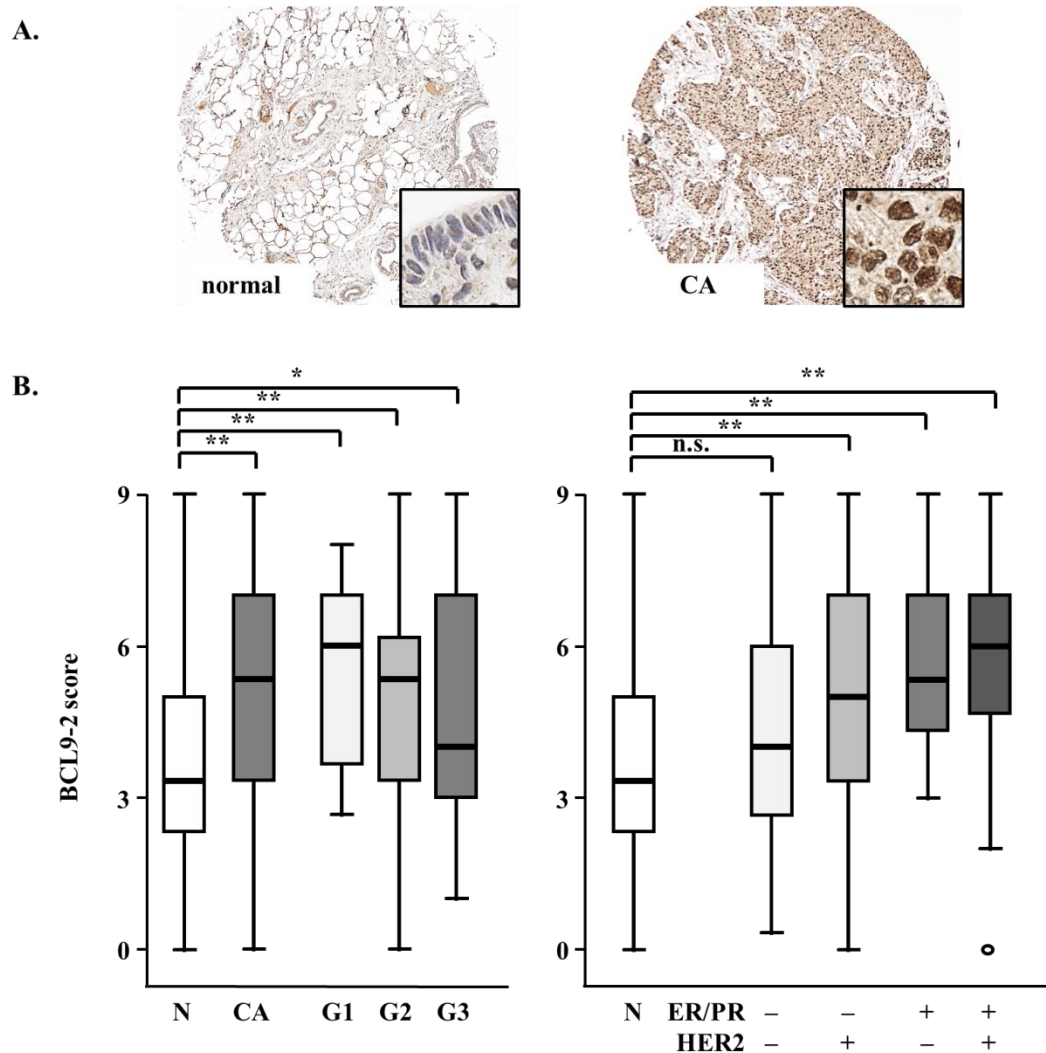


Figure 35. Human breast cancer express higher levels of BCL9-2 compared to normal breast tissue and correlates with the expression of ER,PR and HER2.

A. Representative images of immunohistochemical staining of BCL9-2 in normal human breast tissue and in invasive ductal carcinoma of the breast. **B.** Left: Expression of BCL9-2 was compared between 30 samples of normal breast tissue samples and 194 breast cancer tissue samples and for the pathological grade of the tumors. Right: Expression of BCL9-2 was compared between 30 samples of normal breast tissue samples and 194 breast cancer tissue samples based on the expression of nuclear hormone receptors and Neu. For statistical analyses a Mann-Whitney test was performed. * $p < 0.05$, ** $p < 0.005$.

Taken together, the analyses of BCL9-2 expression on human breast cancer tissue further confirm a correlation between high BCL9-2 expression and development of hormone receptor positive breast tumors in humans.

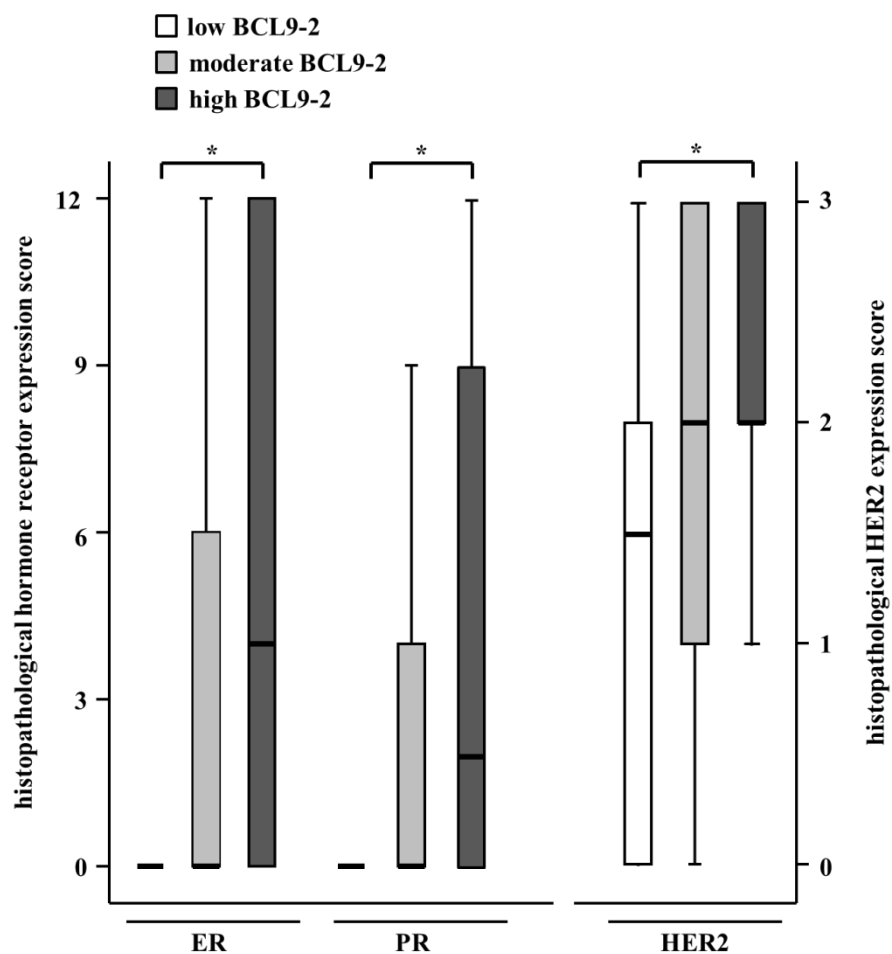


Figure 36. High nuclear ER α and PR and HER2 expression correlates with high expression of BCL9-2 in human breast cancer.

The graphs show the box plot analyses of nuclear hormone receptor and Neu expression score in breast cancer samples with low, moderate and high BCL9-2 expression score. For statistical analyses a Mann-Whitney test was performed. * $p < 0.05$

6. Discussion

The role of BCL9 proteins has been discussed the recent years. While a connection of BCL9 to B-cell Lymphoma was clearly established (87, 91), BCL9-2 was found to be involved in tumorigenesis in the epithelial tissues. We and others recently demonstrated the relevance of BCL9-2 in intestinal tumorigenesis in human and mice (89, 91, 93, 95). We found that BCL9-2 was highly expressed in adenoma of APC^{Min/+} mice and in humans. Moreover overexpression of BCL9-2 enhanced adenoma formation in APC^{Min/+} mice and led to progression by inducing local invasion of the tumor cells beyond the mucosa. In addition, we found that BCL9-2 was highly expressed in human colorectal cancers. The role of BCL9-2 in other carcinoma was not analyzed in details yet. Toya et al. 2007 presented the only immunohistochemical study on human ductal carcinoma in situ and invasive ductal carcinoma of the breast. Here, BCL9-2 was overexpressed in the breast tumors compared to the normal breast epithelium.

The study presented here shows for the first time, that overexpression of BCL9-2 *in vivo* leads to breast tumor development. Moreover, the results suggest a mechanism of BCL9-2 oncogenic action in the breast by interfering with ER α signaling.

6.1 Overexpression of BCL9-2 leads to tumorigenesis *in vivo*

To examine the oncogenic potential of BCL9-2 *in vivo*, a novel transgenic mouse model on a C57BL/6N background was established. The overexpression of the transgene was regulated by the keratin 19 (K19) promoter. K19 is expressed in the simple epithelia of several organs including the proliferative compartments of the stomach, small intestine, colon and ductal epithelia of the pancreas and mammary gland (106-109). Aged transgenic animals (older than 15 month) developed macroscopic tumors of the pancreas and small intestine with higher incidence than control animals. Females of all analyzed founder lines developed mammary gland tumors, whereas tumors of the breast were never found in control animals. In addition, a number of transgenic females displayed macroscopic breast tumors, developed pulmonary metastases. The transgene was established on a pure C57BL/6N background,

which is known to be more resistant to tumor development compared to other different mouse strains (134, 135), already indicating an oncogenic potential of BCL9-2 overexpression.

Breeding K19-BCL9-2 mice with APC^{Min/+} mice increased breast tumor number. Compound MMTV^{Cre};Catnb^{+/ Δ ex3}; K19-BCL9-2 developed macroscopic tumors of the breast, whereas MMTV^{Cre};Catnb^{+/ Δ ex3} only displayed breast epithelial hyperplasia. These results indicate that overexpression of BCL9-2 can lead or contribute to development of macroscopic tumors.

No macroscopic tumors were observed in K5-CreER^{T/+}; Catnb^{+/ Δ ex3}; K19-BCL9-2 females. The absence of macroscopic tumors in these compound females may be due to distinct spatial promoter activity used in this model. Keratin 5 (K5) is a basal epithelium specific keratin (71). Therefore, the Cre-mediated stabilization of β -catenin and the resulting hyperactivation of Wnt signaling take place within the myoepithelial cells of the breast epithelium, using K5 promoter-driven Cre recombinase expression. The overexpression of BCL9-2 under the K19 promoter occurs exclusively in the luminal breast epithelia. Thus, the simultaneous expression of both, stabilized β -catenin and BCL9-2, within the same cell is not achieved. In contrast, usage of MMTV-Cre system enables a coincident expression of stabilized β -catenin and BCL9-2 in the same luminal cells, since the MMTV promoter is reported to be activated predominantly in the luminal epithelial compartment of the breast (105, 129). The APC^{Min/+} model also provides a coexistent expression of stabilized β -catenin and of BCL9-2 in the same cell, since the mutation of the APC gene is maintained in every cell of the organism (136, 137). The simultaneous deregulation of β -catenin and BCL9-2 in the same ductal cell may have therefore synergistic effect leading to oncogenic transformation of the cell.

6.2 Overexpression of BCL9-2 leads to mammary gland hyperplasia *in vivo*

The epithelial hyperplasia in the breast is associated with higher cancer risk. Serial transplantation of hyperplastic mouse breast epithelium from p53 heterozygous or

homozygous null mice or mice infected with MMTV (Mouse Mammary Tumor Virus) results in the development of tumors, impressively demonstrating the malignant potential of hyperplastic lesions (13, 119-121, 138). Enhanced development of hyperplastic alveolar nodules (HANs) in the terminal parts of the ducts and ductal dilatation in the K19-BCL9-2 transgenics compared to controls were detected in this study. Moreover, increased hyperplastic foci in the glands of compound MMTV^{Cre};Catnb^{+/ Δ ex3}; K19-BCL9-2 females were found, too.

In humans and mice, there is a process taking place as the organism ages, called age-related involution. During this process, the mammary gland loses its complexity and function due to regression of its glandular/secretory structures such as alveoli and terminal ducts. Progressed age-related involution was shown to negatively correlate with risk of breast cancer (4, 122). Different studies showed an extensive alveolar phenotype of the breast, accompanied by breast tumor development. This is the case for several Wnt/ β -catenin pathway-deregulated mouse models, such as MMTV-Wnt10b, MMTV-CyclinD1 or MMTV-Wnt1 (43, 64, 69, 70, 139-141). The surprising finding of the present study was the extensive alveolar morphology, which still persisted in the mammary glands of aged transgenic females. This morphology was very reminiscent of a mammary gland from pregnant or lactating females which is characterized by extensive alveolar development. Our findings indicate a delayed age-related involution accompanied by hyperplasia of the aged transgenic mammary gland, which is consistent with preneoplastic changes.

Delayed postlactational involution is correlated with higher breast cancer risk. The work on different mouse models clearly demonstrated a connection between prolonged mammary postpartum involution and mammary tumor development (64, 73). Based on that, postlactational involution was defined as a special window for breast cancer susceptibility (122, 142, 143). In this thesis, we analyzed females during the phase of the postlactational involution at day 10 and 20. We found greater alveolar structures persisting in the glands of transgenic females on day 10 of involution, which were less present in controls. Based on this, we concluded that K19-BCL9-2 animals displayed delayed involution. Interestingly, the transgenic alveolar epithelium showed a higher proportion of BrdU-labeled cells than found in control glands. This result indicates that the extensive alveolar morphology may be a consequence of

an enhanced proliferation of the transgenic epithelium after weaning. Capuco et al. reported that pregnancy indirectly inhibited mammary involution by increasing the proliferation of mammary epithelial cells. This was indicated by an increased number of BrdU incorporating epithelial cells in the mammary gland of mice which were pregnant at the time point of weaning (144). In the present study high BCL9-2 expression was found during ductal outgrowth and pregnancy in the wild-type mammary gland, which overlaps with Wnt/ β -catenin signaling activity at these stages (145). Based in that, one could speculate that high expression of BCL9-2 may be linked to high proliferation and /or differentiation of the mammary epithelia, which usually takes place during puberty and pregnancy.

Taken together, using the K19-BCL9-2 mouse model, we could target mammary epithelial cells for the overexpression of BCL9-2. We demonstrated for the first time that elevated level of BCL9-2 in the epithelia of the mammary gland has the potential to mediate a premalignant state of the epithelium. Moreover, we showed that overexpression of BCL9-2 leads to tumor development *in vivo*, confirming an oncogenic potential of BCL9-2.

6.3 BCL9-2 overexpression may mediate EMT in breast tumors

The breast tumor from K19-BCL9-2 females barely expressed E-cadherin, as was detected by immunohistological staining of the tissue samples. Loss or inactivation of E-cadherin is associated with invasive lobular carcinoma and EMT (epithelial-mesenchymal transition), which enables a tumor to invade and metastasize (110, 112, 113, 146-150). Interestingly, Mani et al., 2008 showed that human and murine mammary cells defined by expression of CD24^{low}/CD44^{high} displayed stem cell like properties and showed expression of markers associated with EMT, including loss of E-cadherin expression (147). Our previous studies already showed, that overexpression of BCL9-2 in normal epithelial cells induces EMT and an increase in cell migration capacity. siRNA mediated down regulation of BCL9-2 could revert the cells to the epithelial phenotype (54). Moreover, we found that overexpression of BCL9-2 *in vivo* induces invasion of adenoma in compound APC^{Min/+}; K19-BCL9-2 mice (93).

These data was consistent with reduced expression of EMT markers in adenomas from BCL9/BCL9-2 double knockout mice (95). Taken together, these findings suggest that BCL9-2 may regulate E-cadherin expression, thereby mediating invasion and EMT.

6.4 Overexpression of BCL9-2 may interfere with ER α

Histological examinations of the breast tumors from K19-BCL9-2 females revealed a spectrum of distinct tissue differentiation. This morphological variety was previously described for Wnt signaling associated tumors in different mouse models (13, 126, 140, 151). We found well differentiated tumors, with well-established luminal and myoepithelial layers. This type of tumor tissue differentiation is described as “type-P” (Pregnancy-dependent or Plaque-like) tumors and show predominantly ductule architecture (126). Interestingly, those well-differentiated breast tumors from K19-BCL9-2 females displayed distinct, myoepithelial-like differentiated areas. Such less differentiated, myoepithelial-like tumor pattern can be found adjacent to well differentiated type-P-like pattern in Wnt pathway tumors (126). However, a panel of K19-BCL9-2 cancers showed a differentiation reminiscent of lobular carcinoma found in humans. These tumors expressed markers of the luminal and basal breast epithelium, too.

Intriguingly, BCL9-2 expression among the distinct histological pattern of K19-BCL9-2 mammary tumors changed. It was high in the well differentiated tumors, in luminal-like as well as in myoepithelial areas. In contrast, the lobular-like tumor tissues displayed defined BCL9-2 expression with the high expression limited to ductal cells and a weak staining of BCL9-2 in single tumor cells. The staining of K19 luminal marker revealed similar expression pattern in the lobular-like K19-BCL9-2 tumors. However, transgenic BCL9-2 RNA expression was high in the lobular-like tumors, indicating that the transgenic BCL9-2 contributed to the development and progression of this type of tumors.

The probably most impressing result of this study is the nuclear expression of ER α and PR in all K19-BCL9-2 mammary tumors. This finding represents a unique characteristic of the K19-BCL9-2 mouse model, since the most mouse breast cancer models show no or low levels of nuclear ER α and PR and are not hormone respon-

sive (117). In contrast, many human breast cancers are characterized by nuclear ER expression and a subtype of these tumors are also hormone responsive. In fact, ER α is the most common anti-hormonal therapeutic target for the treatment of such tumors (130, 152, 153). There are a few Wnt pathway models that develop ER α positive breast tumors (117, 152). A tumor growth dependency on hormones was already demonstrated for Wnt1 transgenic mice (154). In this study we showed that the proliferation of the primary K19-BCL9-2 tumor cells was reduced by tamoxifen, an antagonist of the estrogen receptor. In addition, in 2D collagen culture, the tumor cells developed ductal-like epithelial colonies. The number of those structures was higher after estrogen treatment. Treated with tamoxifen, the number of the epithelial colonies was lower compared to vehicle control and the cells died after several days. Moreover, examination of primary cells revealed higher ER α protein levels in K19-BCL9-2 mammary tumor cells compared to non-transgenic control cells. These results indicate that the growth of the K19-BCL9-2 breast tumors is dependent on ER α , thus implying a possible correlation between overexpression of BCL9-2 and ER α expression.

This assumption is further supported by the immunohistological BCL9-2 expression data, obtained from wild-type animals in this thesis. The strongest expression of endogenous BCL9-2 was detected during the puberty within the epithelium of the terminal end buds (TEBs), and in the late pregnancy. Interestingly, the proliferating activity of the outgrowing pubertal ductal epithelium is regulated by estrogen and its receptor (10, 11). In addition, in the mammary glands the levels of ER α are high during pregnancy (13, 155-157). These findings indicate a time matched high expression of both, ER α and BCL9-2 in the proliferating mammary epithelium of pubertal and pregnant females, and in mammary tumor cells. Thus, BCL9-2 may be a novel candidate to interfere with ER α expression and action.

6.5 Overexpression of BCL9-2 may lead to oncogenic transformation of stem/ progenitor cells in the mammary gland

No pillar-like differentiation or squamous metaplasia was detected in the K19-BCL9-2 breast tumors. Those pillar-like differentiation and squamous metaplasia of tumor

tissue are usually found in APC^{Min/+} mammary tumors (123, 124, 126). In addition, the pattern of transdifferentiation into epidermis combined with squamous metaplasia was described within the mammary glands of MMTV^{Cre};Catnb^{+/ Δ ex3} females (127). We found the same differentiation within the glands and tumors from APC^{Min/+}; K19-BCL9-2 and MMTV^{Cre};Catnb^{+/ Δ ex3}; K19-BCL9-2 females. Thus, overexpression of BCL9-2 drives the hyperplasia caused by accumulation of β -catenin to progress to macroscopic cancers, and enhances tumorigenesis in APC^{Min/+} mice. However, overexpression of BCL9-2 at least in a K19 promoter-driven system is not sufficient to alternate the characteristic squamous metaplasia of mammary glands in APC^{Min/+} or MMTV^{Cre};Catnb^{+/ Δ ex3} models. Thus, it may act as a co-factor of Wnt/ β -catenin signaling enhancing tumorigenesis.

Based on the immunohistochemical analyses and primary tumor cell culture experiments on K19-BCL9-2 tumors, it is evident that K19-BCL9-2 mammary tumors are more reminiscent of breast tumors induced by overexpression of Wnt1 compared to breast cancers from APC^{Min/+} or MMTV^{Cre};Catnb^{+/ Δ ex3} mice. K19-BCL9-2 and MMTV-Wnt1 cancers share similar tissue differentiation and they depend on ER α action. One explanation for the disparity of these models could be the different levels of Wnt/ β -catenin levels induced by distinct mutations. Several studies confirmed the possibility of a tissue specific level of Wnt/ β -catenin signaling, so that only specific alternations of Wnt/ β -catenin pathway components could cause a “just right” level of signaling to induce tumorigenesis in the mammary gland (123, 124). These and other studies showed in addition that special mutations affect different epithelial stem/progenitor cells in the mammary gland (123, 124, 128, 158). Using an expression of different cell surface markers, Teissedre et al. 2009 analyzed differences between mammary tumors caused by MMTV-Wnt1 and MMTV- Δ N89 β -catenin transgenes. They found that although driven by the same promoter, the activation of Wnt- β -catenin signaling targeted different cell types within the mammary epithelium. MMTV- Δ N89 β -catenin expression induced autocrine canonical signaling and affected bipotent alveolar/ductal progenitor population, which resulted in well differentiated and hormone receptor negative tumors. The tumors induced by MMTV-Wnt1 expression originated from paracrine Wnt/ β -catenin signaling which affected multipotent mammary progenitors, defined by the low expression of CD24 and high

expression of CD49f (128). The progenitor origin of the tumors detected in the studies described above was confirmed by immunohistochemical expression of luminal and basal/myoepithelial specific markers in the tumor tissue. The tumors from K19-BCL9-2 females displayed K19 and SMA α positive cells, indicating a possible progenitor cell origin of the tumors. Moreover, immunofluorescent staining on the breast tumor tissue from K19-BCL9-2 mice showed that the expression of BCL9-2 was activated in luminal and myoepithelial cell, indicating a common BCL9-2 positive progenitor of the tumor cells. The exact progenitor specific cell surface marker expression of tumor cells from K19-BCL9-2 females was not analyzed in this thesis. However, it is plausible though to expect that the overexpression of BCL9-2 using a K19 promoter could target mammary progenitor cell lineages. K19 was described as a marker for lobular mammary stem cells, which express ER α (159, 160). Moreover, the majority of human breast cancers are characterized by expression of both, ER α and K19, suggesting these cells as a target for oncogenic transformations (161). Recently, a down regulation of BCL9 and BCL9-2 was shown to reduce stem cell marker and to impair regeneration of the epithelium in the intestine, confirming the role of BCL9-2 in regulation of stem cell functions (95). These findings indicate that K19-BCL9-2 mouse model may possibly mimic specific oncogenic transformation processes taking place during breast cancer development in humans.

6.6 BCL9-2 overexpression in human breast cancer correlates with high hormone receptor expression

To analyze the role of BCL9-2 in human breast cancers this study made use of human breast cancer tissue microarrays. The immunohistological examination of the invasive ductal carcinoma samples revealed overexpression of BCL9-2 compared to normal breast tissues, provided by the microarrays. This finding was consistent with the results of the study performed on human ductal carcinoma in situ (DCIS) and invasive ductal carcinoma (IDC) for the immunohistochemical expression of BCL9-2 by Toya et al. 2007.

Furthermore, we found a correlation between high BCL9-2 expression and nuclear hormone receptor positivity. The highest BCL9-2 levels were detected in ER and/or PR positive tumors and in tumors, which displayed the expression of nuclear hormone receptors and HER2. The modern classification of the breast cancers is based on their hormone expression profile. The combination of their expression is applied to define the tumors into following subtypes: the luminal A (ER+, PR+, HER2-), luminal B (ER+, PR+, HER2+), HER2-overexpressing (ER-, PR-, HER2+) and triple-negative (ER-, PR-, HER2-) (25, 27, 28, 162). Thus, the tumor samples from the microarrays with the highest BCL9-2 expression are defined as luminal A and B type of breast cancers, according to their hormone receptor and HER2 expression profile.

These data are consistent with our results obtained from the Western blot analyses of BCL9-2 expression in different human breast cancer cell lines. BCL9-2 was expressed in all analyzed cancer cell lines regardless of their subtype. However, the level of BCL9-2 was highest in breast cancer cell lines of the luminal type, MCF7 and T47D, which express ER, and SK-BR-3, a HER2-positive luminal cell line (163, 164). Compared to that, the BCL9-2 levels were only moderate in the triple negative breast cancer lines MDA-MB-231 and BT 549. Similarly, the expression of BCL9-2 was only slightly elevated in the triple-negative cancer samples of the tissue arrays compared to the normal mammary breast.

These data are in part consistent with the results published by Toya et al. 2007. In this publication, high BCL9-2 expression correlated with the expression of HER2, similar to our findings. However, the statistical analyses of BCL9-2 and ER expression did not reveal a significant correlation of the expression of these molecules. That may be due to the lower patients numbers used in the mentioned study (99). Taken together, our data from the tissue microarrays strongly indicate, that BCL9-2 could play an important role for development and/or progression of breast tumors, especially of the luminal, ER positive type.

In this study, BCL9-2 was not only highly expressed in ER and/or PR positive human breast cancers. Higher expression levels were detected in HER2 positive and in tumors with ER, PR and HER2 expression. Although the majority of human breast cancers are ER positive, and a large number of patients respond to the tamoxifen therapy, a significant number of breast cancer evolve into tamoxifen resistant type.

Recent studies suggest different mechanism of tamoxifen resistance, such as decrease or loss of ER expression, changes in expression of ER α co-factors, and interference with other signaling pathways (30, 35, 165, 166). Whether BCL9-2 may play a role in maintenance of tamoxifen action and balancing the crosstalk among ER α and other pathways is yet to be determined.

To find out if BCL9-2 interferes with ER α signaling, we used RNAi to knock down BCL9-2 in the ER α positive human breast cancer cell line MCF7. We found reduced ER α mRNA and protein levels after 48 hours of BCL9-2 knock down. In addition, the mRNA level of the ER α target genes PR (progesterone receptor) and GREB1 (growth regulation by estrogen in breast cancer 1) was down regulated simultaneously. However, after 72 hours of BCL9-2 knock down, ER α and its target genes increased again, although the knock down of BCL9-2 still persisted. These results suggest that reduction of BCL9-2 protein leads to a reduction of ER α and its transcriptional activity. However, this effect seems to be transient and the expression of ER α and its targets recovers rapidly. Studies on MCF7 cell line reported a rapid dynamic process of ER α degradation and synthesis as a general estrogen response (167). Moreover, a cross-regulatory mechanism between ER α and its target genes such as PR and GATA3 (trans-acting T-cell-specific transcription factor GATA-3) was reported (168, 169). Furthermore, ER α was shown to have an auto-regulating ability (170-172). Together these findings indicate that the maintenance of ER α levels is a very dynamic cell process, rapidly controlled by various mechanisms. Thus, being a co-factor, BCL9-2 could be a part of a regulatory machinery of feedback loops, which influence the expression of ER α and, consequently, of its targets. However, a validation of BCL9-2 knock down experiments and immunoprecipitation studies in MCF7 and further ER α positive breast cancer cell lines would help to gain more details about the interaction of BCL9-2 and ER α .

It is possible that BCL9-2 acts as a co-factor of β -catenin in this context. An interaction between ER α and Wnt/ β -catenin signaling in different tissues was previously reported (173-176). Recent studies suggest a mechanism via inhibition of GSK3 β by estrogen that leads to an induction of Wnt/ β -catenin signaling (177, 178). However, the findings concerning the direct interaction between ER α and β -catenin are controversial (173, 179, 180). Nevertheless, β -catenin was reported to positively regulate

ER α signaling in breast cancer cell lines (173, 179). Thus, BCL9-2 could indirectly co-regulate ER α function by acting as a co-factor of β -catenin. An alternative model could be that BCL9-2 directly binds to ER or is a part of a protein complex with ER α . Such BCL9-2/ER complexes could bind to regulatory sequences and regulate ER target gene expression. This speculation is supported on the findings from our recent study. We found that BCL9-2 regulates a subset of Wnt/ β -catenin dependent target genes in colon cancer cells, indicating a context specific mode of action of BCL9-2. Furthermore, it is able to act as a transcriptional regulator in a Wnt/ β -catenin independent manner (84). Of note, canonical Wnt/ β -catenin signaling is almost inactive in human breast luminal breast cancer cell line MCF7 which were used in this thesis to analyze the expression of ER α and its target genes after BCL9-2 knock down (179). Therefore, BCL9-2 could indeed act in a Wnt/ β -catenin independent mode in this model. Sustmann et al., 2008 detected a transactivation domain in the C-terminus of BCL9, a homologue of BCL9-2. The C-terminal domains of BCL9 and BCL9-2 are highly conserved between vertebrate BCL9 proteins but not in *Drosophila* Legless (48, 54, 88, 89, 91). The function of C-terminal domains in BCL9-2 seem to be important for promotion of Wnt/ β -catenin signaling, since a deletion of a C-terminus in both, BCL9 and BCL9-2 reduced the Wnt/ β -catenin dependent expression of a reporter construct in cultured cells (54, 91). However, a definite function of any of three C-terminal domains was not addressed yet precisely. Thus, C-terminus of BCL9-2 could be a candidate to bind to further not yet described interaction partners, in a β -catenin dependent or independent manner. Finally, BCL9-2 could act on the protein level as a regulator of ER α stability. However, the precise mechanism of how BCL9-2 interferes with ER α signaling is not apparent from the results of this study and yet has to be analyzed.

7. Summary

One of a few highly conserved signaling pathways, which regulate cell proliferation and tissue organization during embryogenesis and in the adult organism, is the Wnt/ β -catenin signaling cascade. The mutations of different Wnt/ β -catenin signaling components lead to an aberrant activation of β -catenin and to an abnormal expression of diverse target genes. A deregulated Wnt signal transduction results in a malignant transformation followed by tumor progression in many tissues, including the breast. Recently, BCL9-2, the member of the novel BCL9/legless oncogene family, was identified as essential co-activator of β -catenin dependent regulation of target gene transcription. The oncogenic potential of BCL9-2 in colorectal cancer is becoming more apparent. Its implication in breast tumor development is not yet investigated. This study shows for the first time, that overexpression of BCL9-2 *in vivo* leads to breast tumor development. Moreover, the results suggest a mechanism of BCL9-2 oncogenic activity by interfering with ER α signaling.

Overexpression of BCL9-2 using a keratin 19 (K19) specific promoter sequence in transgenic mice led to breast tumor development in aged females. Moreover, BCL9-2 overexpression was sufficient to increase the breast tumor incidence in APC^{Min/+} females and to induce macroscopic tumors of the breast in MMTV^{Cre};Catnb^{+/ Δ ex3} mice. Aged transgenic females displayed mammary gland hyperplasia characterized by enlarged ducts and hyperplastic alveolar nodules (HANs), which are described as premalignant foci in mice and in human. In addition, they displayed increased alveolar morphology and delayed postlactational involution of mammary epithelium, possibly associated with tumorigenesis in the breast. Interestingly, the mammary tumors of transgenic K19-BCL9-2 females showed nuclear estrogen receptor alpha (ER α) and progesterone receptor (PR) expression, representing a unique feature of the K19-BCL9-2 model. Moreover, the tumor growth was dependent on estrogen stimulation, as was shown by MTT and BrdU assays.

Comparing different human breast cancer cell lines, the highest BCL9-2 protein levels were found in ER α and HER2 positive cells. Additionally, a siRNA-mediated transient knock down of BCL9-2 resulted in a transient mRNA reduction of ER α and corresponding target genes, indicating that BCL9-2 may regulate the ER α expression

and interferes with downstream signaling. Finally, immunohistochemical analyses of human breast cancer tissues showed that BCL9-2 overexpression significantly correlated with high expression of ER α , PR and HER2 and that the expression of BCL9-2 is higher in malignant than in healthy mammary tissue.

Taken together, this study demonstrates, for the first time, an implication of BCL9-2 in mammary tumorigenesis and suggests BCL9-2 as a novel modulator of estrogen receptor α signaling.

8. Zusammenfassung

Einer der wenigen hoch konservierten Signalwege, welche die Zellproliferation und Gewebeorganisation während der Embryogenese aber auch im adulten Organismus regulieren, ist die Wnt/ β -Catenin Signalkaskade. Mutationen verschiedenster Wnt/ β -Catenin Signalkomponenten führen zu einer aberranten Aktivierung von β -Catenin und zu einer abnormalen Expression diverser Zielgene. Eine solche deregulierte Wnt Signaltransduktion verursacht in vielen Geweben, inklusive des Brustgewebes, eine maligne Transformation mit anschließender Ausbildung von Tumoren. Kürzlich wurde BCL9-2, ein Mitglied der neuen onkogenen BCL9/legless Familie, als essentieller Co-Aktivator der β -Catenin-abhängigen Regulation der Transkription von Zielgenen identifiziert. Im kolorektalen Karzinom zeichnet sich das onkogene Potential von BCL9-2 immer mehr ab. Seine Implikation in der Entstehung von Brusttumoren wurde dagegen noch nicht untersucht. Diese Arbeit zeigt zum ersten Mal, dass eine Überexpression von BCL9-2 zur Bildung von Brusttumoren *in vivo* führt. Zudem weisen die Ergebnisse auf einen Mechanismus der onkogenen Aktivität hin, bei dem BCL9-2 in die ER Signaltransduktion eingreift.

Nach Überexpression von BCL9-2 unter einem Keratin 19 (K19) -spezifischen Promotor kam es in älteren transgenen Weibchen zur Ausbildung von Brusttumoren. Zudem reichte eine BCL9-2 Überexpression aus, um die Brusttumor-Inzidenz in APC^{Min/+} Weibchen zu erhöhen und makroskopische Tumore der Brust in MMTV^{Cre};Catnb^{+/ Δ ex3} Mäusen zu induzieren. Gealterte transgene Weibchen zeigten Milchdrüsenhyperplasien, welche durch erweiterte Gänge und hyperplastische alveoläre Knoten (hyperplastic alveolar nodules; HANs) charakterisiert und als prä-maligne Foci in Maus und Mensch beschrieben sind. Zusätzlich weisen sie eine erhöhte alveolare Morphologie und eine verzögerte post-laktationale Rückbildung des Brustepithels auf, was möglicherweise mit einer Tumorbildung in der Brust assoziiert ist. Interessanterweise wiesen Brusttumoren der transgenen K19-BCL9-2 Weibchen eine nukleäre Estrogenrezeptor alpha- (ER α) und Progesteronrezeptor- (PR) Expression auf, was eine Besonderheit des K19-BCL9-2 Mausmodells darstellt. Darüber hinaus zeigten MTT und BrdU Assays, dass das Tumorstadium abhängig von der Stimulation mit Estrogen ist.

Der Vergleich verschiedener humaner Brustkrebs-Zelllinien zeigte, dass ER α - und HER2- positive Zellen die höchsten Level an BCL9-2 Protein aufweisen. Zusätzlich resultierte ein siRNA-vermittelter transienter knock down von BCL9-2 in einer transienten mRNA Reduktion des ER α und entsprechender Zielgene. Dies weist auf eine mögliche Regulation der ER α -Expression durch BCL9-2 und ein Eingreifen in die ER α downstream Signaltransduktion hin. Schließlich zeigten immunhistochemische Analysen an humanen Brustkrebsgewebeproben eine signifikante Korrelation zwischen BCL9-2 Überexpression und erhöhter Expression des ER α , PR und HER2 sowie eine deutlich stärkere BCL9-2 Expression in malignem verglichen mit gesundem Brustgewebe.

Zusammenfassend veranschaulicht diese Arbeit erstmals eine Implikation von BCL9-2 in der Tumorgenese von Mamma Tumoren und lässt BCL9-2 als neuen Modulator der ER α Signalkaskade vermuten.

9. References

- (1) Cardiff RD, Bern HA, Faulkin LJ, Daniel CW, Smith GH, Young LJ, et al. Contributions of mouse biology to breast cancer research. *Comp Med* 2002;52:12-31.
- (2) Visvader JE. Keeping abreast of the mammary epithelial hierarchy and breast tumorigenesis. *Genes Dev* 2009;23:2563-77.
- (3) Richert MM, Schwertfeger KL, Ryder JW, Anderson SM. An atlas of mouse mammary gland development. *J Mammary Gland Biol Neoplasia* 2000;5:227-41.
- (4) Radisky DC, Hartmann LC. Mammary involution and breast cancer risk: transgenic models and clinical studies. *J Mammary Gland Biol Neoplasia* 2009;14:181-91.
- (5) Veltmaat JM, Van VW, Thiery JP, Bellusci S. Identification of the mammary line in mouse by Wnt10b expression. *Dev Dyn* 2004;229:349-56.
- (6) Hens JR, Wysolmerski JJ. Key stages of mammary gland development: molecular mechanisms involved in the formation of the embryonic mammary gland. *Breast Cancer Res* 2005;7:220-4.
- (7) Cowin P, Wysolmerski J. Molecular mechanisms guiding embryonic mammary gland development. *Cold Spring Harb Perspect Biol* 2010;2:a003251.
- (8) Curtis HS, Couse JF, Korach KS. Estrogen receptor transcription and transactivation: Estrogen receptor knockout mice: what their phenotypes reveal about mechanisms of estrogen action. *Breast Cancer Res* 2000;2:345-52.
- (9) Bocchinfuso WP, Lindzey JK, Hewitt SC, Clark JA, Myers PH, Cooper R, et al. Induction of mammary gland development in estrogen receptor- α knockout mice. *Endocrinology* 2000;141:2982-94.
- (10) Sternlicht MD. Key stages in mammary gland development: the cues that regulate ductal branching morphogenesis. *Breast Cancer Res* 2006;8:201.
- (11) Hinck L, Silberstein GB. Key stages in mammary gland development: the mammary end bud as a motile organ. *Breast Cancer Res* 2005;7:245-51.
- (12) Incassati A, Chandramouli A, Eelkema R, Cowin P. Key signaling nodes in mammary gland development and cancer: beta-catenin. *Breast Cancer Res* 2010;12:213.
- (13) Cardiff RD, Wellings SR. The comparative pathology of human and mouse mammary glands. *J Mammary Gland Biol Neoplasia* 1999;4:105-22.

- (14) Watson CJ. Involution: apoptosis and tissue remodelling that convert the mammary gland from milk factory to a quiescent organ. *Breast Cancer Res* 2006;8:203.
- (15) Howard BA, Gusterson BA. Human breast development. *J Mammary Gland Biol Neoplasia* 2000;5:119-37.
- (16) Fridriksdottir AJ, Petersen OW, Ronnov-Jessen L. Mammary gland stem cells: current status and future challenges. *Int J Dev Biol* 2011;55:719-29.
- (17) Nusse R. Wnt signaling and stem cell control. *Cell Res* 2008;18:523-7.
- (18) Roarty K, Rosen JM. Wnt and mammary stem cells: hormones cannot fly wingless. *Curr Opin Pharmacol* 2010;10:643-9.
- (19) Shackleton M, Vaillant F, Simpson KJ, Stingl J, Smyth GK, Asselin-Labat ML, et al. Generation of a functional mammary gland from a single stem cell. *Nature* 2006;439:84-8.
- (20) Stingl J, Eirew P, Ricketson I, Shackleton M, Vaillant F, Choi D, et al. Purification and unique properties of mammary epithelial stem cells. *Nature* 2006;439:993-7.
- (21) Sleeman KE, Kendrick H, Robertson D, Isacke CM, Ashworth A, Smalley MJ. Dissociation of estrogen receptor expression and in vivo stem cell activity in the mammary gland. *J Cell Biol* 2007;176:19-26.
- (22) Perou CM, Sorlie T, Eisen MB, van de Rijn M, Jeffrey SS, Rees CA, et al. Molecular portraits of human breast tumours. *Nature* 2000;406:747-52.
- (23) Gusterson BA, Ross DT, Heath VJ, Stein T. Basal cytokeratins and their relationship to the cellular origin and functional classification of breast cancer. *Breast Cancer Res* 2005;7:143-8.
- (24) Stingl J, Caldas C. Molecular heterogeneity of breast carcinomas and the cancer stem cell hypothesis. *Nat Rev Cancer* 2007;7:791-9.
- (25) Gruver AM, Portier BP, Tubbs RR. Molecular pathology of breast cancer: the journey from traditional practice toward embracing the complexity of a molecular classification. *Arch Pathol Lab Med* 2011;135:544-57.
- (26) Leong AS, Zhuang Z. The changing role of pathology in breast cancer diagnosis and treatment. *Pathobiology* 2011;78:99-114.
- (27) Rakha EA, Ellis IO. Modern classification of breast cancer: should we stick with morphology or convert to molecular profile characteristics. *Adv Anat Pathol* 2011;18:255-67.
- (28) Reis-Filho JS, Pusztai L. Gene expression profiling in breast cancer: classification, prognostication, and prediction. *Lancet* 2011;378:1812-23.

- (29) Osborne CK. Tamoxifen in the treatment of breast cancer. *N Engl J Med* 1998;339:1609-18.
- (30) Criscitiello C, Fumagalli D, Saini KS, Loi S. Tamoxifen in early-stage estrogen receptor-positive breast cancer: overview of clinical use and molecular biomarkers for patient selection. *Onco Targets Ther* 2011;4:1-11.
- (31) Wiebe VJ, Osborne CK, Fuqua SA, DeGregorio MW. Tamoxifen resistance in breast cancer. *Crit Rev Oncol Hematol* 1993;14:173-88.
- (32) Zhao JJ, Lin J, Yang H, Kong W, He L, Ma X, et al. MicroRNA-221/222 negatively regulates estrogen receptor alpha and is associated with tamoxifen resistance in breast cancer. *J Biol Chem* 2008;283:31079-86.
- (33) Cittelly DM, Das PM, Spoelstra NS, Edgerton SM, Richer JK, Thor AD, et al. Downregulation of miR-342 is associated with tamoxifen resistant breast tumors. *Mol Cancer* 2010;9:317.
- (34) Ring A, Dowsett M. Mechanisms of tamoxifen resistance. *Endocr Relat Cancer* 2004;11:643-58.
- (35) Shou J, Massarweh S, Osborne CK, Wakeling AE, Ali S, Weiss H, et al. Mechanisms of tamoxifen resistance: increased estrogen receptor-HER2/neu cross-talk in ER/HER2-positive breast cancer. *J Natl Cancer Inst* 2004;96:926-35.
- (36) Choo JR, Nielsen TO. Biomarkers for Basal-like Breast Cancer. *Cancers* 2010;2:1040-65.
- (37) Higgins MJ, Baselga J. Targeted therapies for breast cancer. *J Clin Invest* 2011;121:3797-803.
- (38) Gusterson B. Do 'basal-like' breast cancers really exist? *Nat Rev Cancer* 2009;9:128-34.
- (39) Ben-Porath I, Thomson MW, Carey VJ, Ge R, Bell GW, Regev A, et al. An embryonic stem cell-like gene expression signature in poorly differentiated aggressive human tumors. *Nat Genet* 2008;40:499-507.
- (40) Herschkowitz JJ, Simin K, Weigman VJ, Mikaelian I, Usary J, Hu Z, et al. Identification of conserved gene expression features between murine mammary carcinoma models and human breast tumors. *Genome Biol* 2007;8:R76.
- (41) Polakis P. Wnt Signaling in Cancer. *Cold Spring Harb Perspect Biol* 2012.
- (42) Klaus A, Birchmeier W. Wnt signalling and its impact on development and cancer. *Nat Rev Cancer* 2008;8:387-98.
- (43) Brennan KR, Brown AM. Wnt proteins in mammary development and cancer. *J Mammary Gland Biol Neoplasia* 2004;9:119-31.

- (44) Logan CY, Nusse R. The Wnt signaling pathway in development and disease. *Annu Rev Cell Dev Biol* 2004;20:781-810.
- (45) Clevers H. Wnt/beta-catenin signaling in development and disease. *Cell* 2006;127:469-80.
- (46) Tanaka SS, Kojima Y, Yamaguchi YL, Nishinakamura R, Tam PP. Impact of WNT signaling on tissue lineage differentiation in the early mouse embryo. *Dev Growth Differ* 2011;53:843-56.
- (47) Bienz M, Clevers H. Linking colorectal cancer to Wnt signaling. *Cell* 2000;103:311-20.
- (48) Brembeck FH, Rosario M, Birchmeier W. Balancing cell adhesion and Wnt signaling, the key role of beta-catenin. *Curr Opin Genet Dev* 2006;16:51-9.
- (49) Wodarz A, Nusse R. Mechanisms of Wnt signaling in development. *Annu Rev Cell Dev Biol* 1998;14:59-88.
- (50) MacDonald BT, Tamai K, He X. Wnt/beta-catenin signaling: components, mechanisms, and diseases. *Dev Cell* 2009;17:9-26.
- (51) Smalley MJ, Dale TC. Wnt signalling in mammalian development and cancer. *Cancer Metastasis Rev* 1999;18:215-30.
- (52) Stadeli R, Hoffmans R, Basler K. Transcription under the control of nuclear Arm/beta-catenin. *Curr Biol* 2006;16:R378-R385.
- (53) Mosimann C, Hausmann G, Basler K. Beta-catenin hits chromatin: regulation of Wnt target gene activation. *Nat Rev Mol Cell Biol* 2009;10:276-86.
- (54) Brembeck FH, Schwarz-Romond T, Bakkers J, Wilhelm S, Hammerschmidt M, Birchmeier W. Essential role of BCL9-2 in the switch between beta-catenin's adhesive and transcriptional functions. *Genes Dev* 2004;18:2225-30.
- (55) Belenkaya TY, Han C, Standley HJ, Lin X, Houston DW, Heasman J, et al. pygopus Encodes a nuclear protein essential for wingless/Wnt signaling. *Development* 2002;129:4089-101.
- (56) Parker DS, Jemison J, Cadigan KM. Pygopus, a nuclear PHD-finger protein required for Wingless signaling in *Drosophila*. *Development* 2002;129:2565-76.
- (57) Kramps T, Peter O, Brunner E, Nellen D, Froesch B, Chatterjee S, et al. Wnt/wingless signaling requires BCL9/legless-mediated recruitment of pygopus to the nuclear beta-catenin-TCF complex. *Cell* 2002;109:47-60.
- (58) Carrera I, Janody F, Leeds N, Dubeau F, Treisman JE. Pygopus activates Wingless target gene transcription through the mediator complex subunits Med12 and Med13. *Proc Natl Acad Sci U S A* 2008;105:6644-9.

- (59) Jessen S, Gu B, Dai X. Pygopus and the Wnt signaling pathway: a diverse set of connections. *Bioessays* 2008;30:448-56.
- (60) Chu EY, Hens J, Andl T, Kairo A, Yamaguchi TP, Briskin C, et al. Canonical WNT signaling promotes mammary placode development and is essential for initiation of mammary gland morphogenesis. *Development* 2004;131:4819-29.
- (61) Lindvall C, Evans NC, Zylstra CR, Li Y, Alexander CM, Williams BO. The Wnt signaling receptor Lrp5 is required for mammary ductal stem cell activity and Wnt1-induced tumorigenesis. *J Biol Chem* 2006;281:35081-7.
- (62) Gu B, Sun P, Yuan Y, Moraes RC, Li A, Teng A, et al. Pygo2 expands mammary progenitor cells by facilitating histone H3 K4 methylation. *J Cell Biol* 2009;185:811-26.
- (63) Lindvall C, Zylstra CR, Evans N, West RA, Dykema K, Furge KA, et al. The Wnt co-receptor Lrp6 is required for normal mouse mammary gland development. *PLoS One* 2009;4:e5813.
- (64) Lane TF, Leder P. Wnt-10b directs hypermorphic development and transformation in mammary glands of male and female mice. *Oncogene* 1997;15:2133-44.
- (65) Zhang J, Li Y, Liu Q, Lu W, Bu G. Wnt signaling activation and mammary gland hyperplasia in MMTV-LRP6 transgenic mice: implication for breast cancer tumorigenesis. *Oncogene* 2010;29:539-49.
- (66) Jarde T, Dale T. Wnt signalling in murine postnatal mammary gland development. *Acta Physiol (Oxf)* 2012;204:118-27.
- (67) Boras-Granic K, Chang H, Grosschedl R, Hamel PA. Lef1 is required for the transition of Wnt signaling from mesenchymal to epithelial cells in the mouse embryonic mammary gland. *Dev Biol* 2006;295:219-31.
- (68) Tsukamoto AS, Grosschedl R, Guzman RC, Parslow T, Varmus HE. Expression of the int-1 gene in transgenic mice is associated with mammary gland hyperplasia and adenocarcinomas in male and female mice. *Cell* 1988;55:619-25.
- (69) Imbert A, Eelkema R, Jordan S, Feiner H, Cowin P. Delta N89 beta-catenin induces precocious development, differentiation, and neoplasia in mammary gland. *J Cell Biol* 2001;153:555-68.
- (70) Wang TC, Cardiff RD, Zukerberg L, Lees E, Arnold A, Schmidt EV. Mammary hyperplasia and carcinoma in MMTV-cyclin D1 transgenic mice. *Nature* 1994;369:669-71.
- (71) Teuliere J, Faraldo MM, Deugnier MA, Shtutman M, Ben-Ze'ev A, Thierry JP, et al. Targeted activation of beta-catenin signaling in basal mammary

- epithelial cells affects mammary development and leads to hyperplasia. *Development* 2005;132:267-77.
- (72) Briskin C, Heineman A, Chavarria T, Elenbaas B, Tan J, Dey SK, et al. Essential function of Wnt-4 in mammary gland development downstream of progesterone signaling. *Genes Dev* 2000;14:650-4.
 - (73) Li X, Gonzalez ME, Toy K, Filzen T, Merajver SD, Kleer CG. Targeted overexpression of EZH2 in the mammary gland disrupts ductal morphogenesis and causes epithelial hyperplasia. *Am J Pathol* 2009;175:1246-54.
 - (74) Nusse R, Varmus HE. Many tumors induced by the mouse mammary tumor virus contain a provirus integrated in the same region of the host genome. *Cell* 1982;31:99-109.
 - (75) Hayes MJ, Thomas D, Emmons A, Giordano TJ, Kleer CG. Genetic changes of Wnt pathway genes are common events in metaplastic carcinomas of the breast. *Clin Cancer Res* 2008;14:4038-44.
 - (76) Khramtsov AI, Khramtsova GF, Tretiakova M, Huo D, Olopade OI, Goss KH. Wnt/beta-catenin pathway activation is enriched in basal-like breast cancers and predicts poor outcome. *Am J Pathol* 2010;176.
 - (77) Lin SY, Xia W, Wang JC, Kwong KY, Spohn B, Wen Y, et al. Beta-catenin, a novel prognostic marker for breast cancer: its roles in cyclin D1 expression and cancer progression. *Proc Natl Acad Sci U S A* 2000;97.
 - (78) Prasad CP, Gupta SD, Rath G, Ralhan R. Wnt signaling pathway in invasive ductal carcinoma of the breast: relationship between beta-catenin, dishevelled and cyclin D1 expression. *Oncology* 2007;73:112-7.
 - (79) Jonsson M, Borg A, Nilbert M, Andersson T. Involvement of adenomatous polyposis coli (APC)/beta-catenin signalling in human breast cancer. *Eur J Cancer* 2000;36.
 - (80) Andrews PG, Lake BB, Popadiuk C, Kao KR. Requirement of Pygopus 2 in breast cancer. *Int J Oncol* 2007;30.
 - (81) Kleer CG, Cao Q, Varambally S, Shen R, Ota I, Tomlins SA, et al. EZH2 is a marker of aggressive breast cancer and promotes neoplastic transformation of breast epithelial cells. *Proc Natl Acad Sci U S A* 2003;100.
 - (82) Zeng YA, Nusse R. Wnt proteins are self-renewal factors for mammary stem cells and promote their long-term expansion in culture. *Cell Stem Cell* 2010;6.
 - (83) Li Y, Welm B, Podsypanina K, Huang S, Chamorro M, Zhang X, et al. Evidence that transgenes encoding components of the Wnt signaling

- pathway preferentially induce mammary cancers from progenitor cells. *Proc Natl Acad Sci U S A* 2003;100.
- (84) Liu BY, McDermott SP, Khwaja SS, Alexander CM. The transforming activity of Wnt effectors correlates with their ability to induce the accumulation of mammary progenitor cells. *Proc Natl Acad Sci U S A* 2004;101.
 - (85) Liu CC, Prior J, Piwnica-Worms D, Bu G. LRP6 overexpression defines a class of breast cancer subtype and is a target for therapy. *Proc Natl Acad Sci U S A* 2010;107.
 - (86) Geyer FC, Lacroix-Triki M, Savage K, Arnedos M, Lambros MB, MacKay A, et al. beta-Catenin pathway activation in breast cancer is associated with triple-negative phenotype but not with CTNNB1 mutation. *Mod Pathol* 2011;24.
 - (87) Willis TG, Zalcborg IR, Coignet LJ, Wlodarska I, Stul M, Jadayel DM, et al. Molecular cloning of translocation t(1;14)(q21;q32) defines a novel gene (BCL9) at chromosome 1q21. *Blood* 1998;91.
 - (88) Hoffmans R, Basler K. BCL9-2 binds Arm/beta-catenin in a Tyr142-independent manner and requires Pygopus for its function in Wg/Wnt signaling. *Mech Dev* 2007;124.
 - (89) Adachi S, Jigami T, Yasui T, Nakano T, Ohwada S, Omori Y, et al. Role of a BCL9-related beta-catenin-binding protein, B9L, in tumorigenesis induced by aberrant activation of Wnt signaling. *Cancer Res* 2004;64:8496-501.
 - (90) Townsley FM, Thompson B, Bienz M. Pygopus residues required for its binding to Legless are critical for transcription and development. *J Biol Chem* 2004;279.
 - (91) Sustmann C, Flach H, Ebert H, Eastman Q, Grosschedl R. Cell-type-specific function of BCL9 involves a transcriptional activation domain that synergizes with beta-catenin. *Mol Cell Biol* 2008;28.
 - (92) Brack AS, Murphy-Seiler F, Hanifi J, Deka J, Eyckerman S, Keller C, et al. BCL9 is an essential component of canonical Wnt signaling that mediates the differentiation of myogenic progenitors during muscle regeneration. *Dev Biol* 2009;335.
 - (93) Brembeck FH, Wiese M, Zatula N, Grigoryan T, Dai Y, Fritzmann J, et al. BCL9-2 promotes early stages of intestinal tumor progression. *Gastroenterology* 2011;141.
 - (94) Matsuura K, Jigami T, Taniue K, Morishita Y, Adachi S, Senda T, et al. Identification of a link between Wnt/beta-catenin signalling and the cell fusion pathway. *Nat Commun* 2011;2.

- (95) Deka J, Wiedemann N, Anderle P, Murphy-Seiler F, Bultinck J, Eyckerman S, et al. Bcl9/Bcl9l are critical for Wnt-mediated regulation of stem cell traits in colon epithelium and adenocarcinomas. *Cancer Res* 2010;70.
- (96) de la Roche M, Worm J, Bienz M. The function of BCL9 in Wnt/beta-catenin signaling and colorectal cancer cells. *BMC Cancer* 2008;8.
- (97) Herath NI, Boyd AW. The role of Eph receptors and ephrin ligands in colorectal cancer. *Int J Cancer* 2010;126.
- (98) Sakamoto I, Ohwada S, Toya H, Togo N, Kashiwabara K, Oyama T, et al. Up-regulation of a BCL9-related beta-catenin-binding protein, B9L, in different stages of sporadic colorectal adenoma. *Cancer Sci* 2007;98.
- (99) Toya H, Oyama T, Ohwada S, Togo N, Sakamoto I, Horiguchi J, et al. Immunohistochemical expression of the beta-catenin-interacting protein B9L is associated with histological high nuclear grade and immunohistochemical ErbB2/HER-2 expression in breast cancers. *Cancer Sci* 2007;98.
- (100) Jia W, Eneh JO, Ratnaparkhe S, Altman MK, Murph MM. MicroRNA-30c-2* expressed in ovarian cancer cells suppresses growth factor-induced cellular proliferation and downregulates the oncogene BCL9. *Mol Cancer Res* 2011;9.
- (101) Keydar I, Chen L, Karby S, Weiss FR, Delarea J, Radu M, et al. Establishment and characterization of a cell line of human breast carcinoma origin. *Eur J Cancer* 1979;15.
- (102) Su LK, Kinzler KW, Vogelstein B, Preisinger AC, Moser AR, Luongo C, et al. Multiple intestinal neoplasia caused by a mutation in the murine homolog of the APC gene. *Science* 1992;256.
- (103) Harada N, Tamai Y, Ishikawa T, Sauer B, Takaku K, Oshima M, et al. Intestinal polyposis in mice with a dominant stable mutation of the beta-catenin gene. *EMBO J* 1999;18.
- (104) Indra AK, Warot X, Brocard J, Bornert JM, Xiao JH, Chambon P, et al. Temporally-controlled site-specific mutagenesis in the basal layer of the epidermis: comparison of the recombinase activity of the tamoxifen-inducible Cre-ER(T) and Cre-ER(T2) recombinases. *Nucleic Acids Res* 1999;27.
- (105) Hennighausen L, Wall RJ, Tillmann U, Li M, Furth PA. Conditional gene expression in secretory tissues and skin of transgenic mice using the MMTV-LTR and the tetracycline responsive system. *J Cell Biochem* 1995;59.
- (106) Brembeck FH, Moffett J, Wang TC, Rustgi AK. The keratin 19 promoter is potent for cell-specific targeting of genes in transgenic mice. *Gastroenterology* 2001;120.

- (107) Bartek J, Bartkova J, Taylor-Papadimitriou J. Keratin 19 expression in the adult and developing human mammary gland. *Histochem J* 1990;22.
- (108) Brembeck FH, Rustgi AK. The tissue-dependent keratin 19 gene transcription is regulated by GKLF/KLF4 and Sp1. *J Biol Chem* 2000;275.
- (109) Sun P, Yuan Y, Li A, Li B, Dai X. Cytokeratin expression during mouse embryonic and early postnatal mammary gland development. *Histochem Cell Biol* 2010;133.
- (110) Kowalski PJ, Rubin MA, Kleer CG. E-cadherin expression in primary carcinomas of the breast and its distant metastases. *Breast Cancer Res* 2003;5.
- (111) Boussadia O, Kutsch S, Hierholzer A, Delmas V, Kemler R. E-cadherin is a survival factor for the lactating mouse mammary gland. *Mech Dev* 2002;115.
- (112) Prasad CP, Rath G, Mathur S, Bhatnagar D, Parshad R, Ralhan R. Expression analysis of E-cadherin, Slug and GSK3beta in invasive ductal carcinoma of breast. *BMC Cancer* 2009;9.
- (113) Derksen PW, Liu X, Saridin F, van der Gulden H, Zevenhoven J, Evers B, et al. Somatic inactivation of E-cadherin and p53 in mice leads to metastatic lobular mammary carcinoma through induction of anoikis resistance and angiogenesis. *Cancer Cell* 2006;10.
- (114) Kim G, Kim JY, An HJ, Kang H, Kim TH, Shim JY, et al. The Loss of E-cadherin is Associated with the Epigenetic Alteration of CDH1 in Breast Cancer and it is also Associated with an Abnormal + β -catenin Expression in Lobular Carcinoma. *Korean J Pathol* 2009;43:400-7.
- (115) Herzig M, Savarese F, Novatchkova M, Semb H, Christofori G. Tumor progression induced by the loss of E-cadherin independent of beta-catenin/Tcf-mediated Wnt signaling. *Oncogene* 2007;26.
- (116) Ross JS, Fletcher JA. The HER-2/neu oncogene in breast cancer: prognostic factor, predictive factor, and target for therapy. *Stem Cells* 1998;16.
- (117) Mohibi S, Mirza S, Band H, Band V. Mouse models of estrogen receptor-positive breast cancer. *J Carcinog* 2011;10:35.
- (118) Zhang X, Podsypanina K, Huang S, Mohsin SK, Chamness GC, Hatsell S, et al. Estrogen receptor positivity in mammary tumors of Wnt-1 transgenic mice is influenced by collaborating oncogenic mutations. *Oncogene* 2005;24:4220-31.
- (119) Cardiff RD, Moghanaki D, Jensen RA. Genetically engineered mouse models of mammary intraepithelial neoplasia. *J Mammary Gland Biol Neoplasia* 2000;5:421-37.

- (120) Medina D. Preneoplastic lesions in murine mammary cancer. *Cancer Res* 1976;36:2589-95.
- (121) Medina D. The preneoplastic phenotype in murine mammary tumorigenesis. *J Mammary Gland Biol Neoplasia* 2000;5:393-407.
- (122) Milanese TR, Hartmann LC, Sellers TA, Frost MH, Vierkant RA, Maloney SD, et al. Age-related lobular involution and risk of breast cancer. *J Natl Cancer Inst* 2006;98:1600-7.
- (123) Gaspar C, Franken P, Molenaar L, Breukel C, van d, V, Smits R, et al. A targeted constitutive mutation in the APC tumor suppressor gene underlies mammary but not intestinal tumorigenesis. *PLoS Genet* 2009;5:e1000547.
- (124) Kuraguchi M, Ohene-Baah NY, Sonkin D, Bronson RT, Kucherlapati R. Genetic mechanisms in Apc-mediated mammary tumorigenesis. *PLoS Genet* 2009;5:e1000367.
- (125) Prosperi JR, Becher KR, Willson TA, Collins MH, Witte DP, Goss KH. The APC tumor suppressor is required for epithelial integrity in the mouse mammary gland. *J Cell Physiol* 2009;220:319-31.
- (126) Rosner A, Miyoshi K, Landesman-Bollag E, Xu X, Seldin DC, Moser AR, et al. Pathway pathology: histological differences between ErbB/Ras and Wnt pathway transgenic mammary tumors. *Am J Pathol* 2002;161:1087-97.
- (127) Miyoshi K, Shillingford JM, Le PF, Gounari F, Bronson R, von BH, et al. Activation of beta -catenin signaling in differentiated mammary secretory cells induces transdifferentiation into epidermis and squamous metaplasias. *Proc Natl Acad Sci U S A* 2002;99:219-24.
- (128) Teissedre B, Pinderhughes A, Incassati A, Hatsell SJ, Hiremath M, Cowin P. MMTV-Wnt1 and -DeltaN89beta-catenin induce canonical signaling in distinct progenitors and differentially activate Hedgehog signaling within mammary tumors. *PLoS One* 2009;4:e4537.
- (129) Wagner KU, McAllister K, Ward T, Davis B, Wiseman R, Hennighausen L. Spatial and temporal expression of the Cre gene under the control of the MMTV-LTR in different lines of transgenic mice. *Transgenic Res* 2001;10:545-53.
- (130) Levin ER, Pietras RJ. Estrogen receptors outside the nucleus in breast cancer. *Breast Cancer Res Treat* 2008;108:351-61.
- (131) Berthois Y, Katzenellenbogen JA, Katzenellenbogen BS. Phenol red in tissue culture media is a weak estrogen: implications concerning the study of estrogen-responsive cells in culture. *Proc Natl Acad Sci U S A* 1986;83:2496-500.

- (132) Glover JF, Irwin JT, Darbre PD. Interaction of phenol red with estrogenic and antiestrogenic action on growth of human breast cancer cells ZR-75-1 and T-47-D. *Cancer Res* 1988;48:3693-7.
- (133) Moreno-Cuevas JE, Sirbasku DA. Estrogen mitogenic action. III. is phenol red a "red herring"? *In Vitro Cell Dev Biol Anim* 2000;36:447-64.
- (134) Davie SA, Maglione JE, Manner CK, Young D, Cardiff RD, MacLeod CL, et al. Effects of FVB/NJ and C57Bl/6J strain backgrounds on mammary tumor phenotype in inducible nitric oxide synthase deficient mice. *Transgenic Res* 2007;16:193-201.
- (135) Freund R, Dubensky T, Bronson R, Sotnikov A, Carroll J, Benjamin T. Polyoma tumorigenesis in mice: evidence for dominant resistance and dominant susceptibility genes of the host. *Virology* 1992;191:724-31.
- (136) Buchert M, Athineos D, Abud HE, Burke ZD, Faux MC, Samuel MS, et al. Genetic dissection of differential signaling threshold requirements for the Wnt/beta-catenin pathway in vivo. *PLoS Genet* 2010;6:e1000816.
- (137) Moser AR, Pitot HC, Dove WF. A dominant mutation that predisposes to multiple intestinal neoplasia in the mouse. *Science* 1990;247:322-4.
- (138) Marshall LM, Hunter DJ, Connolly JL, Schnitt SJ, Byrne C, London SJ, et al. Risk of breast cancer associated with atypical hyperplasia of lobular and ductal types. *Cancer Epidemiol Biomarkers Prev* 1997;6:297-301.
- (139) Hatsell S, Rowlands T, Hiremath M, Cowin P. Beta-catenin and Tcfs in mammary development and cancer. *J Mammary Gland Biol Neoplasia* 2003;8:145-58.
- (140) Li Y, Hively WP, Varmus HE. Use of MMTV-Wnt-1 transgenic mice for studying the genetic basis of breast cancer. *Oncogene* 2000;19:1002-9.
- (141) Tepera SB, McCrea PD, Rosen JM. A beta-catenin survival signal is required for normal lobular development in the mammary gland. *J Cell Sci* 2003;116:1137-49.
- (142) Monks J, Henson PM. Differentiation of the mammary epithelial cell during involution: implications for breast cancer. *J Mammary Gland Biol Neoplasia* 2009;14:159-70.
- (143) Schedin P, O'Brien J, Rudolph M, Stein T, Borges V. Microenvironment of the involuting mammary gland mediates mammary cancer progression. *J Mammary Gland Biol Neoplasia* 2007;12:71-82.
- (144) Capuco AV, Li M, Long E, Ren S, Hruska KS, Schorr K, et al. Concurrent pregnancy retards mammary involution: effects on apoptosis and proliferation of the mammary epithelium after forced weaning of mice. *Biol Reprod* 2002;66:1471-6.

- (145) Boras-Granic K, Wysolmerski JJ. Wnt signaling in breast organogenesis. *Organogenesis* 2008;4:116-22.
- (146) Derksen PW, Braumuller TM, van der Burg E, Hornsveld M, Mesman E, Wesseling J, et al. Mammary-specific inactivation of E-cadherin and p53 impairs functional gland development and leads to pleomorphic invasive lobular carcinoma in mice. *Dis Model Mech* 2011;4:347-58.
- (147) Mani SA, Guo W, Liao MJ, Eaton EN, Ayyanan A, Zhou AY, et al. The epithelial-mesenchymal transition generates cells with properties of stem cells. *Cell* 2008;133:704-15.
- (148) Schackmann RC, van AM, Haarhuis JH, Vlug EJ, Halim VA, Roodhart JM, et al. Cytosolic p120-catenin regulates growth of metastatic lobular carcinoma through Rock1-mediated anoikis resistance. *J Clin Invest* 2011;121:3176-88.
- (149) Thiery JP. Epithelial-mesenchymal transitions in development and pathologies. *Curr Opin Cell Biol* 2003;15:740-6.
- (150) Vos CB, Cleton-Jansen AM, Berx G, de Leeuw WJ, ter Haar NT, van RF, et al. E-cadherin inactivation in lobular carcinoma in situ of the breast: an early event in tumorigenesis. *Br J Cancer* 1997;76:1131-3.
- (151) Cardiff RD, Anver MR, Gusterson BA, Hennighausen L, Jensen RA, Merino MJ, et al. The mammary pathology of genetically engineered mice: the consensus report and recommendations from the Annapolis meeting. *Oncogene* 2000;19:968-88.
- (152) Cardiff RD. Validity of mouse mammary tumour models for human breast cancer: comparative pathology. *Microsc Res Tech* 2001;52:224-30.
- (153) Nandi S, Guzman RC, Yang J. Hormones and mammary carcinogenesis in mice, rats, and humans: a unifying hypothesis. *Proc Natl Acad Sci U S A* 1995;92:3650-7.
- (154) Bocchinfuso WP, Hively WP, Couse JF, Varmus HE, Korach KS. A mouse mammary tumor virus-Wnt-1 transgene induces mammary gland hyperplasia and tumorigenesis in mice lacking estrogen receptor-alpha. *Cancer Res* 1999;59:1869-76.
- (155) Britt K, Ashworth A, Smalley M. Pregnancy and the risk of breast cancer. *Endocr Relat Cancer* 2007;14:907-33.
- (156) Russo IH, Russo J. Pregnancy-induced changes in breast cancer risk. *J Mammary Gland Biol Neoplasia* 2011;16:221-33.
- (157) Saji S, Jensen EV, Nilsson S, Rylander T, Warner M, Gustafsson JA. Estrogen receptors alpha and beta in the rodent mammary gland. *Proc Natl Acad Sci U S A* 2000;97:337-42.

- (158) Miyoshi K, Hennighausen L. Beta-catenin: a transforming actor on many stages. *Breast Cancer Res* 2003;5:63-8.
- (159) Clarke RB, Spence K, Anderson E, Howell A, Okano H, Potten CS. A putative human breast stem cell population is enriched for steroid receptor-positive cells. *Dev Biol* 2005;277:443-56.
- (160) Villadsen R, Fridriksdottir AJ, Ronnov-Jessen L, Gudjonsson T, Rank F, LaBarge MA, et al. Evidence for a stem cell hierarchy in the adult human breast. *J Cell Biol* 2007;177:87-101.
- (161) Taylor-Papadimitriou J, Stampfer M, Bartek J, Lewis A, Boshell M, Lane EB, et al. Keratin expression in human mammary epithelial cells cultured from normal and malignant tissue: relation to in vivo phenotypes and influence of medium. *J Cell Sci* 1989;94 (Pt 3):403-13.
- (162) Jung SY, Jeong J, Shin SH, Kwon Y, Kim EA, Ko KL, et al. The invasive lobular carcinoma as a prototype luminal A breast cancer: a retrospective cohort study. *BMC Cancer* 2010;10:664.
- (163) Charafe-Jauffret E, Ginestier C, Monville F, Finetti P, Adelaide J, Cervera N, et al. Gene expression profiling of breast cell lines identifies potential new basal markers. *Oncogene* 2006;25:2273-84.
- (164) Riaz M, Elstrodt F, Hollestelle A, Dehghan A, Klijn JG, Schutte M. Low-risk susceptibility alleles in 40 human breast cancer cell lines. *BMC Cancer* 2009;9:236.
- (165) Hurtado A, Holmes KA, Geistlinger TR, Hutcheson IR, Nicholson RI, Brown M, et al. Regulation of ERBB2 by oestrogen receptor-PAX2 determines response to tamoxifen. *Nature* 2008;456:663-6.
- (166) Jones LP, Li M, Halama ED, Ma Y, Lubet R, Grubbs CJ, et al. Promotion of mammary cancer development by tamoxifen in a mouse model of Brca1-mutation-related breast cancer. *Oncogene* 2005;24:3554-62.
- (167) Pinzone JJ, Stevenson H, Strobl JS, Berg PE. Molecular and cellular determinants of estrogen receptor alpha expression. *Mol Cell Biol* 2004;24:4605-12.
- (168) Carroll JS, Meyer CA, Song J, Li W, Geistlinger TR, Eeckhoutte J, et al. Genome-wide analysis of estrogen receptor binding sites. *Nat Genet* 2006;38:1289-97.
- (169) Eeckhoutte J, Keeton EK, Lupien M, Krum SA, Carroll JS, Brown M. Positive cross-regulatory loop ties GATA-3 to estrogen receptor alpha expression in breast cancer. *Cancer Res* 2007;67:6477-83.
- (170) Horwitz KB, McGuire WL. Nuclear mechanisms of estrogen action. Effects of estradiol and anti-estrogens on estrogen receptors and nuclear receptor processing. *J Biol Chem* 1978;253:8185-91.

- (171) Katzenellenbogen BS, Katzenellenbogen JA. Estrogen receptor transcription and transactivation: Estrogen receptor alpha and estrogen receptor beta: regulation by selective estrogen receptor modulators and importance in breast cancer. *Breast Cancer Res* 2000;2:335-44.
- (172) Thomas C, Gustafsson JA. The different roles of ER subtypes in cancer biology and therapy. *Nat Rev Cancer* 2011;11:597-608.
- (173) Gupta N, Schmitt F, Grebhardt S, Mayer D. β -Catenin Is a Positive Regulator of Estrogen Receptor- α Function in Breast Cancer Cells. *Cancers* 2011;3:2990-3001.
- (174) Pinzone JJ, Hall BM, Thudi NK, Vonau M, Qiang YW, Rosol TJ, et al. The role of Dickkopf-1 in bone development, homeostasis, and disease. *Blood* 2009;113:517-25.
- (175) Wandosell F, Varea O, Arevalo MA, Garcia-Segura LM. Oestradiol regulates beta-catenin-mediated transcription in neurones. *J Neuroendocrinol* 2012;24:191-4.
- (176) Wang Y, van der Zee M, Fodde R, Blok LJ. Wnt/Beta-catenin and sex hormone signaling in endometrial homeostasis and cancer. *Oncotarget* 2010;1:674-84.
- (177) Cardona-Gomez P, Perez M, Avila J, Garcia-Segura LM, Wandosell F. Estradiol inhibits GSK3 and regulates interaction of estrogen receptors, GSK3, and beta-catenin in the hippocampus. *Mol Cell Neurosci* 2004;25:363-73.
- (178) Medunjanin S, Hermani A, De SB, Grisouard J, Rincke G, Mayer D. Glycogen synthase kinase-3 interacts with and phosphorylates estrogen receptor alpha and is involved in the regulation of receptor activity. *J Biol Chem* 2005;280:33006-14.
- (179) Kouzmenko AP, Takeyama K, Ito S, Furutani T, Sawatsubashi S, Maki A, et al. Wnt/beta-catenin and estrogen signaling converge in vivo. *J Biol Chem* 2004;279:40255-8.
- (180) Shi B, Liang J, Yang X, Wang Y, Zhao Y, Wu H, et al. Integration of estrogen and Wnt signaling circuits by the polycomb group protein EZH2 in breast cancer cells. *Mol Cell Biol* 2007;27:5105-19.

10. Curriculum Vitae

Dipl.-Biol

Nathalie Zatula

Tumor Biology and Signal Transduction

Department of Hematology/Oncology

Göttingen University Medical School

Robert-Koch-Strasse-40

37075 Göttingen

Germany

Education

2008-2012 PhD at the Department of Hematology/Oncology, Göttingen University Medical School, Göttingen, Germany, supervised by Prof. Dr. F.H. Brembeck

Dissertation title: “Characterization of the Oncogenic Role of BCL9-2 in Breast Tumorigenesis”

2001-2008 Study of Biology (Diploma), Georg-August-University Göttingen, Germany

Grade: 1.4 (sehr gut/A)

Major exam subject: developmental biology

Minor exam subjects: botany, pharmacology

Diploma Thesis: “Untersuchung zur Funktion der Macro-Domäne in *C.elegans* Protein Mdo-1 und in Histon-Variante macroH2A1.2 der Maus”

2000 Abitur

Publications

Felix H. Brembeck, Maria Wiese, **Nathalie Zatula**, Tamara Grigoryan, Yiyang Dai, Johannes Fritzmann, and Walter Birchmeier, *BCL9-2 Promotes Early Stages of Intestinal Tumor Progression*, 2010, Gastroenterology, 14

11. Acknowledgements

An dieser Stelle möchte ich mich bei allen herzlichst bedanken, die zum Gelingen dieser Doktorarbeit beigetragen haben.

Mein besonderer Dank gilt:

Herrn Prof. Dr. Felix H. Brembeck für die Gelegenheit meine Promotion in seiner Arbeitsgruppe „Tumorbilogie und Signaltransduktion“ in der Abteilung Hämatologie/Onkologie am Universitätsklinikum Göttingen durchzuführen, sowie für die Überlassung eines so interessanten und anspruchsvollen Themas und die Betreuung der Arbeit. Des Weiteren gilt mein Dank Abteilungsleiter Herrn Prof. Dr. med. Lorenz Trümper.

Meinen Thesis Committee Mitgliedern, Herrn Prof. Dr. Matthias Dobbstein und Frau Prof. Dr. Heidi Hahn, für ihre Unterstützung und Mitbetreuung meiner Arbeit.

Herrn Prof. Dr. Steven Johnsen für die kompetente Beratung und Unterstützung in Sachen Estrogenrezeptor.

Allen Forschenden aus der Abteilung Hämatologie/Onkologie des Uniklinikums Göttingen für die stetige Hilfe, Unterstützung und Freundlichkeit. Das weiß ich sehr zu schätzen!

Meinen Laborkollegen/innen und meinen „Büromädels“ dafür, dass ihr da wart und ich mich immer auf euch verlassen konnte. Das hat Spaß gemacht mit euch zusammenzuarbeiten!

Frau Dr. rer. nat. Stephanie Plehm für alles eben!

Meinen lieben Freunden und Mitbewohnern fürs Ertragen, Füttern und Trotzallem-liebhaben. Danke!

Meiner Mama und meinem Bruder, das Studieren hat nun ein Ende!